BORON (AND Gd) AT THE ESS

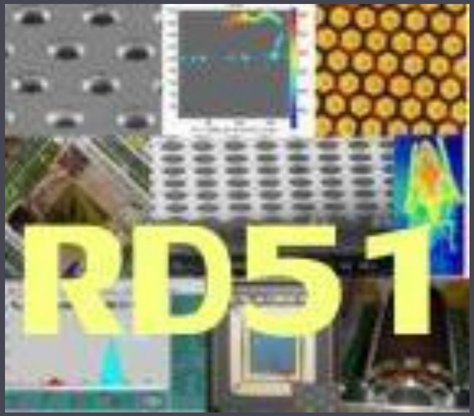

Special thanks to: C. Hoeglund, F. Piscitelli, F. Resnati

Dorothea Pfeiffer on Behalf of the ESS Detector Group

Content

- Boron 10 thin film coatings (C. Hoeglund)
- Boron 10 analytical calculations and measurements (F. Piscitelli: PhD thesis (2014) Uni Perugia/ILL. http://arxiv.org/abs/1406.3133)
- GEMs for thermal neutrons
  - Boron-GEM
  - uTPC analysis
  - Gd-GEM
- Geant4/Garfield interface

- C. Höglund et al, "B4C thin films for neutron detection", Journal of Applied Physics 111, 104908 (2012)
- H. Pedersen, C. Höglund, J. Birch, J. Jensen and A. Henry, "Low temperature chemical vapor deposition of thin, amorphous boron-carbon film for neutron detectors", Chemical Vapor Deposition, 18(7-9), 221-224 (2012)

^{3}He-Crisis → ^{10}B Thin Film Detectors

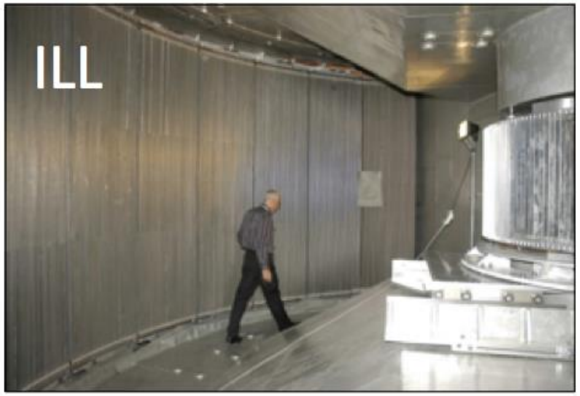

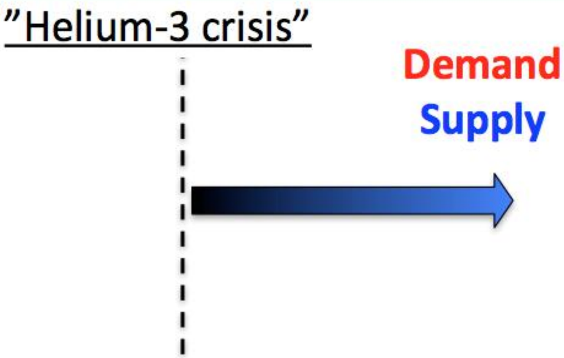

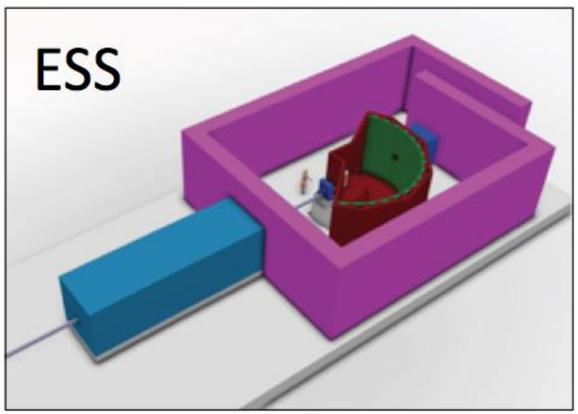

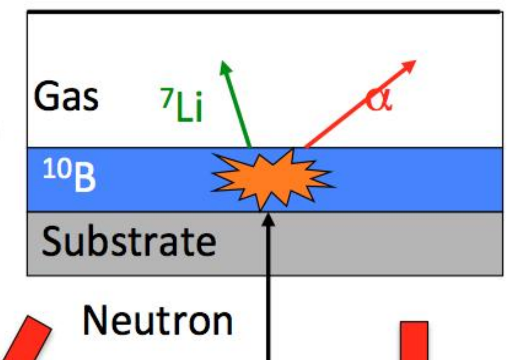

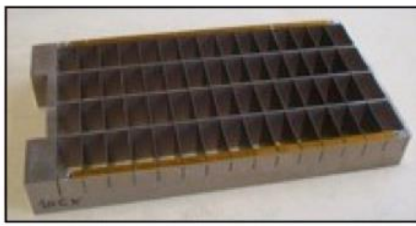

e.g. detectors in the ESS/ILL collaboration

Detector Coatings in Linköping

Linköping University
27 000 students
4 000 employees

Thin film physics division
~55 researchers, 20 MEur/year funding
Design of new multi-functional materials for

- Hard and wear-resistant coatings
- Energy materials
- Magnetic materials
- **Neutron-converting materials**
- Wide-bandgap semiconductors, etc.

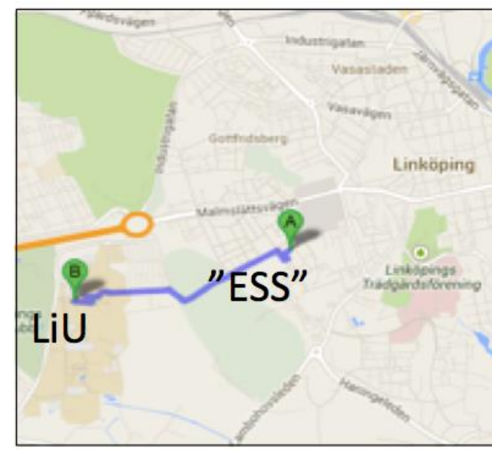

ESS coating workshop in Wahlbecks Företagspark

Plans for the Workshop

<u>The new deposition system</u>
- Only used for $^{10}B_4C$ for neutron detectors
- Fulfills needs for ESS (6000 m^2)

9/2013: Turn-key contract signed
6/2014: Delivery to Linköping

<u>Plan for production:</u>

2014: 150 m^2 of $^{10}B_4C$

2015: 450 m^2 of $^{10}B_4C$

From 2016: >600 m^2 of $^{10}B_4C$ per year

CEMECON 3-axis planetary rotation PVD magnetron sputtering

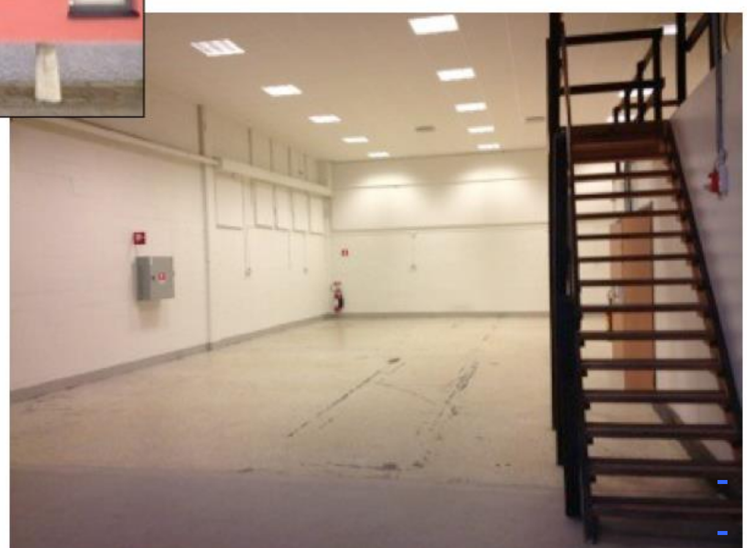

Staff:
- Production engineer
- 1 workman (Q4, 2014)
- Carina Höglund ~50%
- Luis Ortega ~50% (until June)

- Boron targets: RHP technology, Austria
- enriched material: Ceradyne, US

University of Perugia

Institut Laue-Langevin

^{10}B layers
and
Thermal Neutron Gaseous Detectors

Francesco Piscitelli

Francesco Piscitelli, "Boron-10 layers, Neutron Reflectometry and Thermal Neutron Gaseous Detectors", PhD thesis (2014) Uni Perugia/ILL. http://arxiv.org/abs/1406.3133

^{10}B-based Neutron Detectors

$$
\begin{aligned}
{}^{10}B + n \rightarrow {}^{7}Li^{*} + {}^{4}He \rightarrow {}^{7}Li + {}^{4}He + 0.48MeV\,\gamma\text{-ray} + 2.3\ \ MeV \quad (94\%) \\
\rightarrow {}^{7}Li + {}^{4}He \qquad\qquad\qquad\qquad + 2.79\,MeV \quad (6\%)
\end{aligned}
$$

^{10}B

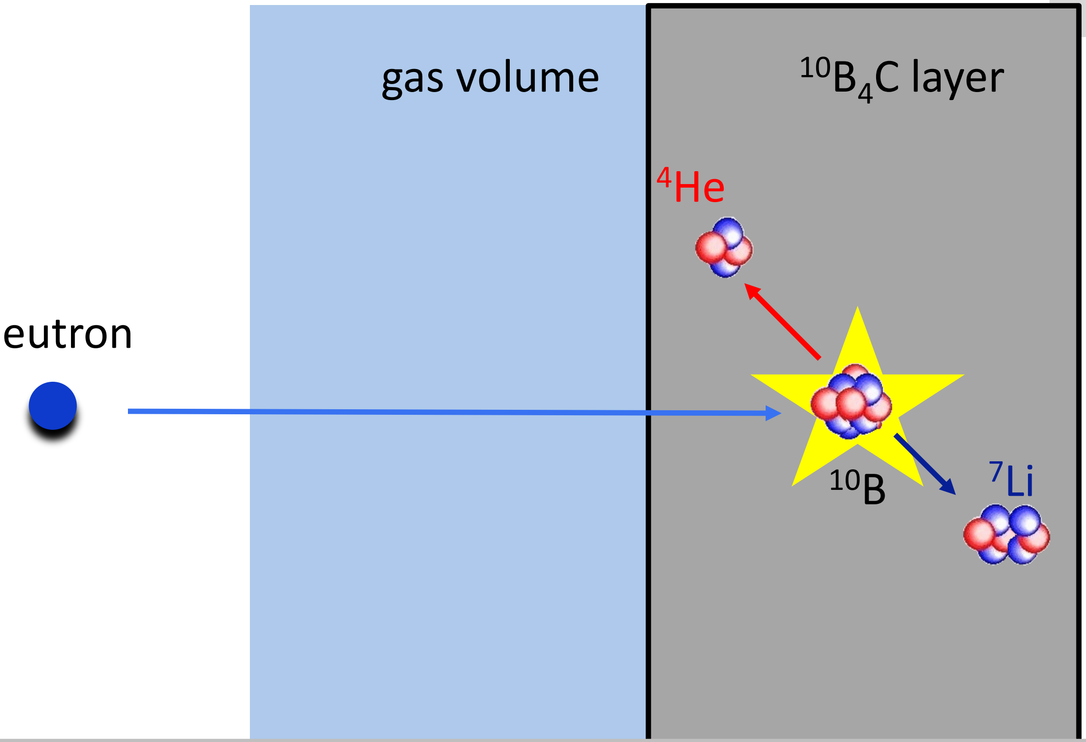

^{10}B-based Neutron Detectors

$$\begin{aligned} {}^{10}B + n \rightarrow {}^{7}Li^{*} + {}^{4}He \rightarrow {}^{7}Li + {}^{4}He + 0.48 MeV\, \gamma\text{-ray} &+ 2.3\ \ MeV \quad (94\%) \\ \rightarrow {}^{7}Li + {}^{4}He \qquad\qquad\qquad\qquad &+ 2.79\, MeV \quad (6\%) \end{aligned}$$

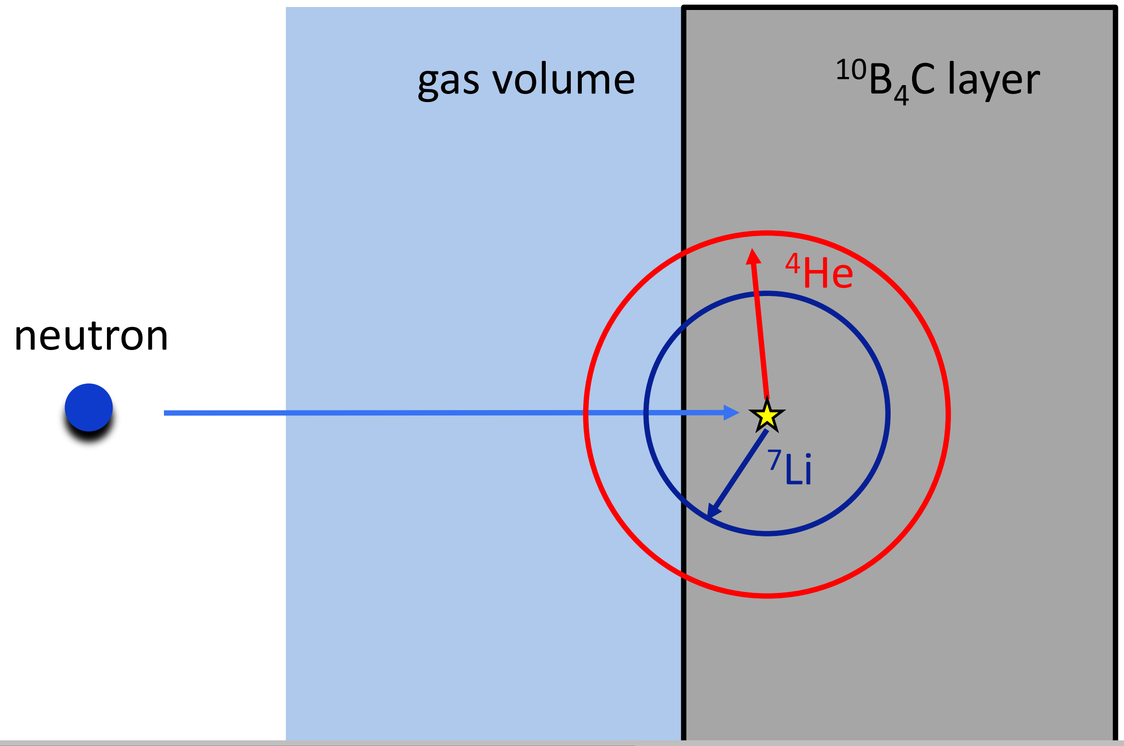

^{10}B-based Neutron Detectors

$$
\begin{aligned}
{}^{10}B + n \rightarrow {}^{7}Li^{*} + {}^{4}He \rightarrow {}^{7}Li + {}^{4}He + 0.48 MeV\,\gamma\text{-ray} + 2.3\ \ MeV \quad (94\%) \\
\rightarrow {}^{7}Li + {}^{4}He \qquad\qquad\qquad + 2.79\,MeV \quad (6\%)
\end{aligned}
$$

Efficiency limited at ~5% (2.5Å) for a single layer

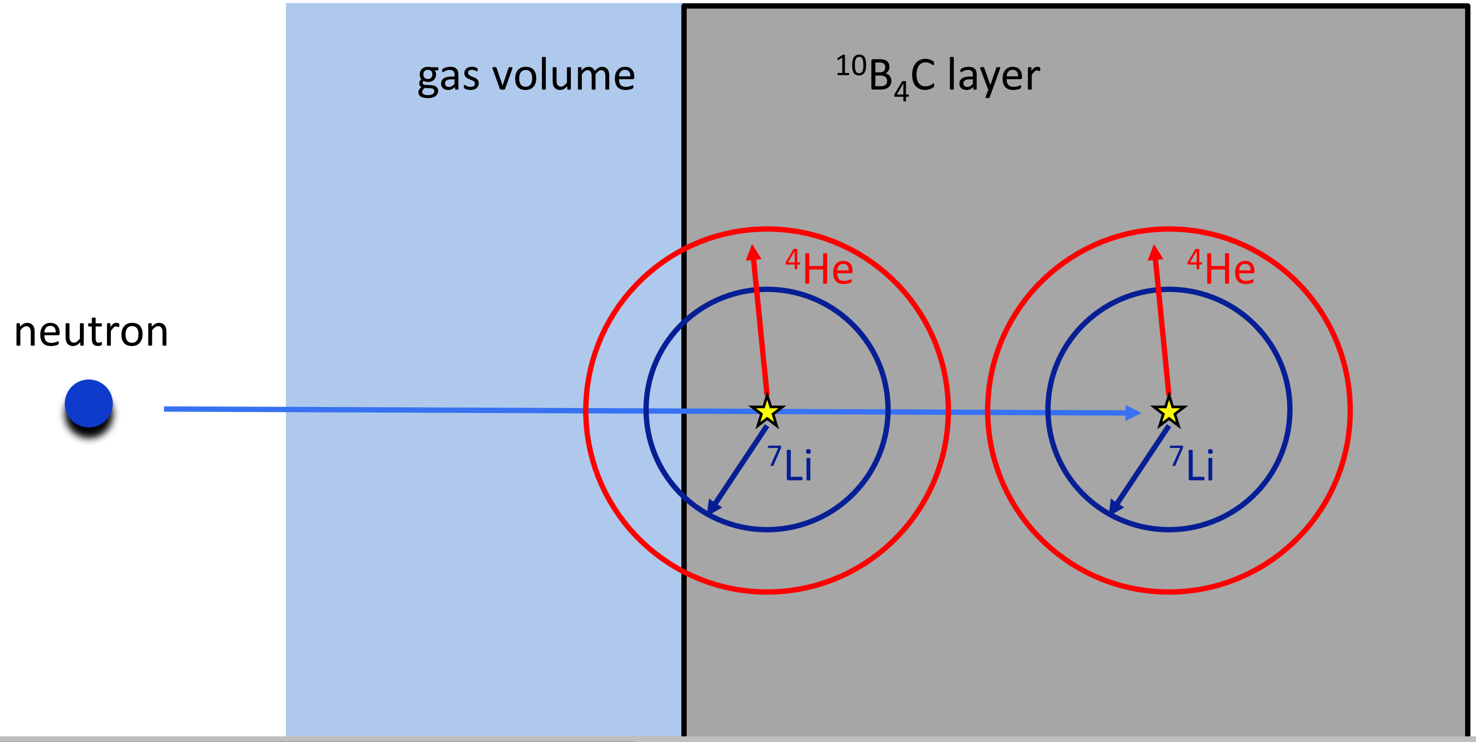

^{10}B-based Neutron Detectors

① Multi-Grid

Multi layer

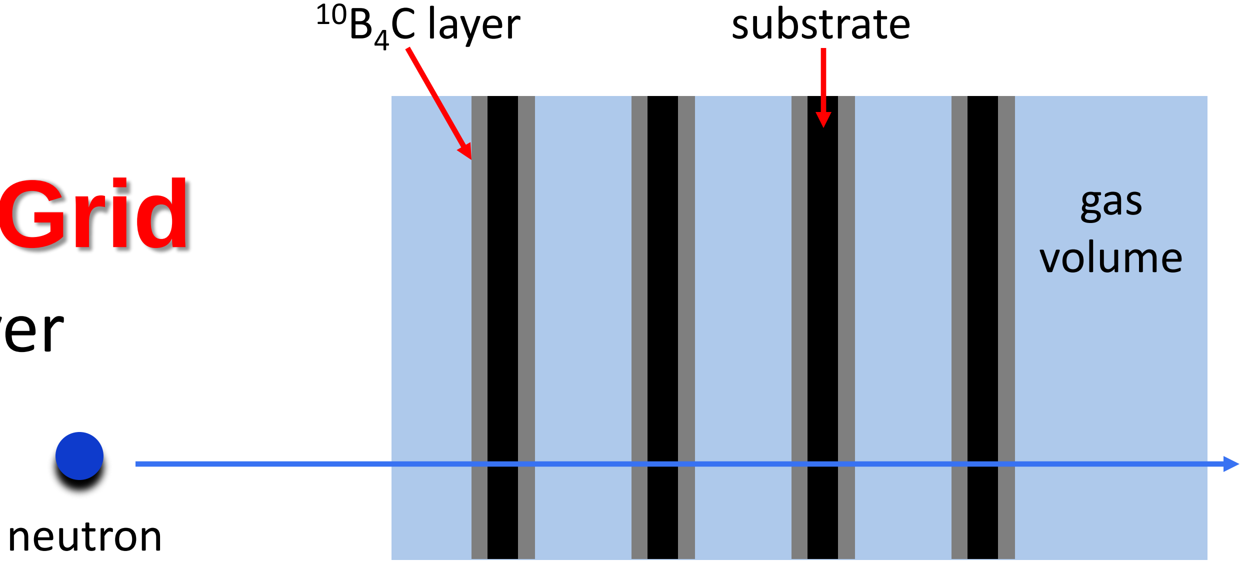

② Multi-Blade

Grazing angle (<10˚)

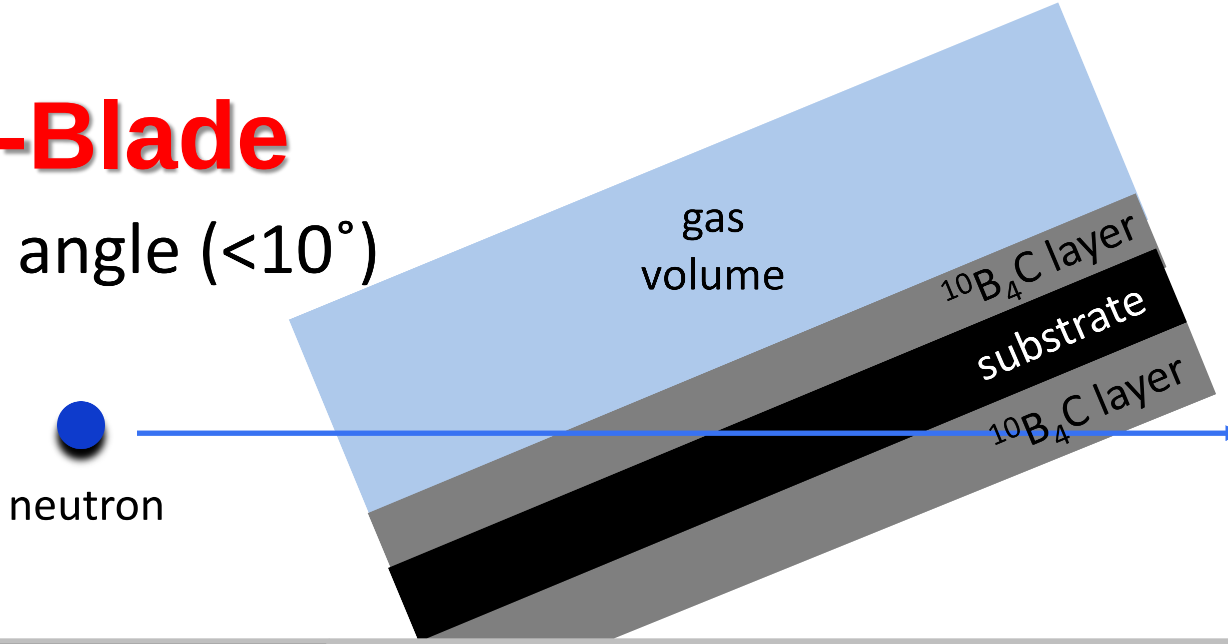

^{10}B-based Neutron Detectors: Efficiency Optimization

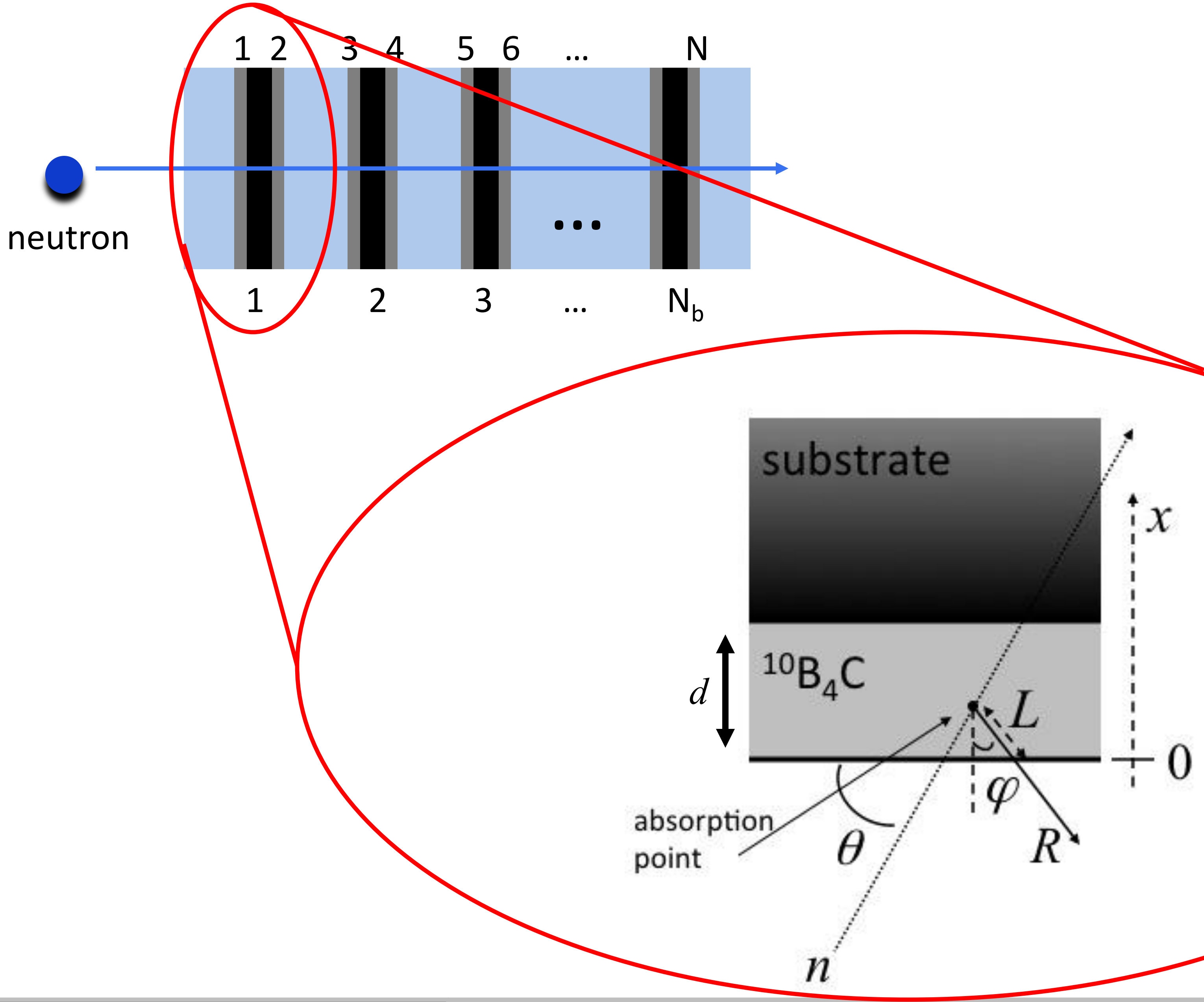

^{10}B-based Neutron Detectors: Efficiency Optimization

efficiency

$$\varepsilon_T(d) = \int_0^d dy K(d-y)\xi(y) = \int_0^d dy \Sigma e^{-(d-y)\Sigma}\left(1 - \frac{y}{2R_1} - \frac{y}{2R_2}\right) =$$

$$= \left(1 + \frac{1}{2\Sigma R_1} + \frac{1}{2\Sigma R_2}\right)\left(1 - e^{-d\Sigma}\right) - \left(\frac{1}{2R_1} + \frac{1}{2R_2}\right) d$$

$$\xi(x) = \begin{cases} \frac{1}{2}\left(2 - \frac{x}{R_1} - \frac{x}{R_2}\right) & \text{if} \quad x \le R_2 < R_1 \\ \frac{1}{2}\left(1 - \frac{x}{R_1}\right) & \text{if} \quad R_2 < x \le R_1 \\ 0 & \text{if} \quad R_2 < R_1 < x \end{cases}$$

$$\Sigma(\lambda, \theta) = n \cdot \frac{\sigma(\lambda)}{\sin(\theta)} = n \cdot \sigma_{1A} \cdot \frac{\lambda}{\sin(\theta)}$$

$$K(x, \lambda) = \Sigma e^{-x\Sigma(\lambda)}$$

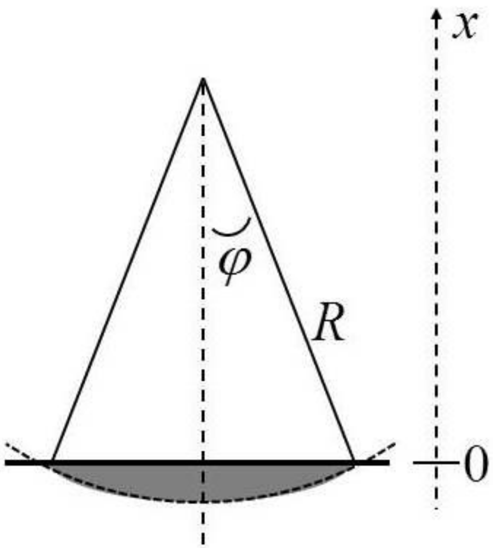

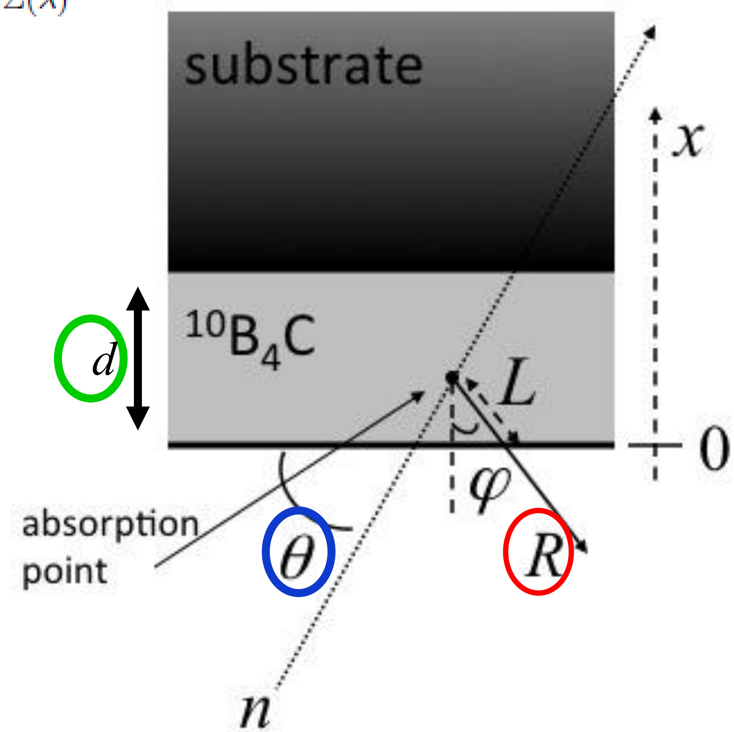

F. Piscitelli and P. Van Esch, JINST, v. 8, p. 04020, 2013

^{10}B-based Neutron Detectors: Multi-Grid Efficiency Optimization

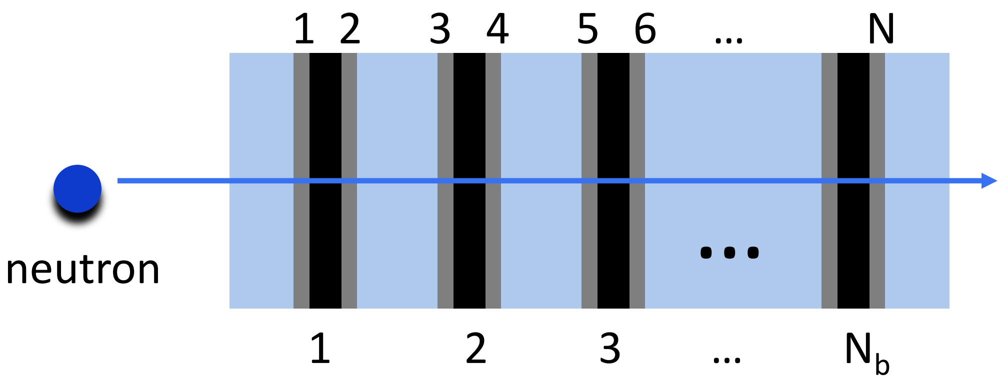

efficiency

$$\varepsilon_{tot}(N_b) = \varepsilon_1(d) + \sum_{k=2}^{N_b} \varepsilon_1(d)\cdot e^{-2\left(\sum_{j=1}^{(k-1)} d\right)\cdot\Sigma} = \varepsilon_1(d)\cdot\sum_{k=1}^{N_b} e^{-2(k-1)d\cdot\Sigma} = \varepsilon_1(d)\cdot\frac{1-e^{-2d\Sigma N_b}}{1-e^{-2d\Sigma}}$$

Monochromatic beam,
Wavelength distribution,
Substrate effects,
Blade-by-blade optimization,
…

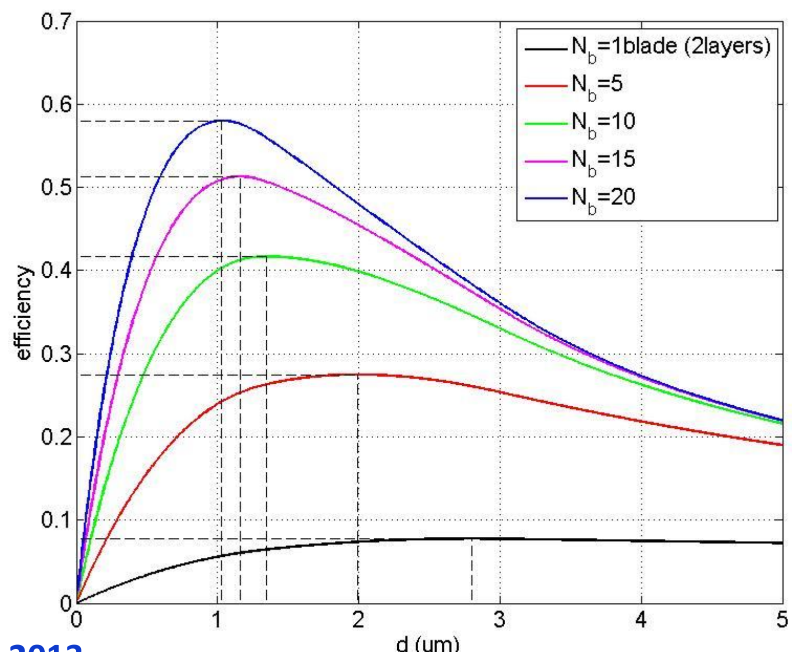

(Θ=90˚, 1.8Å)

F. Piscitelli and P. Van Esch, JINST, v. 8, p. 04020, 2013

^{10}B-based Neutron Detectors: Efficiency Optimization

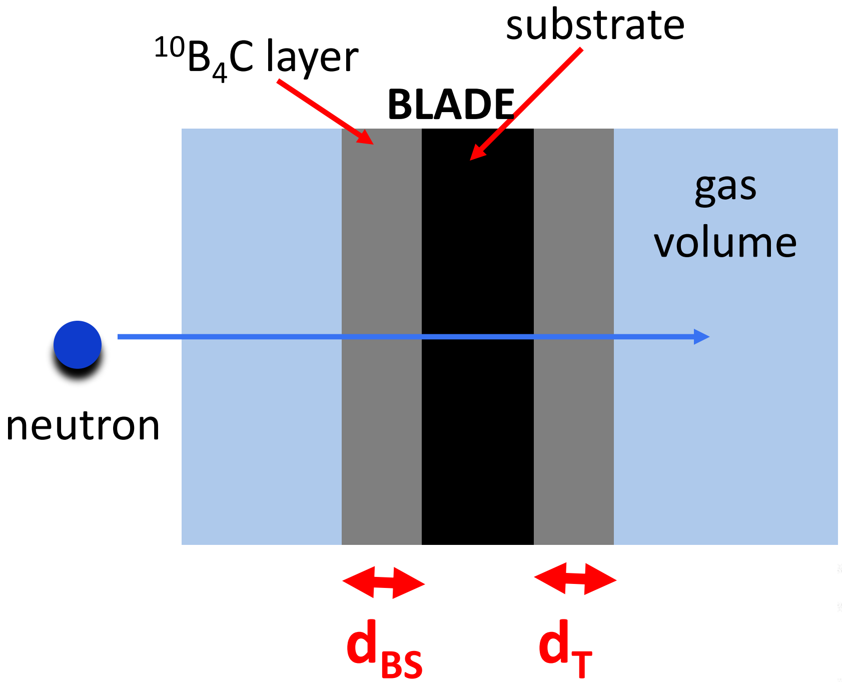

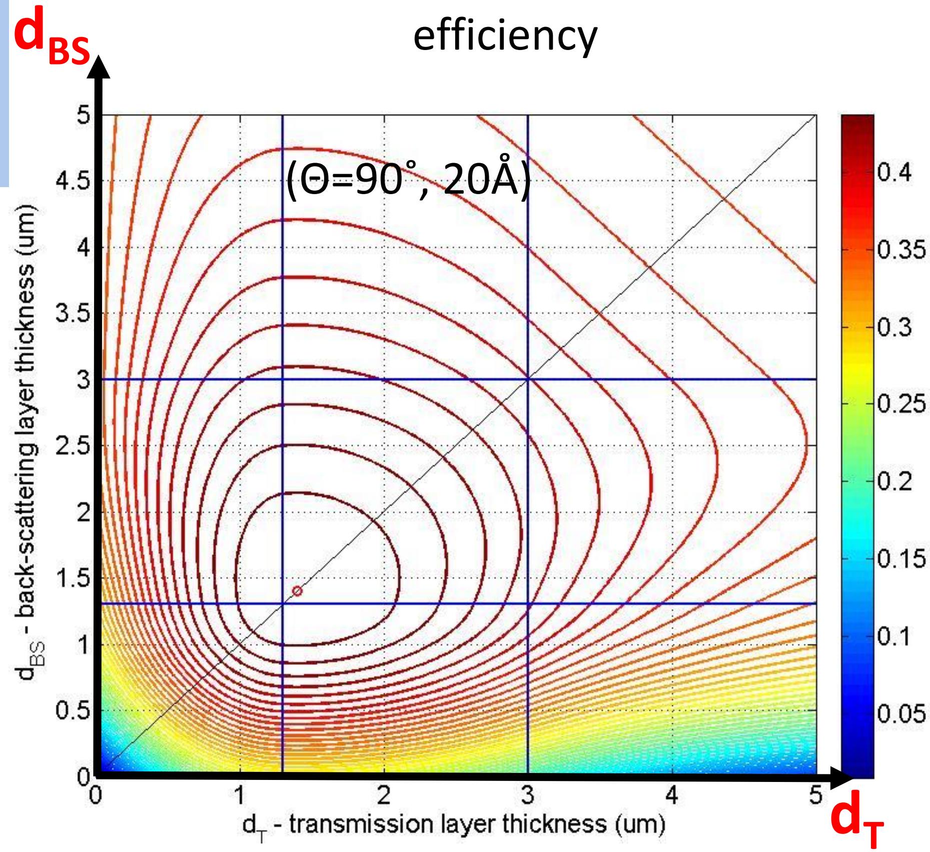

F. Piscitelli and P. Van Esch, JINST, v. 8, p. 04020, 2013

^{10}B-based Neutron Detectors: Efficiency Optimization

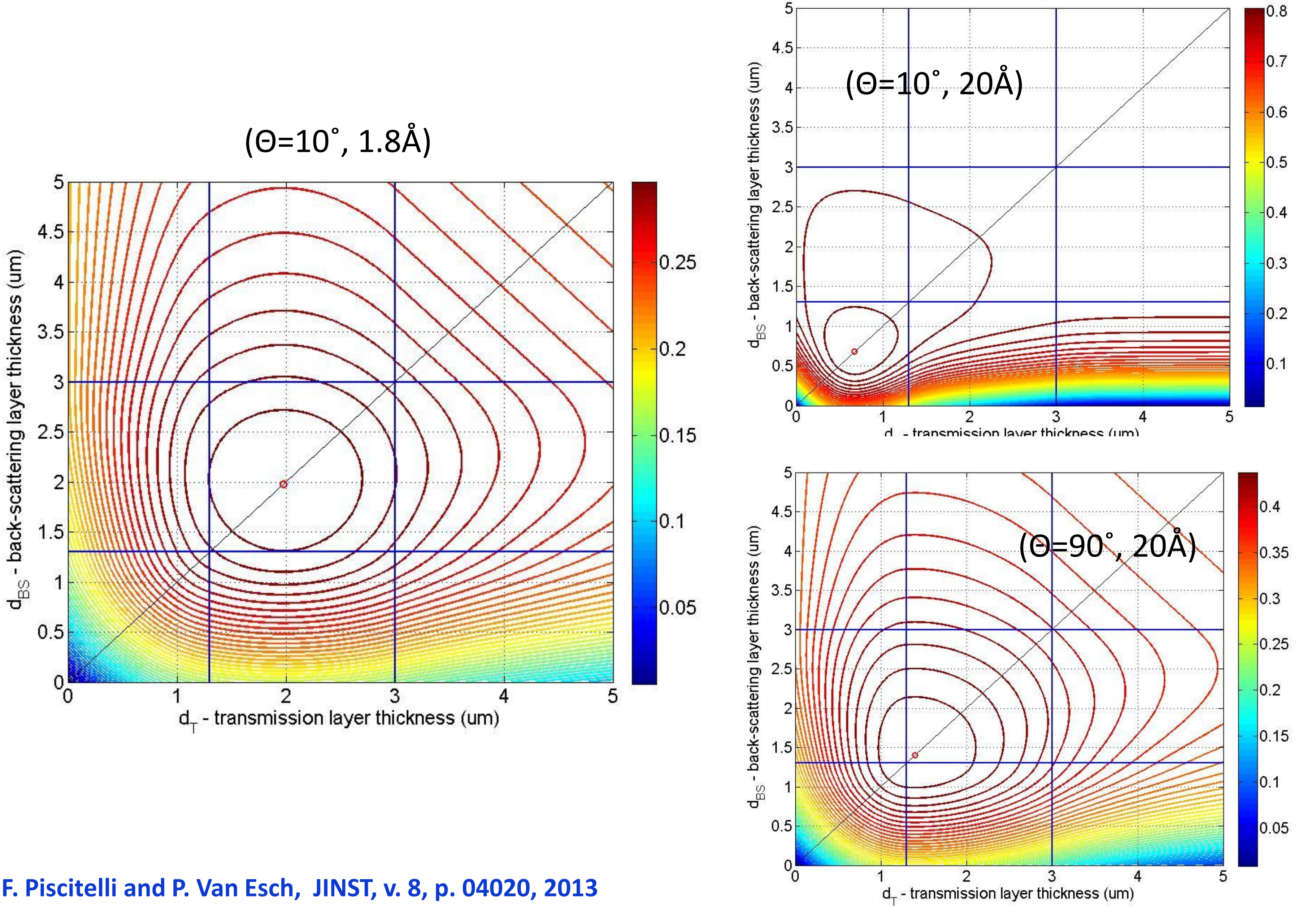

F. Piscitelli and P. Van Esch, JINST, v. 8, p. 04020, 2013

Analytical calculations

^{10}B-based Neutron Detectors: Pulse Height Spectrum

Energy distribution of the fragments

$$
\begin{aligned}
{}^{10}B + n \rightarrow {}^{7}Li^{*} + {}^{4}He \rightarrow {}^{7}Li + {}^{4}He + 0.48MeV\,\gamma\text{-ray} + 2.3\ \ MeV \quad (94\%) \\
\rightarrow {}^{7}Li + {}^{4}He \qquad\qquad\qquad\qquad + 2.79\,MeV \quad (6\%)
\end{aligned}
$$

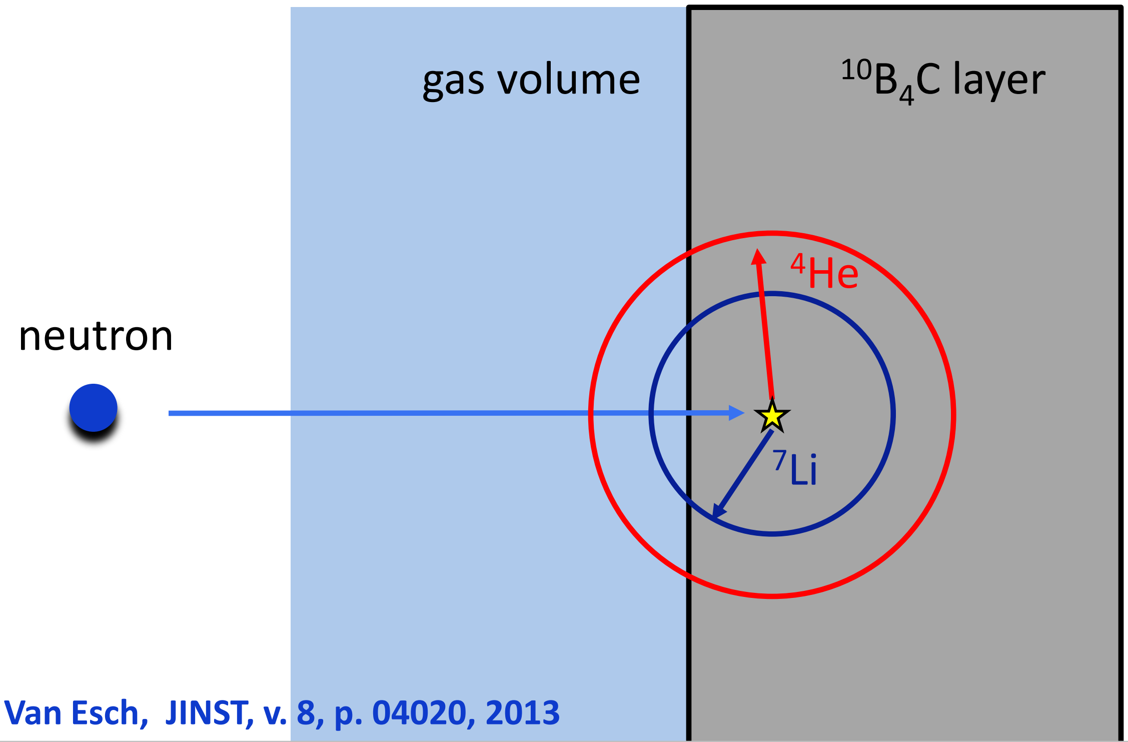

F. Piscitelli and P. Van Esch, JINST, v. 8, p. 04020, 2013

^{10}B-based Neutron Detectors: Pulse Height Spectrum

Energy distribution of the fragments

$$
\begin{aligned}
{}^{10}B + n \rightarrow {}^{7}Li^{*} + {}^{4}He &\rightarrow {}^{7}Li + {}^{4}He + 0.48 MeV \gamma\text{-ray} + 2.3 \ MeV \quad (94\%) \\
&\rightarrow {}^{7}Li + {}^{4}He \qquad\qquad\qquad\qquad + 2.79 MeV \quad (6\%)
\end{aligned}
$$

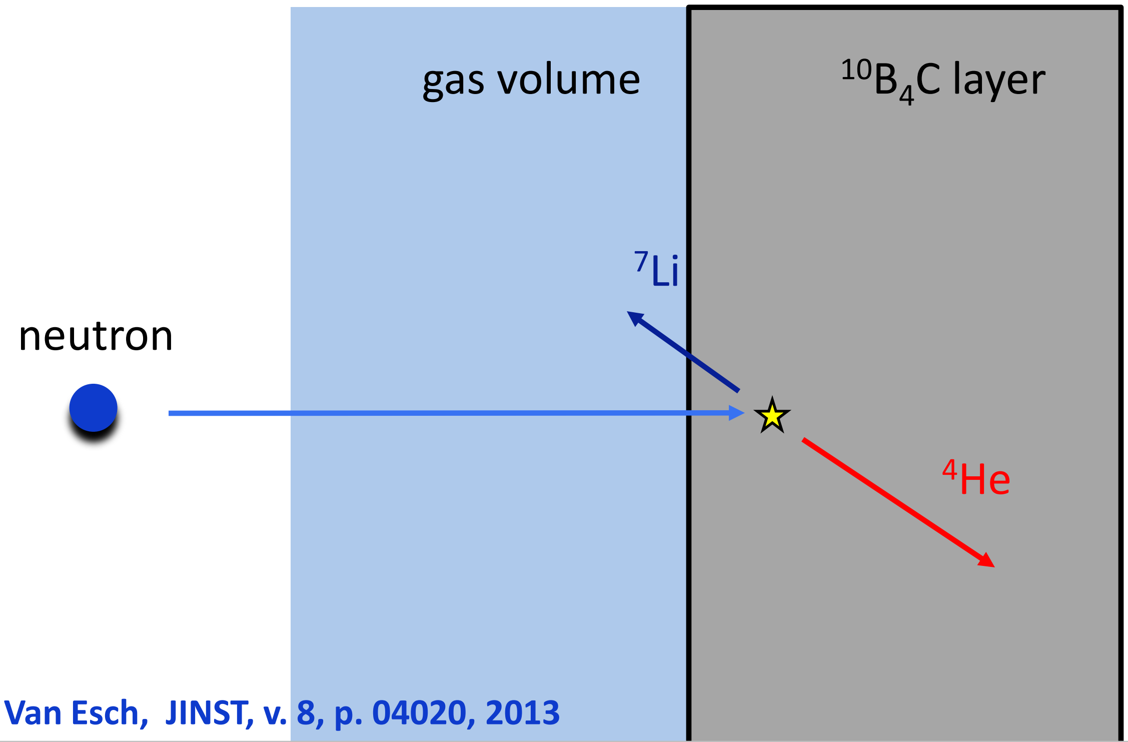

F. Piscitelli and P. Van Esch, JINST, v. 8, p. 04020, 2013

^{10}B-based Neutron Detectors: Pulse Height Spectrum

Energy distribution of the fragments

$$
\begin{aligned}
{}^{10}B + n \rightarrow {}^{7}Li^{*} + {}^{4}He &\rightarrow {}^{7}Li + {}^{4}He + 0.48 MeV\,\gamma\text{-ray} + 2.3 \;\; MeV \quad (94\%) \\
&\rightarrow {}^{7}Li + {}^{4}He \qquad\qquad\qquad\qquad\quad + 2.79\, MeV \quad (6\%)
\end{aligned}
$$

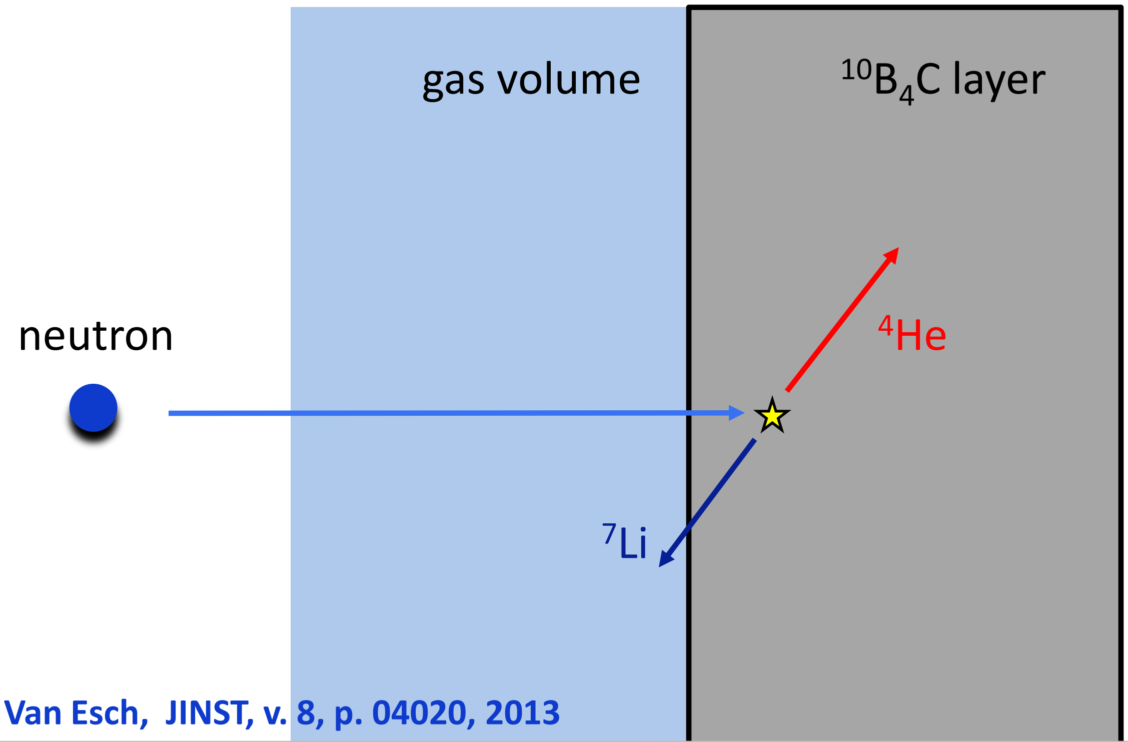

F. Piscitelli and P. Van Esch, JINST, v. 8, p. 04020, 2013

^{10}B-based Neutron Detectors: Pulse Height Spectrum

Energy distribution of the fragments

$$
\begin{aligned}
{}^{10}B + n \rightarrow {}^{7}Li^{*} + {}^{4}He &\rightarrow {}^{7}Li + {}^{4}He + 0.48 MeV\,\gamma\text{-ray} + 2.3\ \ MeV \quad (94\%) \\
&\rightarrow {}^{7}Li + {}^{4}He \qquad\qquad\qquad\qquad + 2.79\,MeV \quad (6\%)
\end{aligned}
$$

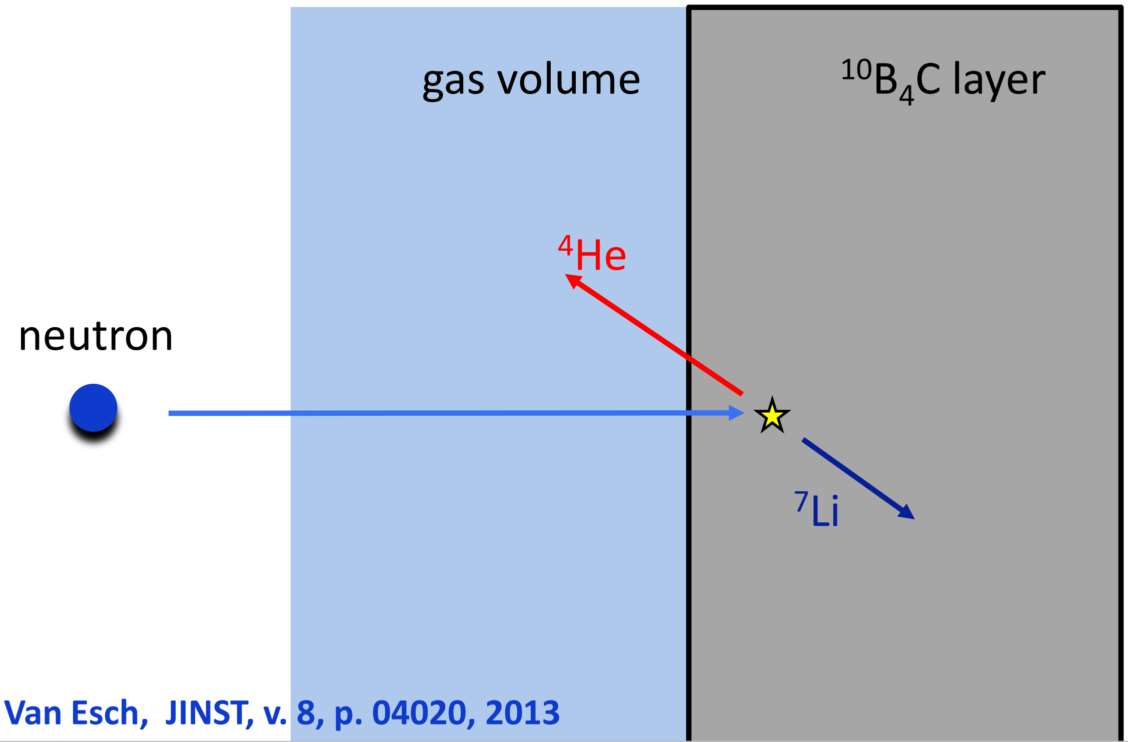

F. Piscitelli and P. Van Esch, JINST, v. 8, p. 04020, 2013

^{10}B-based Neutron Detectors: Pulse Height Spectrum

Energy distribution of the fragments

$$\begin{aligned} {}^{10}B + n \rightarrow {}^{7}Li^{*} + {}^{4}He \rightarrow {}^{7}Li + {}^{4}He + 0.48MeV\,\gamma\text{-ray} + 2.3\ \ MeV \quad (94\%) \\ \rightarrow {}^{7}Li + {}^{4}He \qquad\qquad\qquad\qquad + 2.79\,MeV \quad (6\%) \end{aligned}$$

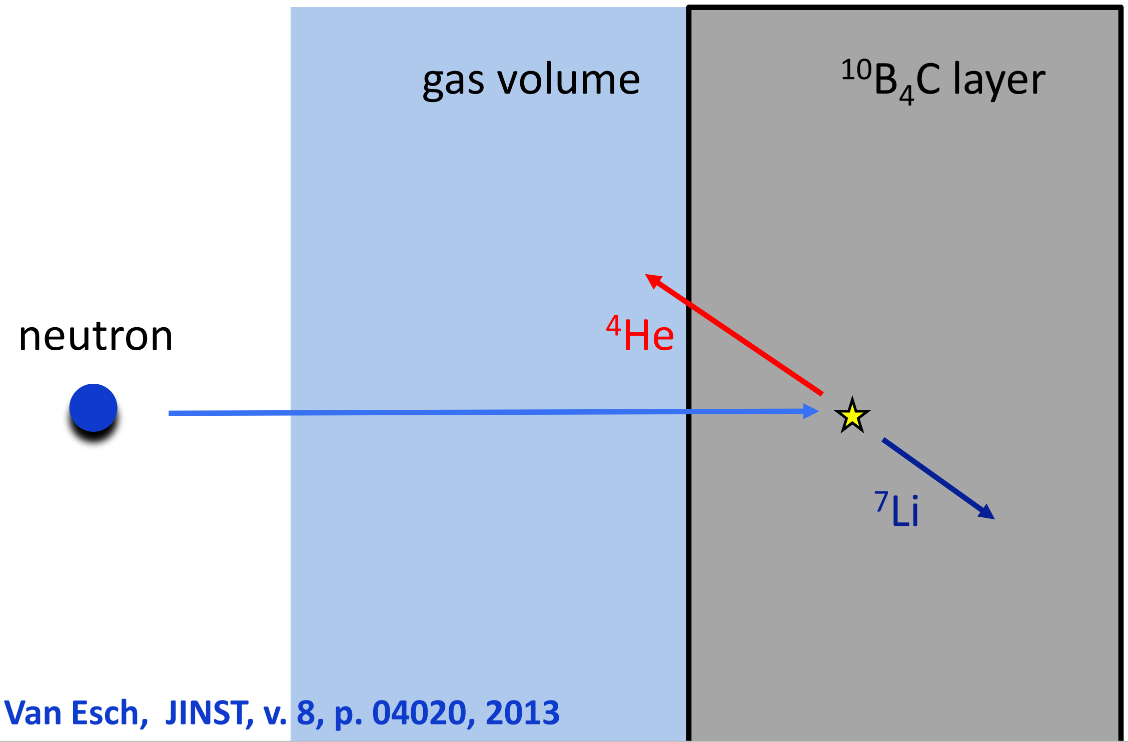

F. Piscitelli and P. Van Esch, JINST, v. 8, p. 04020, 2013

^{10}B-based Neutron Detectors: Pulse Height Spectrum

Energy distribution of the fragments

$$P(L)\,dL = \int_0^d \int_0^1 \delta\left(\frac{x}{u} - L\right) p(x,u)\,dx du = \frac{\Sigma}{2L^2}\int_0^d dx\, x e^{-\Sigma\cdot x}\int_0^1 du\,\delta\left(u - \frac{x}{L}\right) =$$

$$= \frac{\Sigma}{2L^2}\int_0^d dx\, x e^{-\Sigma\cdot x}\left(H(x) - H(x-L)\right) = \begin{cases} \frac{1}{2L^2}\left(\frac{1}{\Sigma} - (\frac{1}{\Sigma} + L)e^{-\Sigma\cdot L}\right) dL & \text{if } L \le d \\ \frac{1}{2L^2}\left(\frac{1}{\Sigma} - (\frac{1}{\Sigma} + d)e^{-\Sigma\cdot d}\right) dL & \text{if } L > d \end{cases}$$

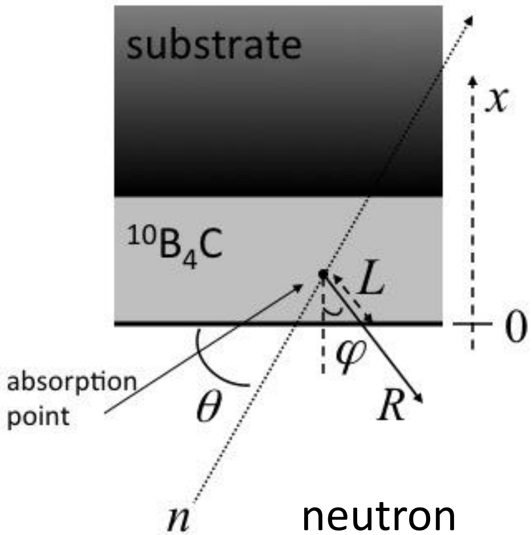

$$Q(E)dE = P(L(E)) \cdot \frac{1}{\left|\frac{dE}{dL}\right|}\cdot dE$$

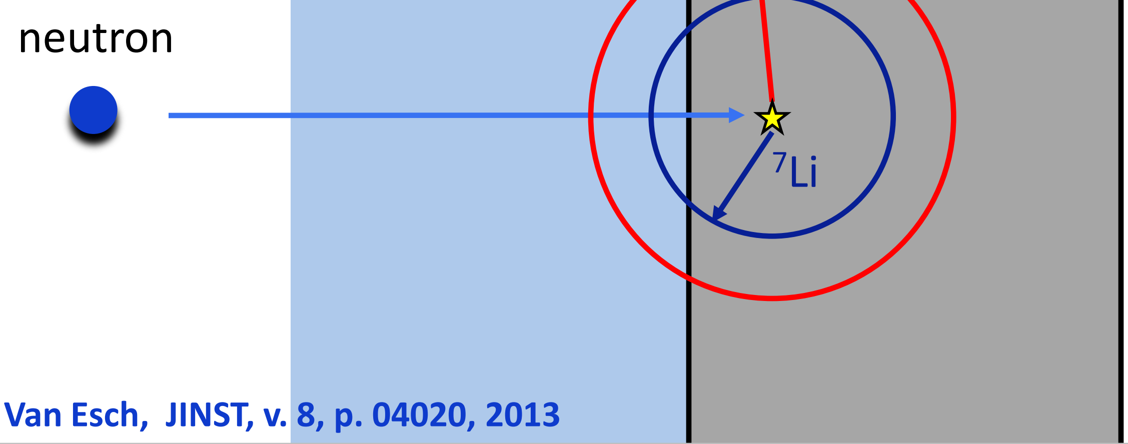

F. Piscitelli and P. Van Esch, JINST, v. 8, p. 04020, 2013

^{10}B-based Neutron Detectors: Pulse Height Spectrum

Energy distribution of the fragments

$$P(L)\,dL = \int_0^d \int_0^1 \delta\left(\frac{x}{u} - L\right) p(x,u)\,dx du = \frac{\Sigma}{2L^2}\int_0^d dx\, x e^{-\Sigma\cdot x}\int_0^1 du\,\delta\left(u - \frac{x}{L}\right) =$$

$$= \frac{\Sigma}{2L^2}\int_0^d dx\, x e^{-\Sigma\cdot x}\left(H(x) - H(x-L)\right) = \begin{cases} \frac{1}{2L^2}\left(\frac{1}{\Sigma} - \left(\frac{1}{\Sigma} + L\right)e^{-\Sigma\cdot L}\right) dL & \text{if } L \le d \\ \frac{1}{2L^2}\left(\frac{1}{\Sigma} - \left(\frac{1}{\Sigma} + d\right)e^{-\Sigma\cdot d}\right) dL & \text{if } L > d \end{cases}$$

$$Q(E)dE = P(L(E)) \cdot \frac{1}{\left|\frac{dE}{dL}\right|} \cdot dE$$

Calculated

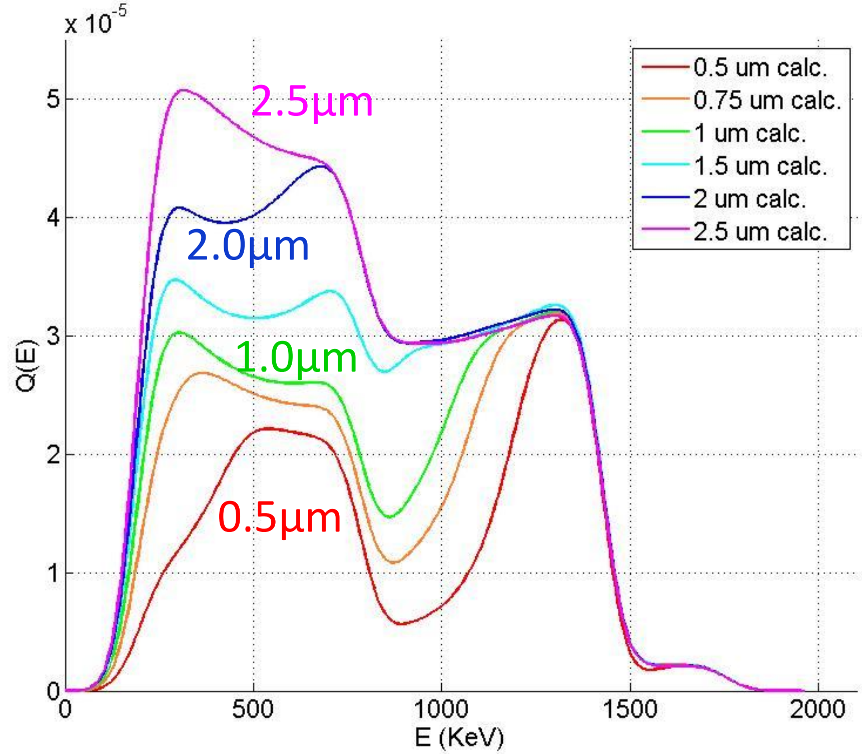

F. Piscitelli and P. Van Esch, JINST, v. 8, p. 04020, 2013

^{10}B-based Neutron Detectors: Pulse Height Spectrum

Energy distribution of the fragments

$$P(L)\,dL = \int_0^d \int_0^1 \delta\left(\frac{x}{u} - L\right) p(x,u)\,dx du = \frac{\Sigma}{2L^2}\int_0^d dx\, x e^{-\Sigma \cdot x} \int_0^1 du\, \delta\left(u - \frac{x}{L}\right) =$$

$$= \frac{\Sigma}{2L^2}\int_0^d dx\, x e^{-\Sigma \cdot x}\left(H(x) - H(x-L)\right) = \begin{cases} \frac{1}{2L^2}\left(\frac{1}{\Sigma} - (\frac{1}{\Sigma} + L)e^{-\Sigma \cdot L}\right) dL & \text{if } L \leq d \\ \frac{1}{2L^2}\left(\frac{1}{\Sigma} - (\frac{1}{\Sigma} + d)e^{-\Sigma \cdot d}\right) dL & \text{if } L > d \end{cases}$$

$$Q(E)dE = P(L(E)) \cdot \frac{1}{\left|\frac{dE}{dL}\right|} \cdot dE$$

Calculated
&
Measured

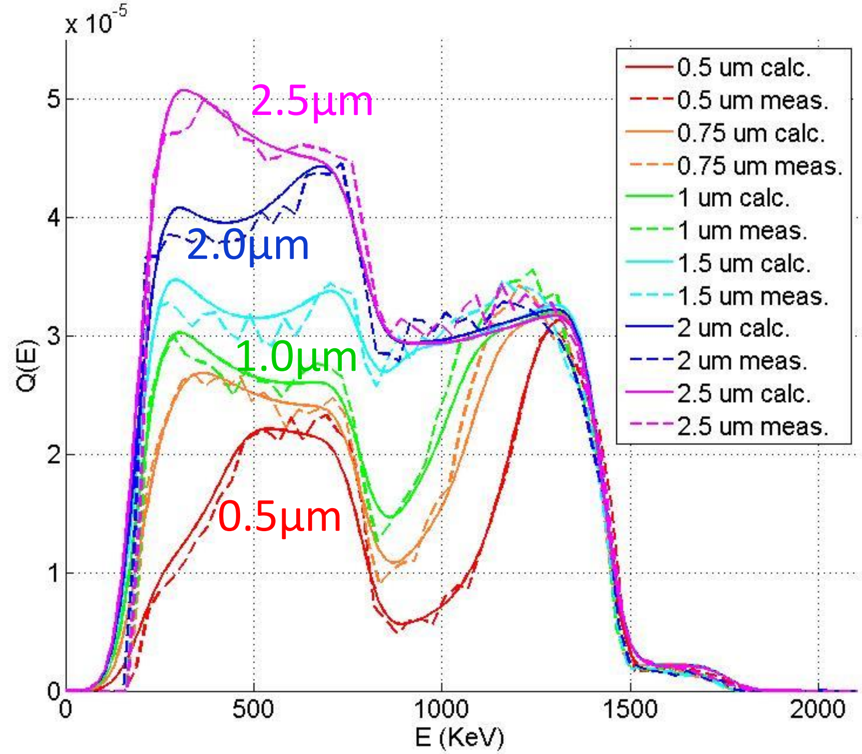

F. Piscitelli and P. Van Esch, JINST, v. 8, p. 04020, 2013

^{10}B-based Neutron Detectors: Pulse Height Spectrum

Energy distribution of the fragments

$$
\begin{aligned}
{}^{10}B + n \rightarrow {}^{7}Li^{*} + {}^{4}He \rightarrow {}^{7}Li + {}^{4}He + 0.48MeV\,\gamma\text{-ray} &+ 2.3\ \ MeV \quad (94\%) \\
\rightarrow {}^{7}Li + {}^{4}He \qquad\qquad\qquad &+ 2.79\,MeV \quad (6\%)
\end{aligned}
$$

$$Q(E)dE = P(L(E)) \cdot \frac{1}{\left|\frac{dE}{dL}\right|} \cdot dE$$

Calculated
&
Measured

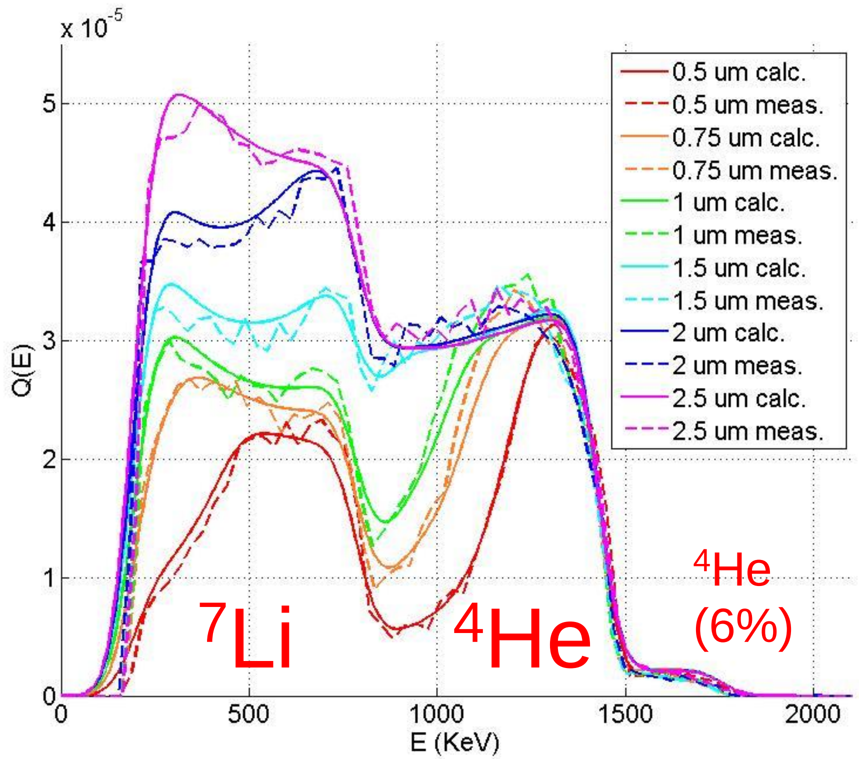

F. Piscitelli and P. Van Esch, JINST, v. 8, p. 04020, 2013

^{10}B-based Neutron Detectors: Gamma Sensitivity

A. Khaplanov , F. Piscitelli et al., JINST, v. 8, p. 10025, 2013

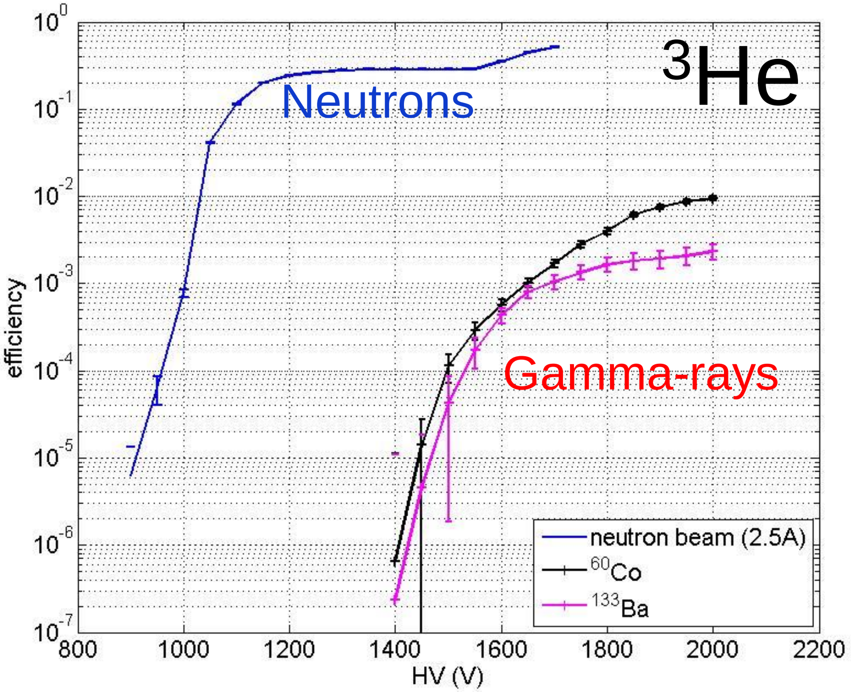

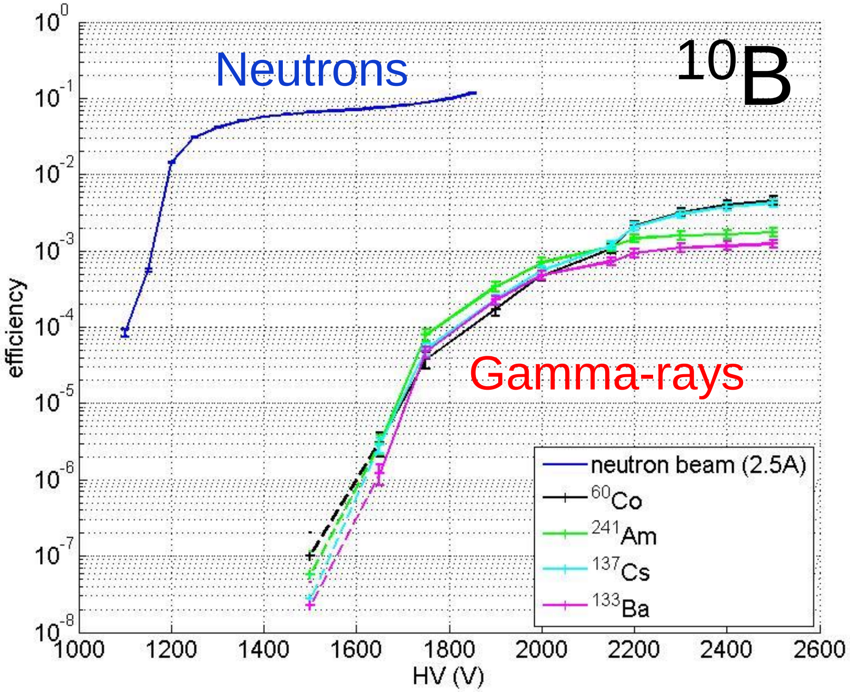

^{10}B-based Neutron Detectors: Gamma Sensitivity

A. Khaplanov , F. Piscitelli et al., JINST, v. 8, p. 10025, 2013

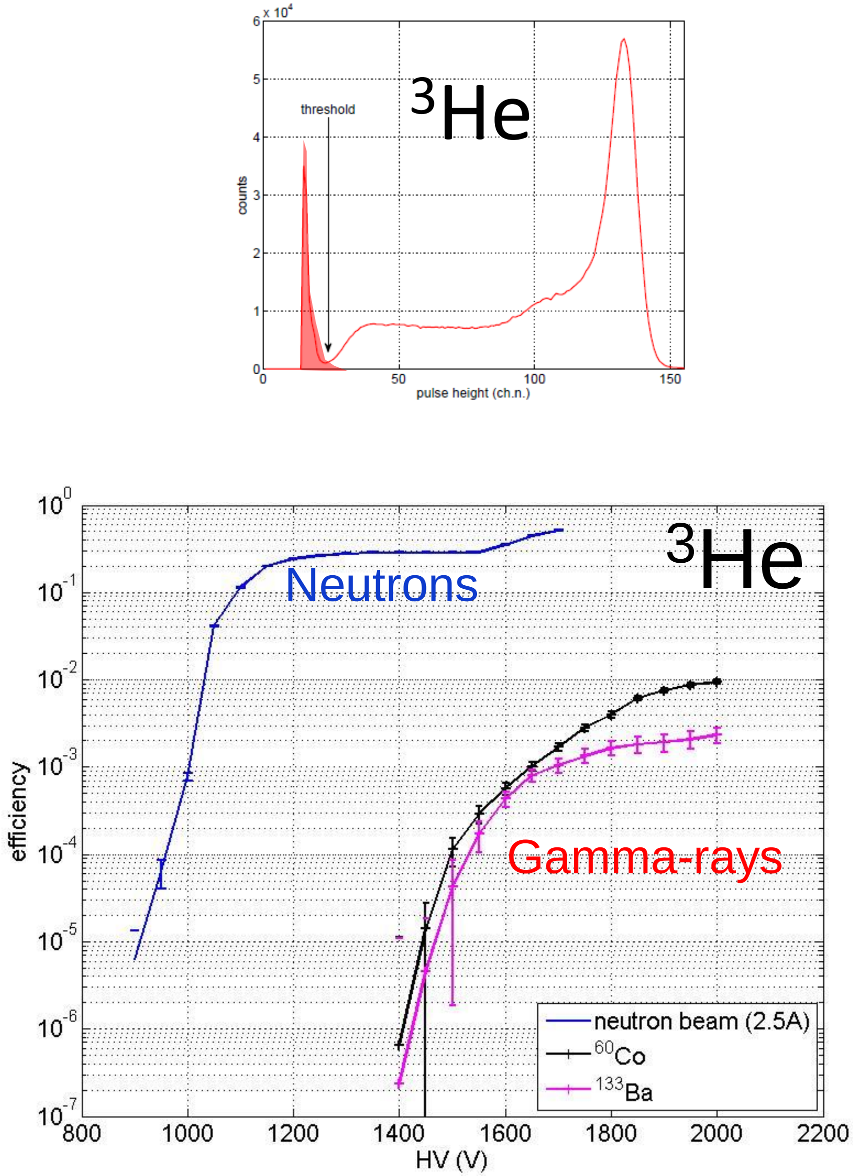

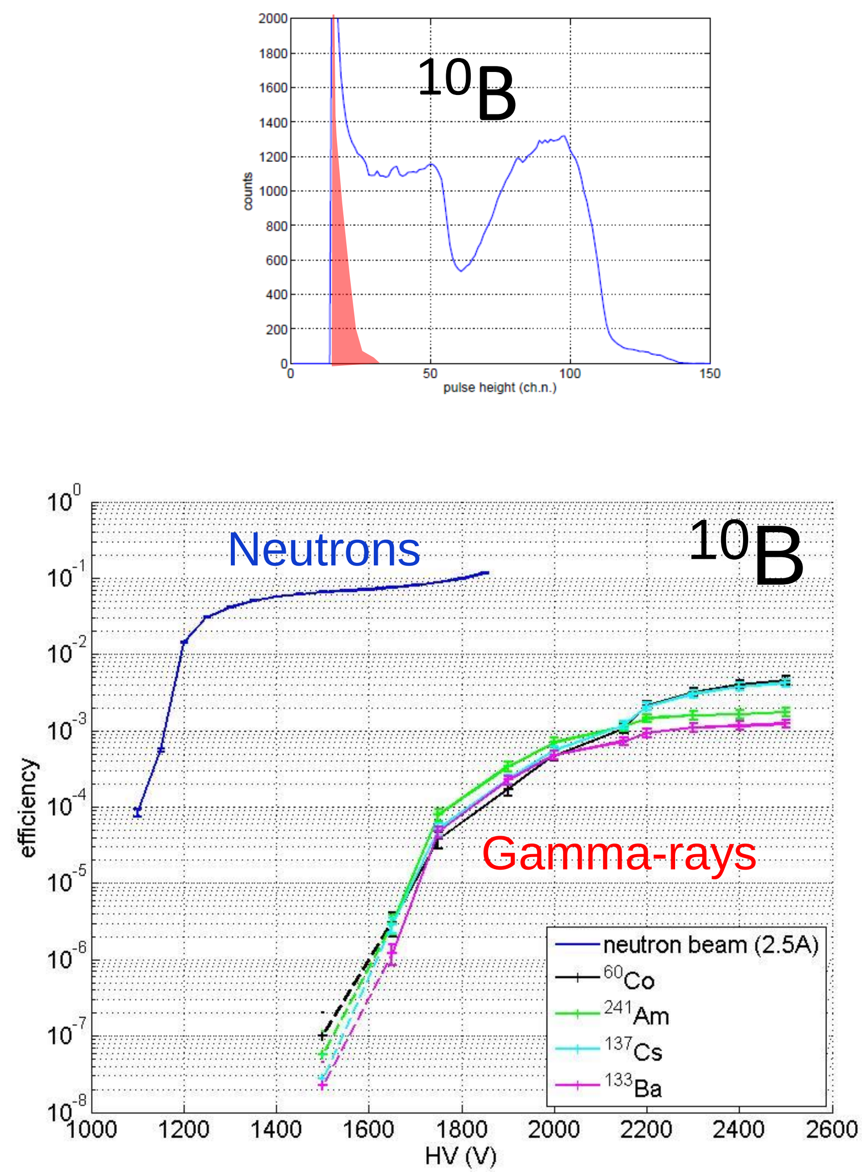

^{10}B-based Neutron Detectors: Gamma Sensitivity

A. Khaplanov , F. Piscitelli et al., JINST, v. 8, p. 10025, 2013

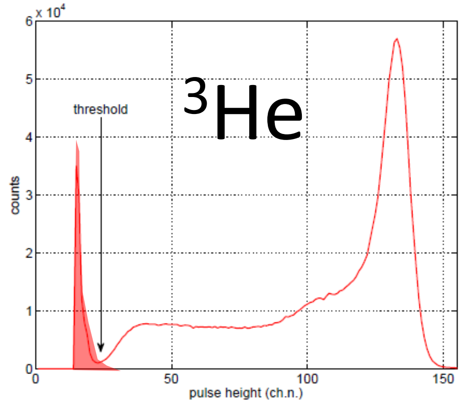

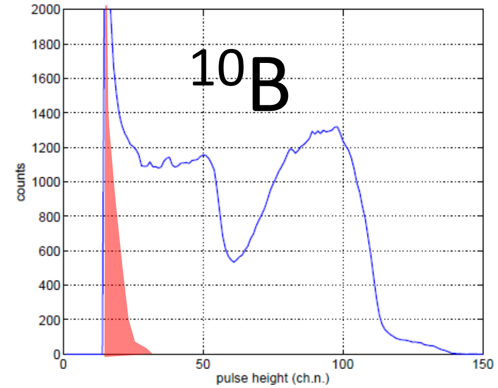

<10^-6

<10^-6

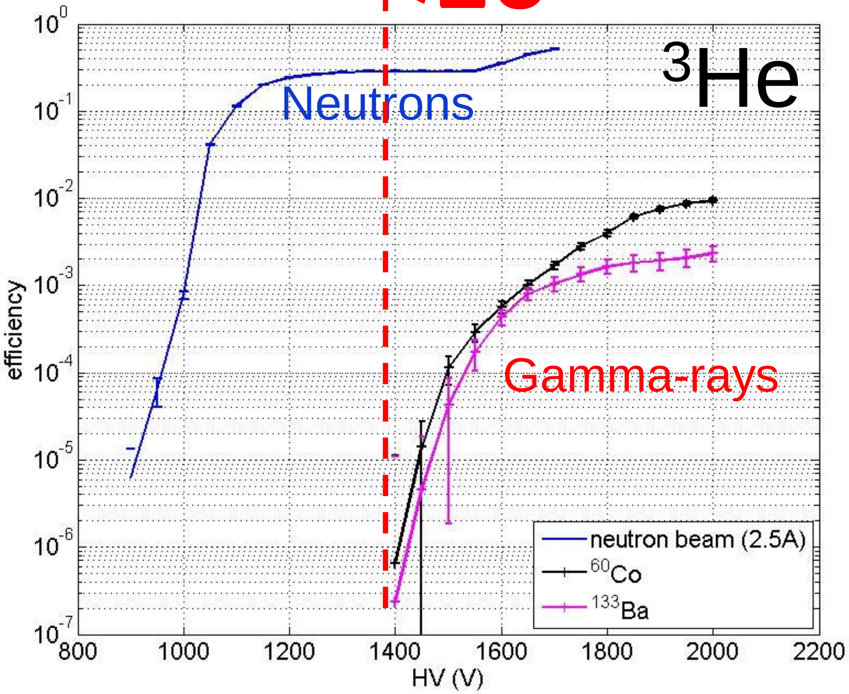

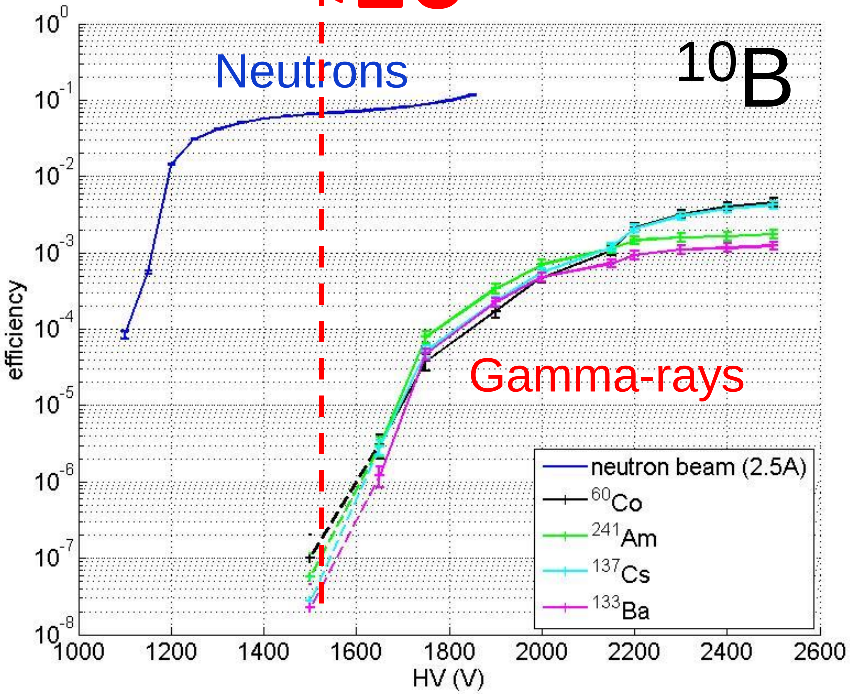

2

Multi-Blade

Grazing angle (<10˚)

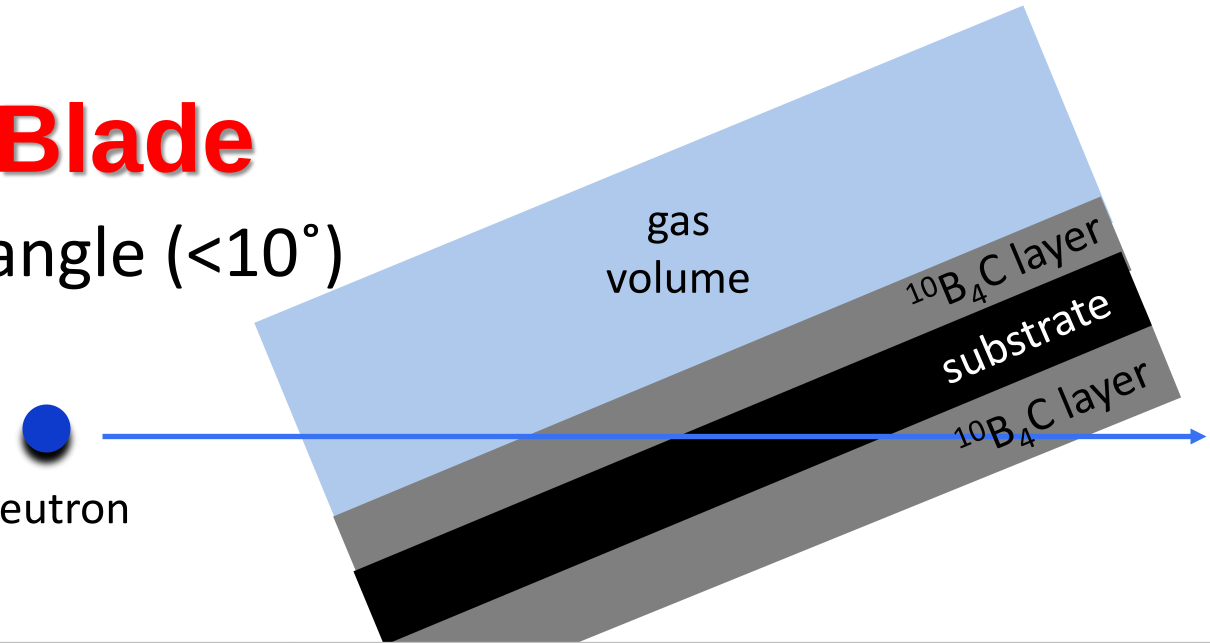

^{10}B-based Neutron Detectors

$$
\begin{array}{lr}
{}^{10}B + n \rightarrow {}^{7}Li^{*} + {}^{4}He \rightarrow {}^{7}Li + {}^{4}He + 0.48 MeV \gamma\text{-ray} + 2.3 \;\; MeV & (94\%) \\
\rightarrow {}^{7}Li + {}^{4}He \qquad\qquad\qquad\qquad + 2.79 MeV & (6\%)
\end{array}
$$

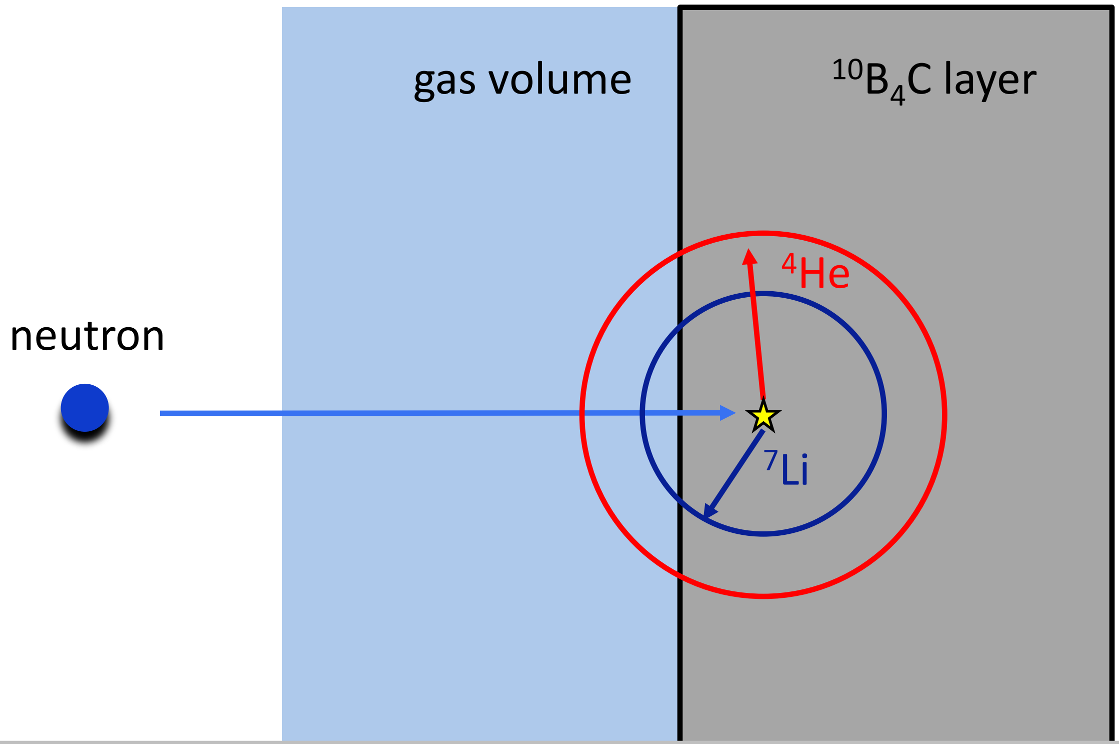

^{10}B-based Neutron Detectors

$$
\begin{aligned}
{}^{10}B + n \rightarrow {}^{7}Li^{*} + {}^{4}He \rightarrow {}^{7}Li + {}^{4}He + 0.48 MeV \gamma\text{-ray} + 2.3 \ \ MeV \quad (94\%) \\
\rightarrow {}^{7}Li + {}^{4}He \quad + 2.79 MeV \quad (6\%)
\end{aligned}
$$

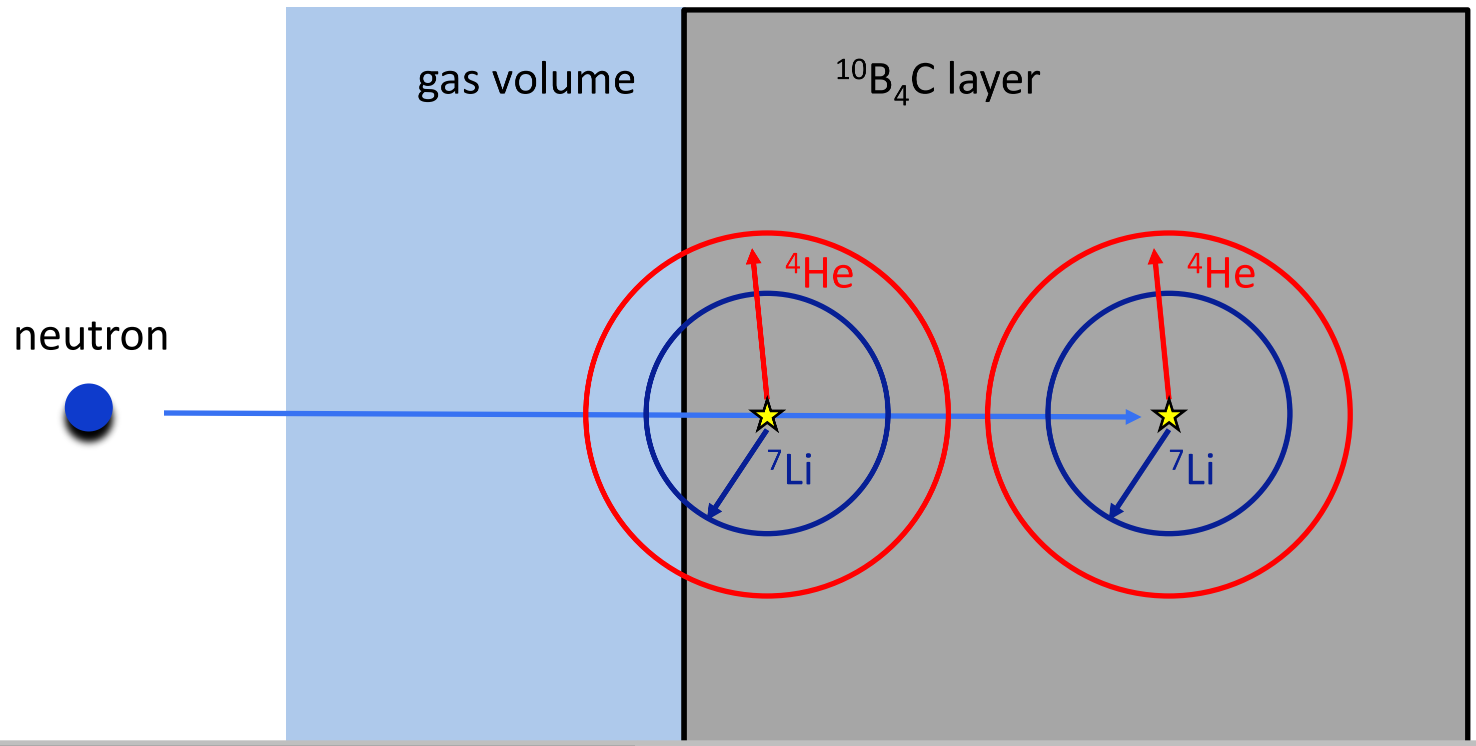

^{10}B-based Neutron Detectors

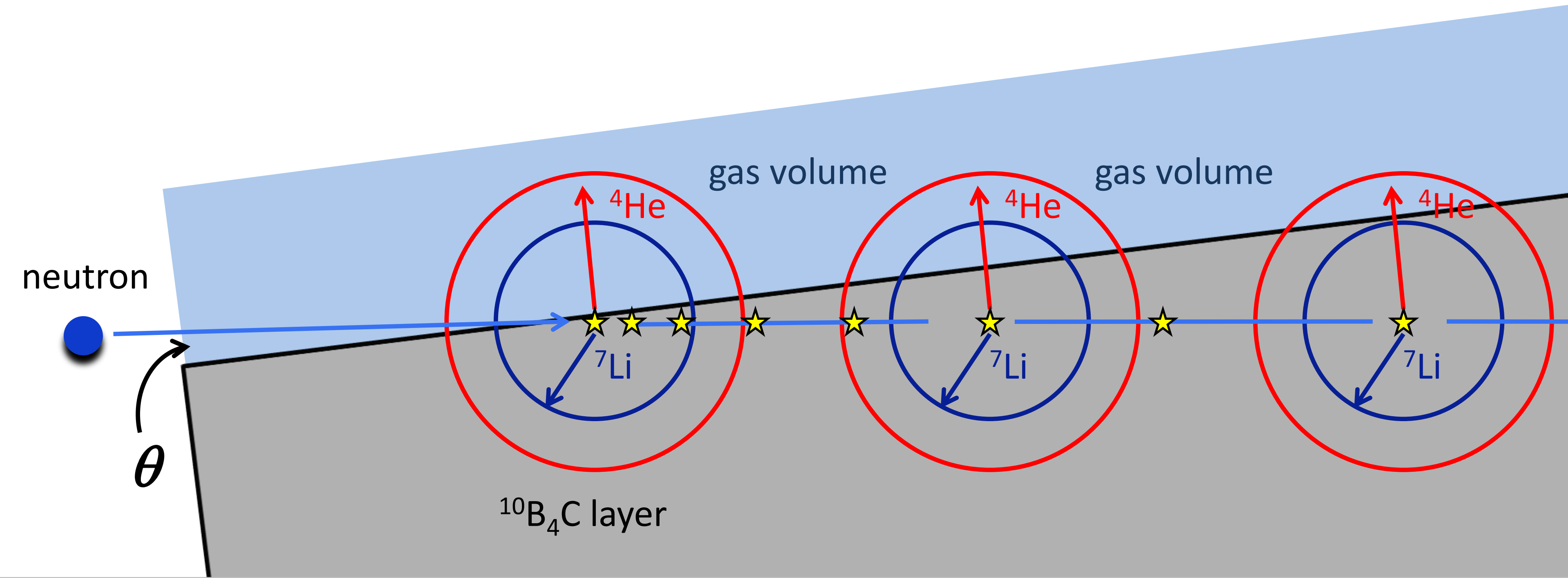

^{10}B-based Neutron Detectors

F. Piscitelli et al., IEEE TNS conf. proc. 2012

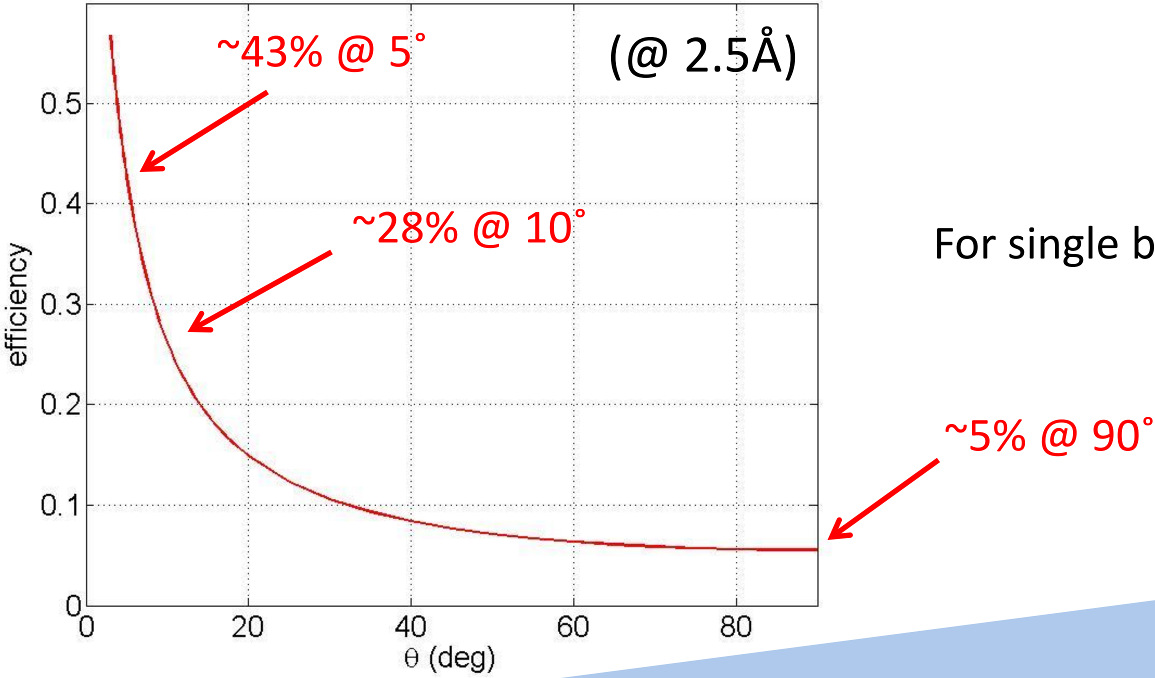

For single back-scattering layer.

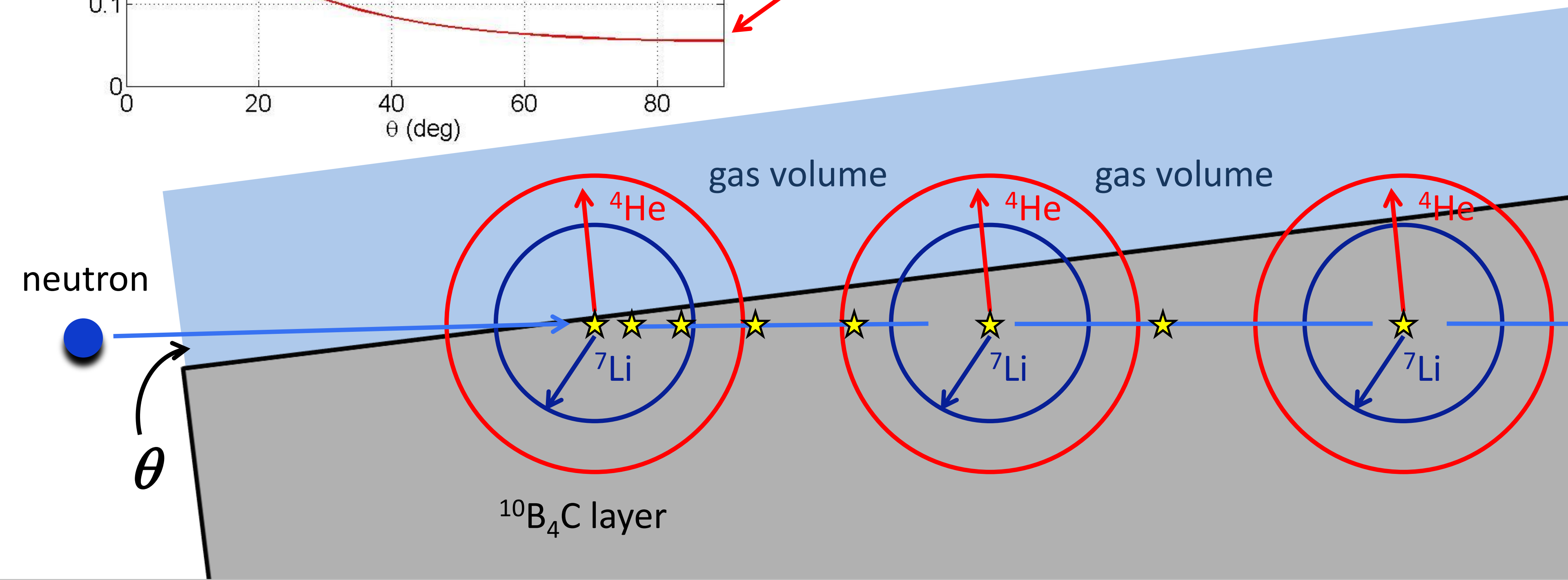

^{10}B-based Neutron Detectors

F. Piscitelli et al., IEEE TNS conf. proc. 2012

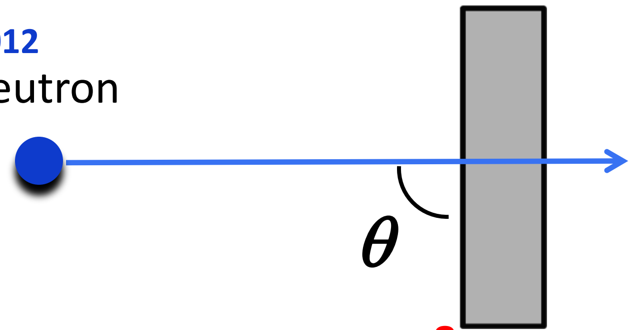

Θ=90˚

Efficiency

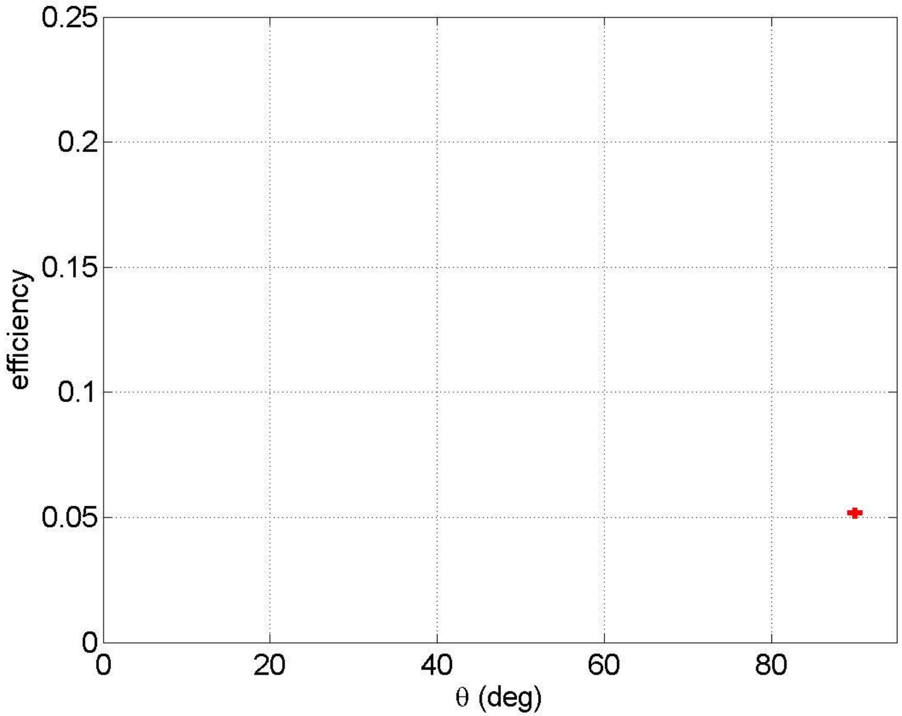

Pulse Height Spectrum

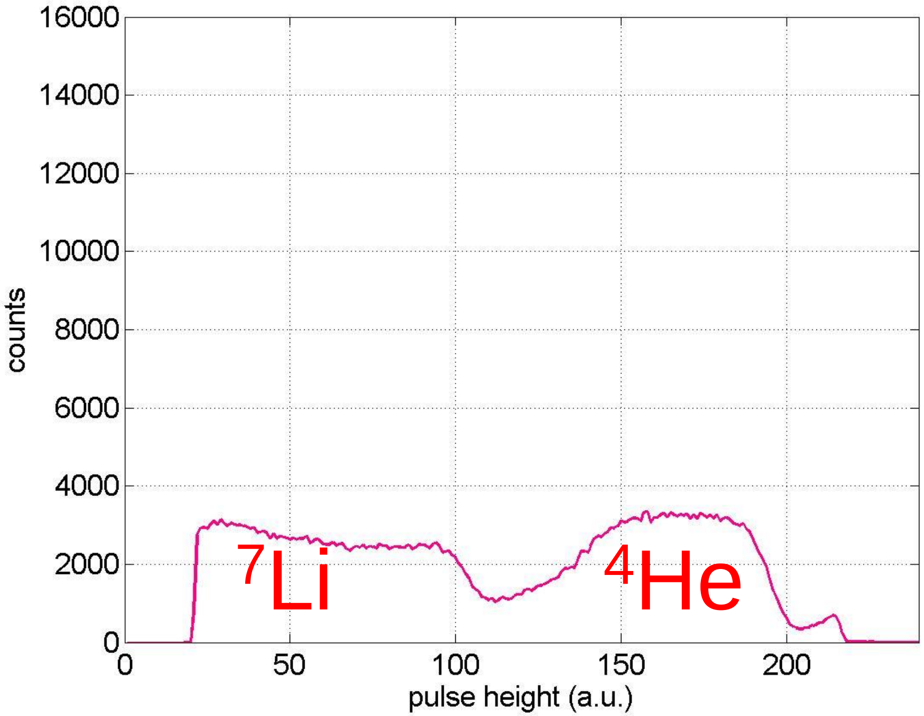

(measured @ 2.5Å, 1um layer)

^{10}B-based Neutron Detectors

F. Piscitelli et al., IEEE TNS conf. proc. 2012

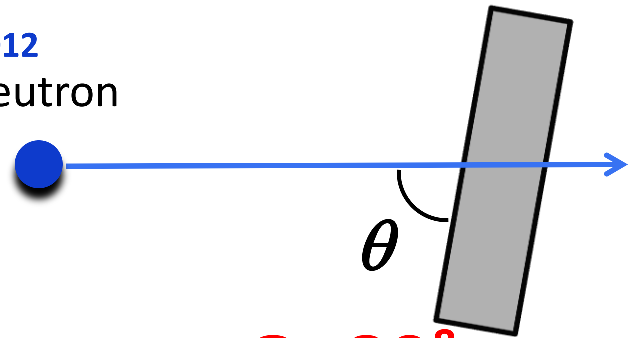

Θ=80˚

Efficiency

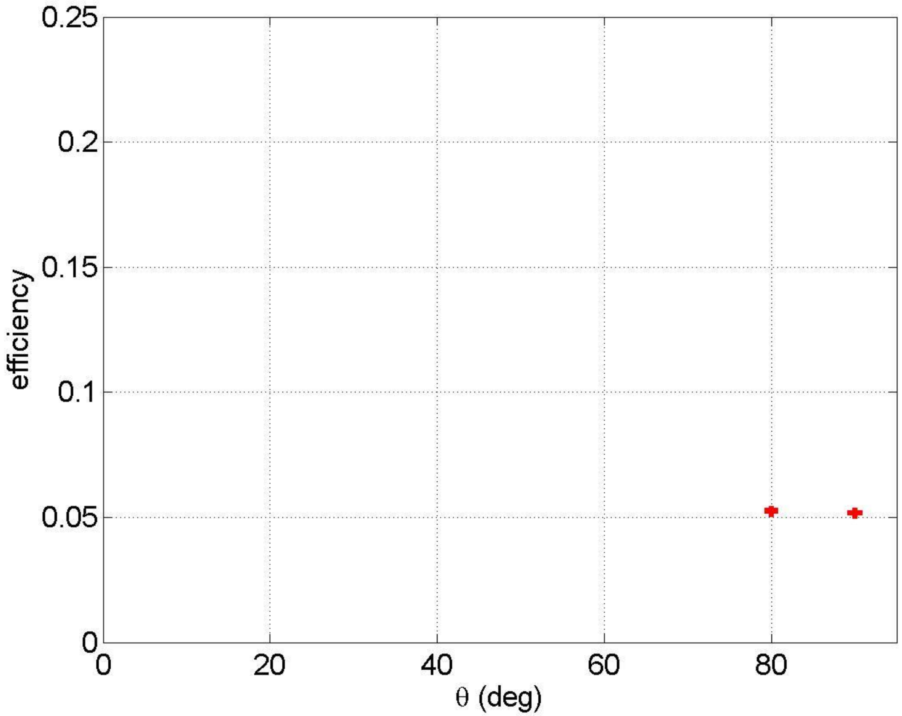

Pulse Height Spectrum

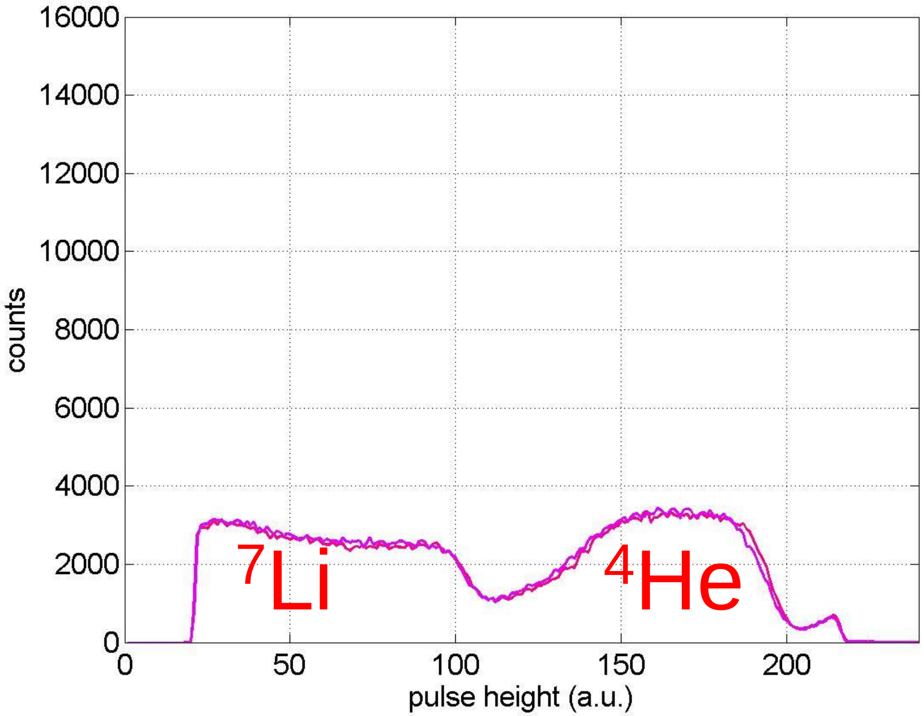

(measured @ 2.5Å, 1um layer)

^{10}B-based Neutron Detectors

F. Piscitelli et al., IEEE TNS conf. proc. 2012

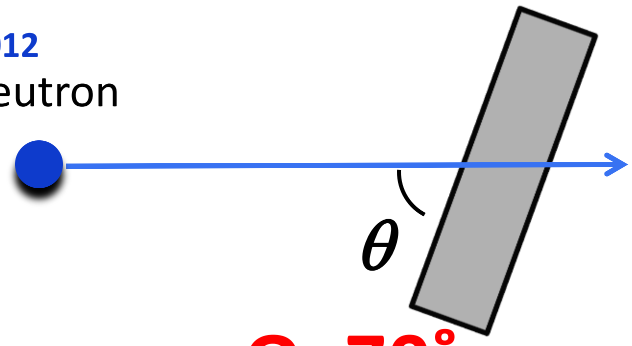

Θ=70˚

Efficiency

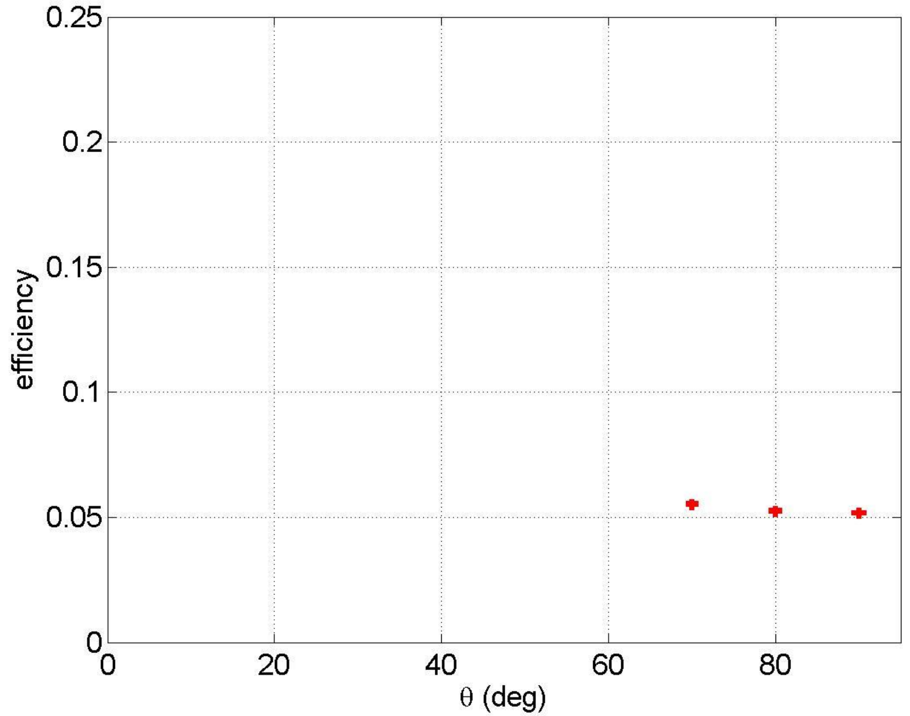

Pulse Height Spectrum

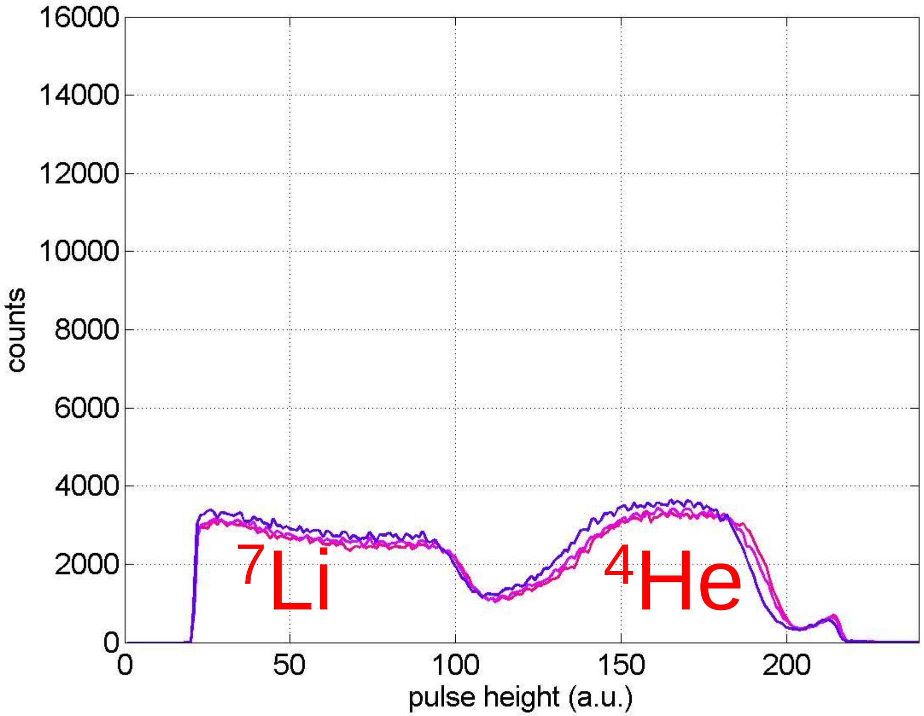

(measured @ 2.5Å, 1um layer)

^{10}B-based Neutron Detectors

F. Piscitelli et al., IEEE TNS conf. proc. 2012

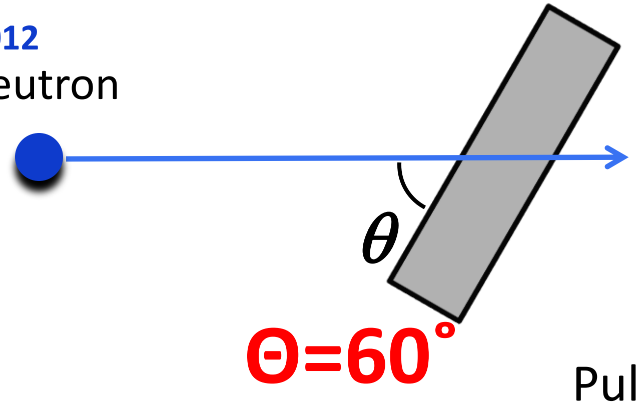

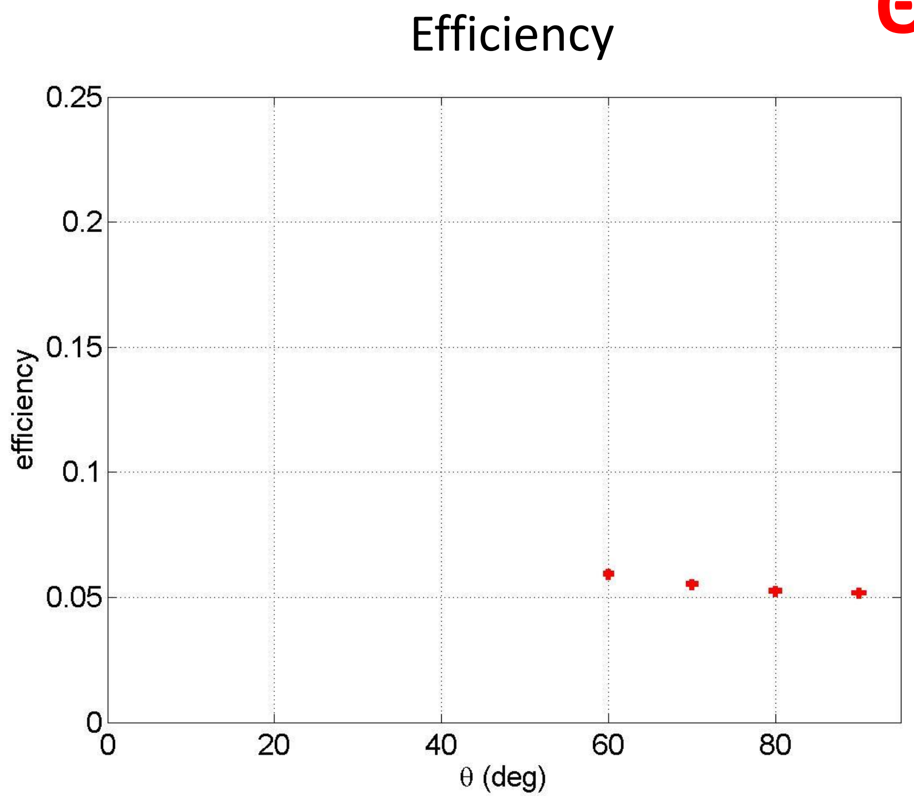

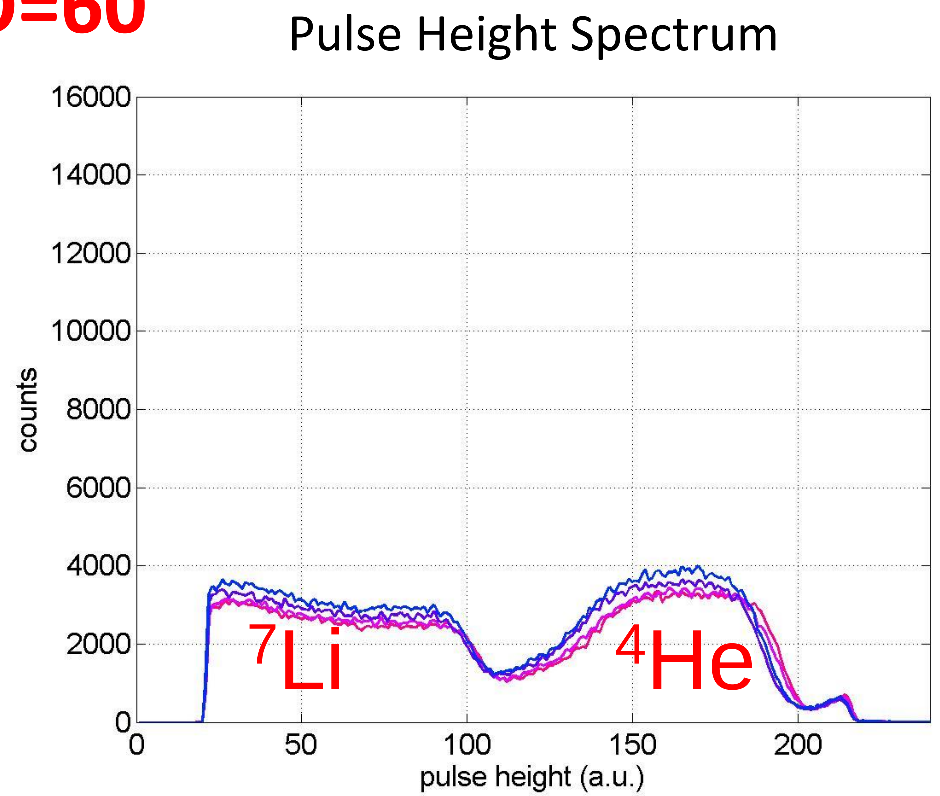

(measured @ 2.5Å, 1um layer)

^{10}B-based Neutron Detectors

F. Piscitelli et al., IEEE TNS conf. proc. 2012

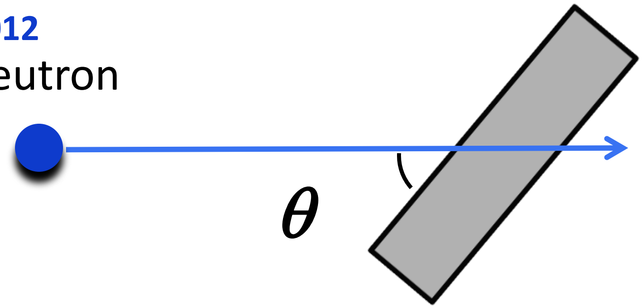

Θ=50˚

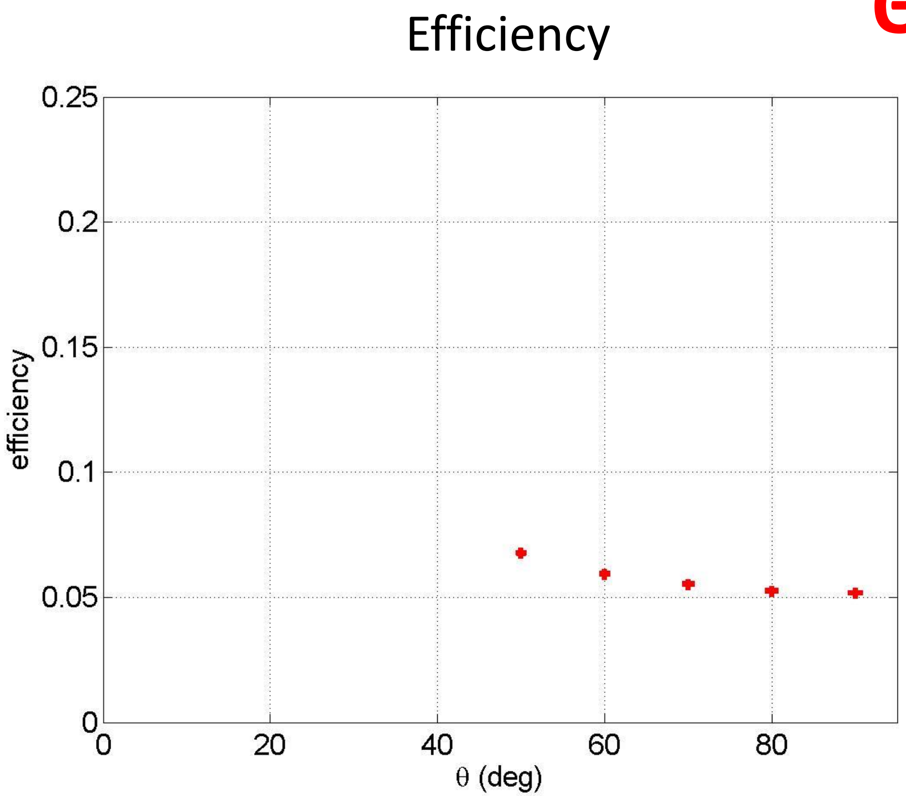

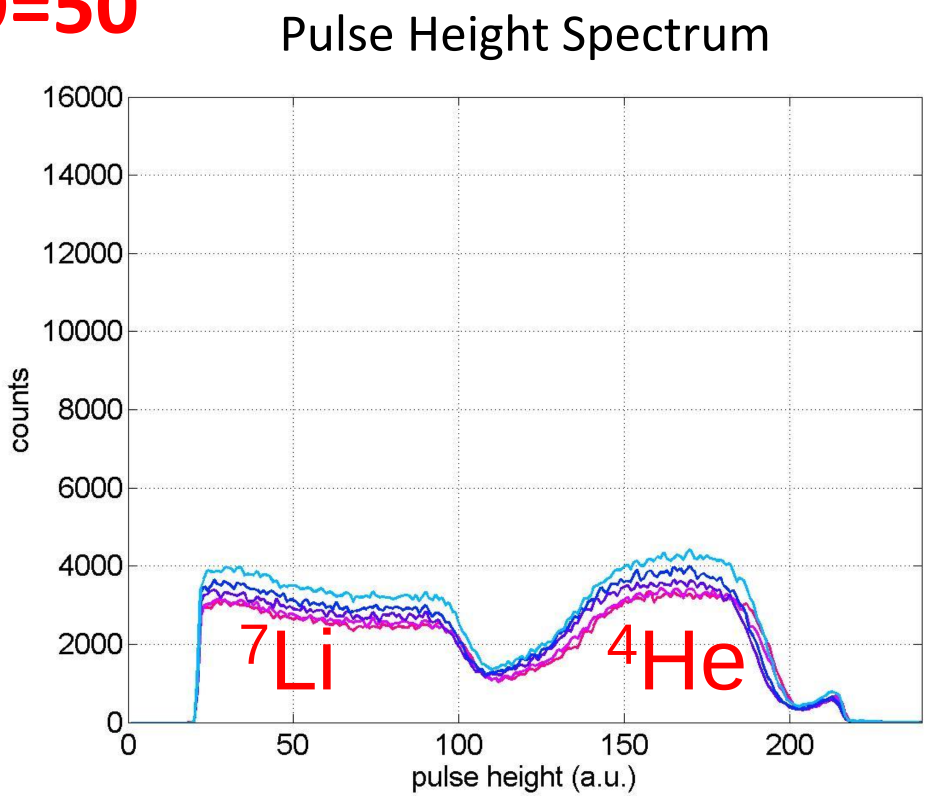

(measured @ 2.5Å, 1um layer)

^{10}B-based Neutron Detectors

F. Piscitelli et al., IEEE TNS conf. proc. 2012

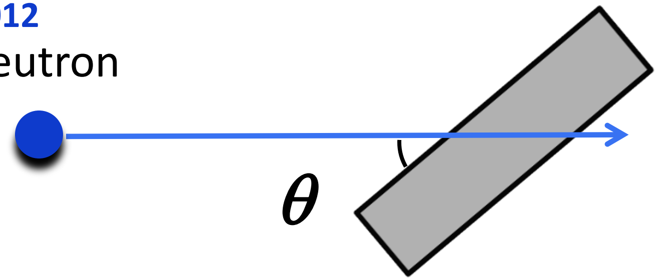

Θ=40˚

Efficiency

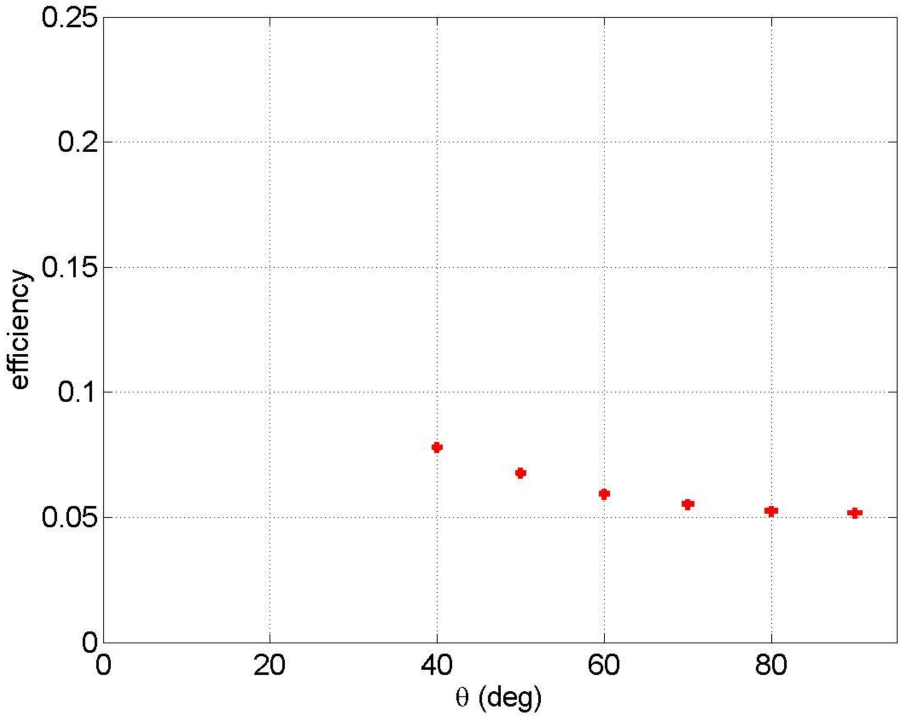

Pulse Height Spectrum

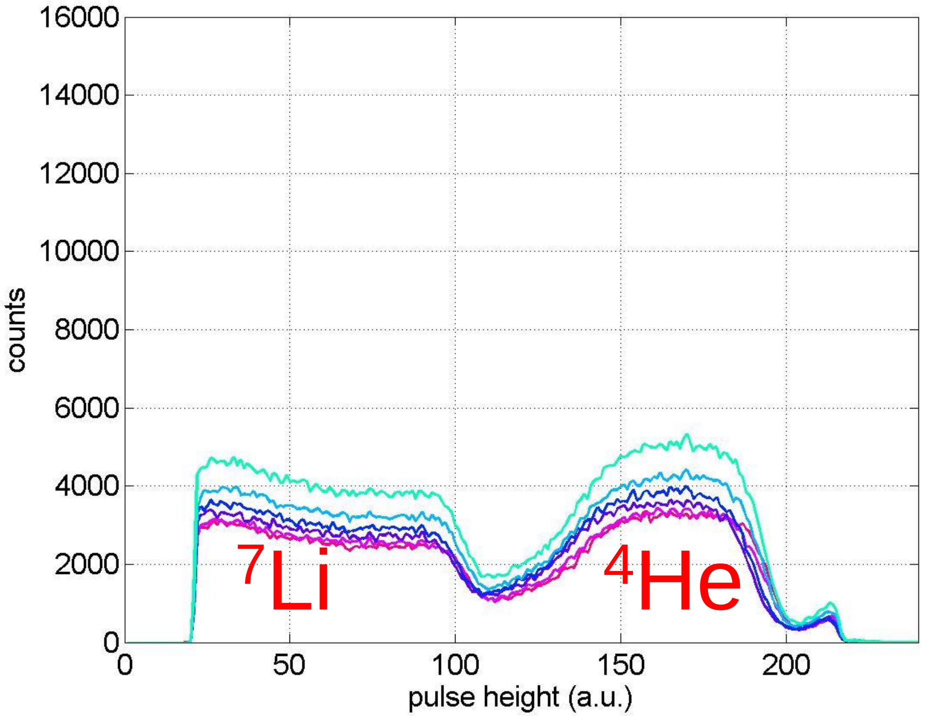

(measured @ 2.5Å, 1um layer)

^{10}B-based Neutron Detectors

F. Piscitelli et al., IEEE TNS conf. proc. 2012

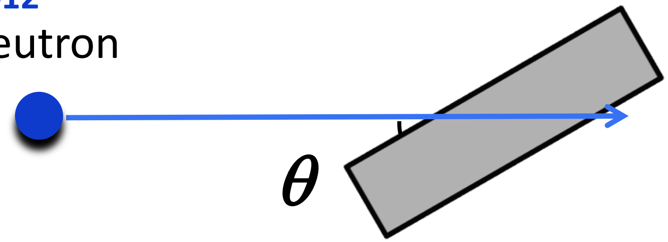

Θ=30˚

Efficiency

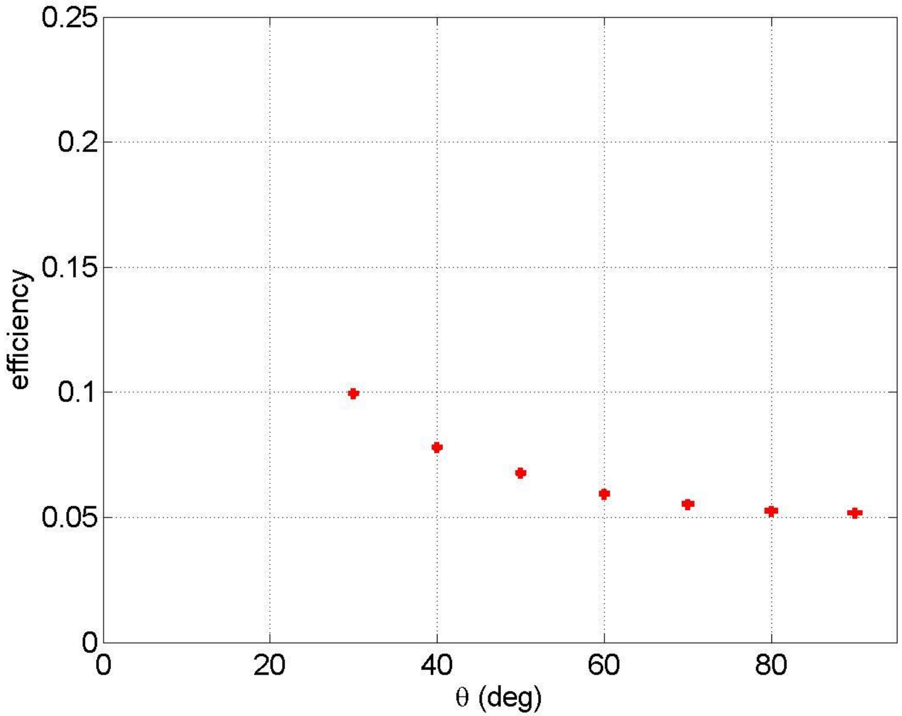

Pulse Height Spectrum

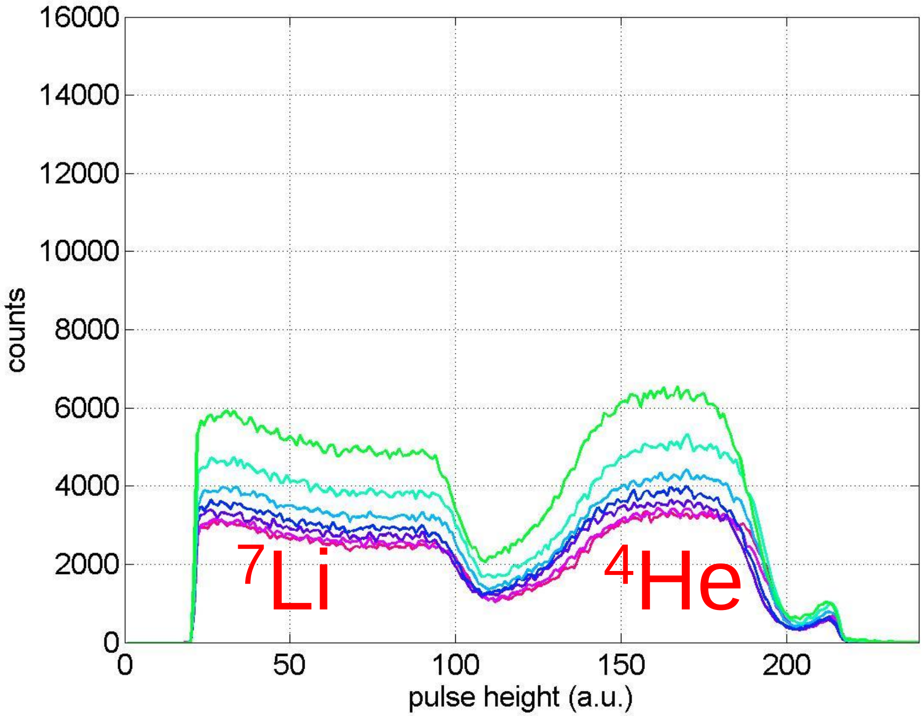

(measured @ 2.5Å, 1um layer)

^{10}B-based Neutron Detectors

F. Piscitelli et al., IEEE TNS conf. proc. 2012

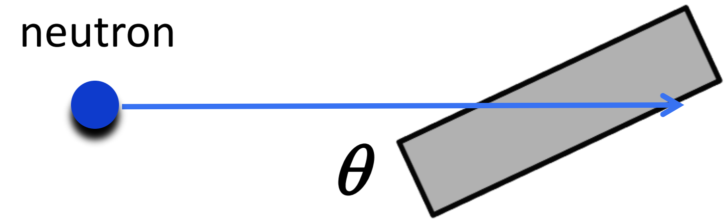

Θ=25˚

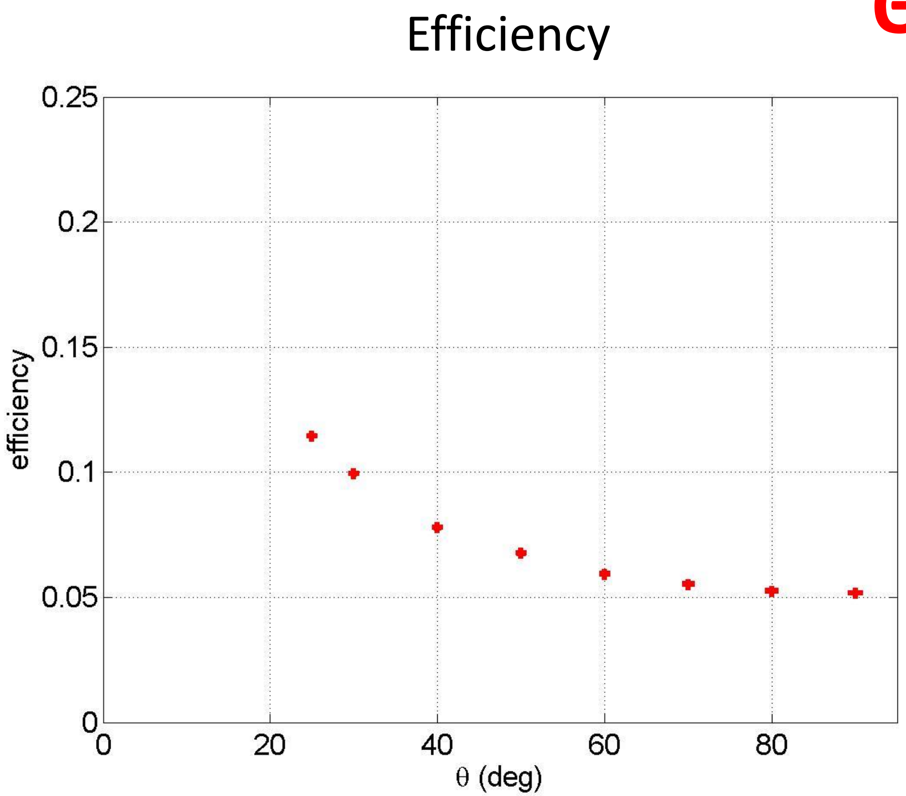

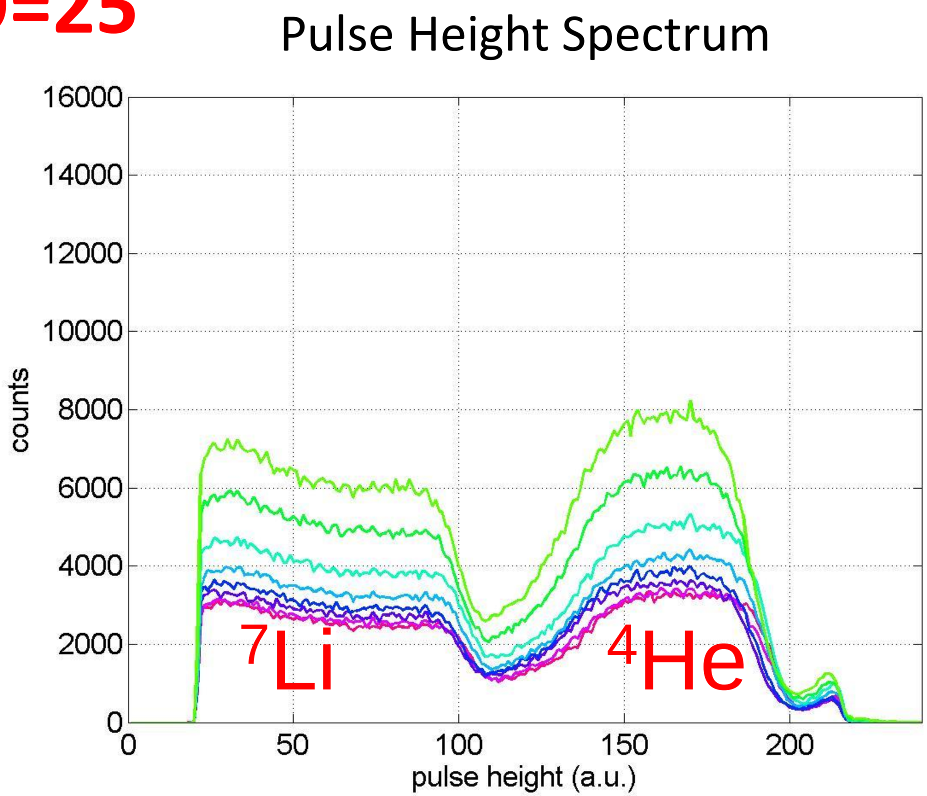

(measured @ 2.5Å, 1um layer)

^{10}B-based Neutron Detectors

F. Piscitelli et al., IEEE TNS conf. proc. 2012

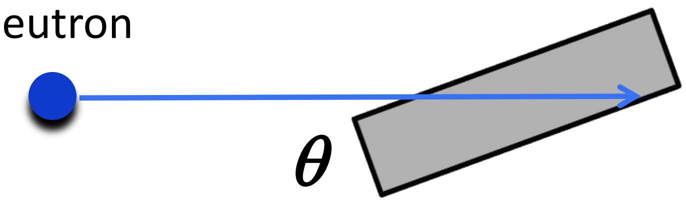

Θ=20˚

Efficiency

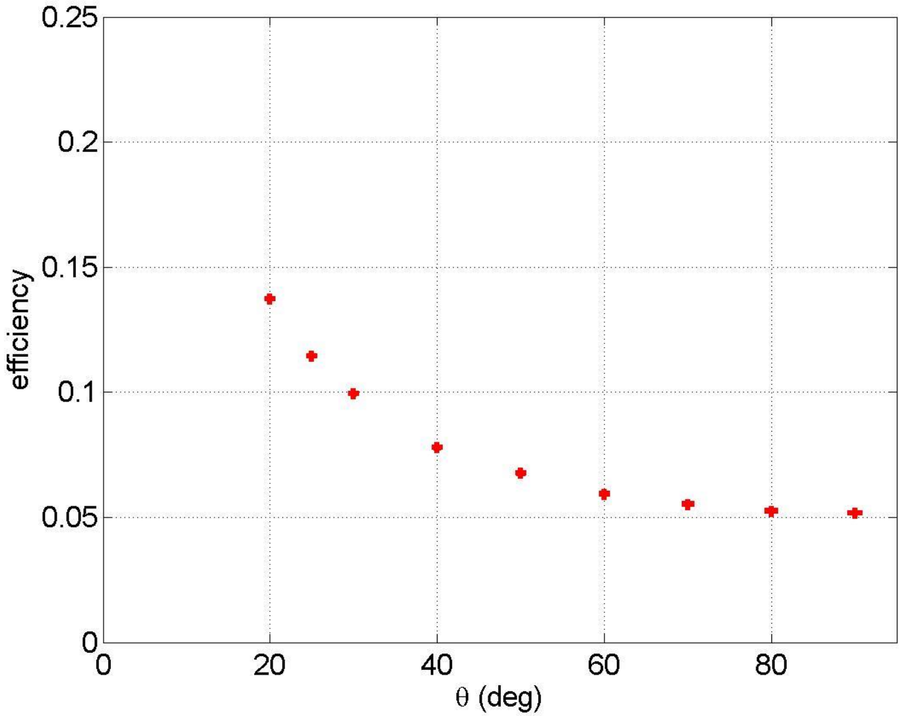

Pulse Height Spectrum

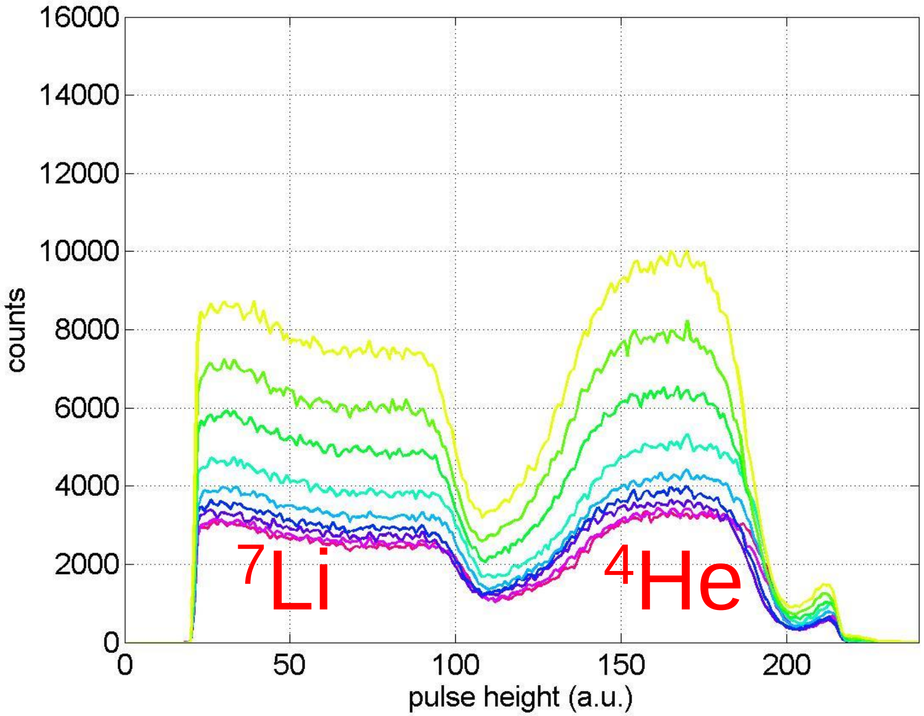

(measured @ 2.5Å, 1um layer)

^{10}B-based Neutron Detectors

F. Piscitelli et al., IEEE TNS conf. proc. 2012

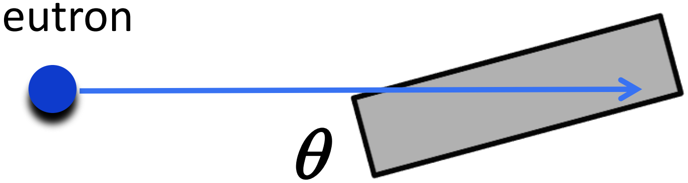

Θ=15˚

Efficiency

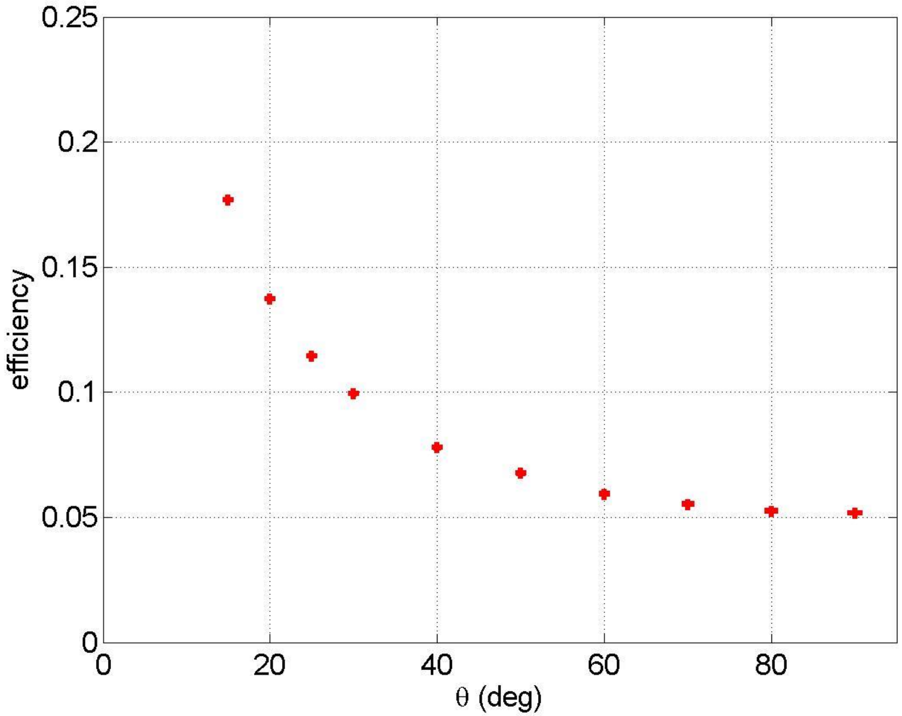

Pulse Height Spectrum

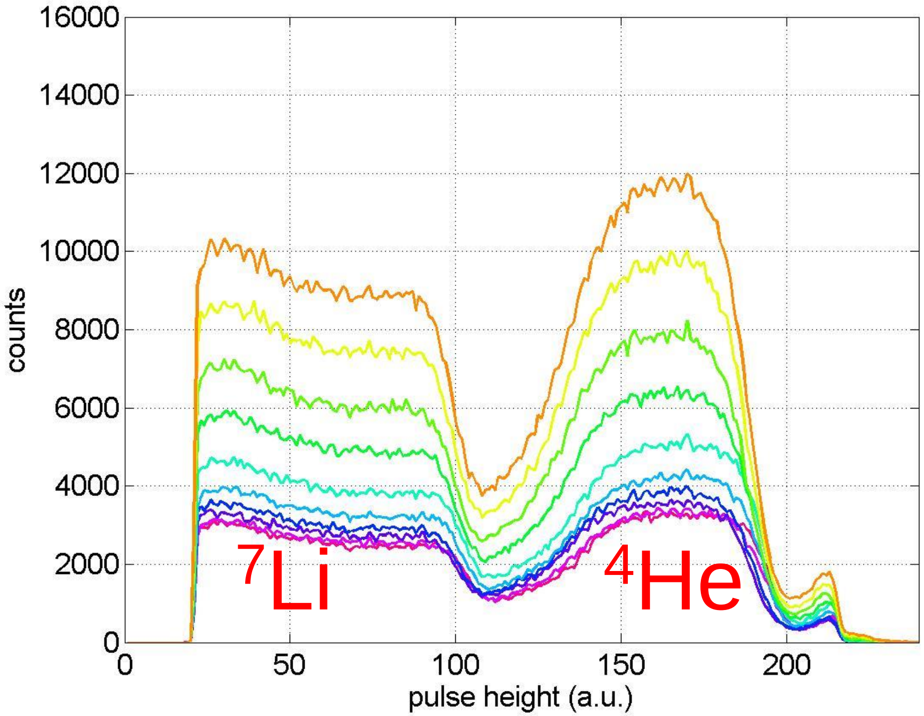

(measured @ 2.5Å, 1um layer)

^{10}B-based Neutron Detectors

F. Piscitelli et al., IEEE TNS conf. proc. 2012

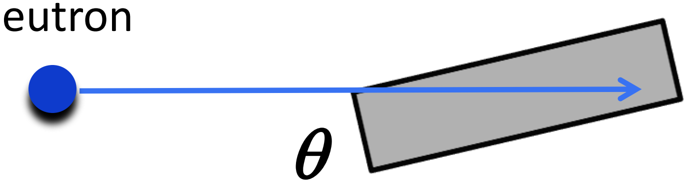

Θ=10˚

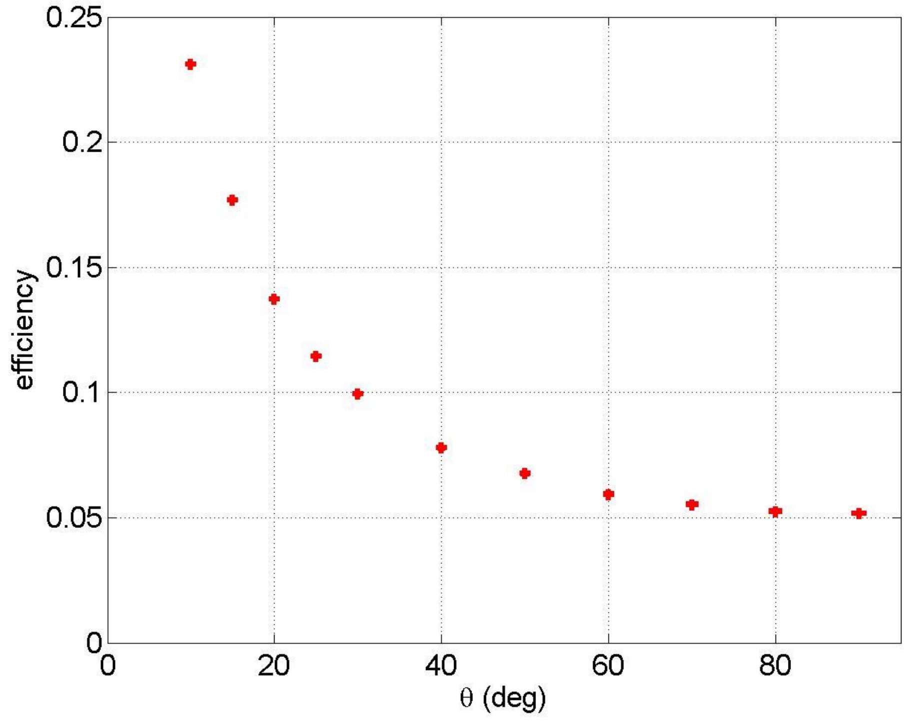

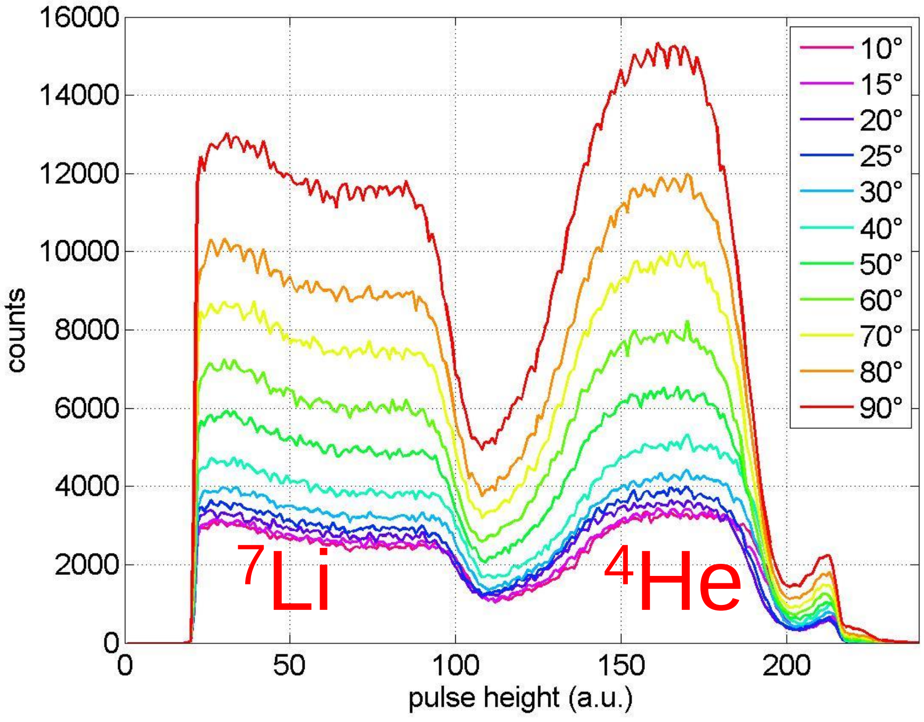

(measured @ 2.5Å, 1um layer)

^{10}B-based Neutron Detectors

F. Piscitelli et al., IEEE TNS conf. proc. 2012

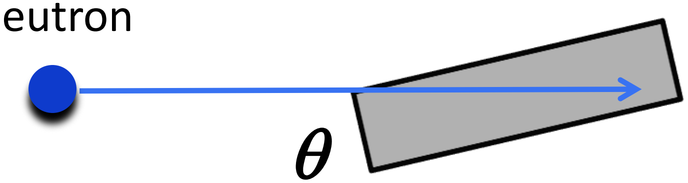

Θ=10°

Efficiency

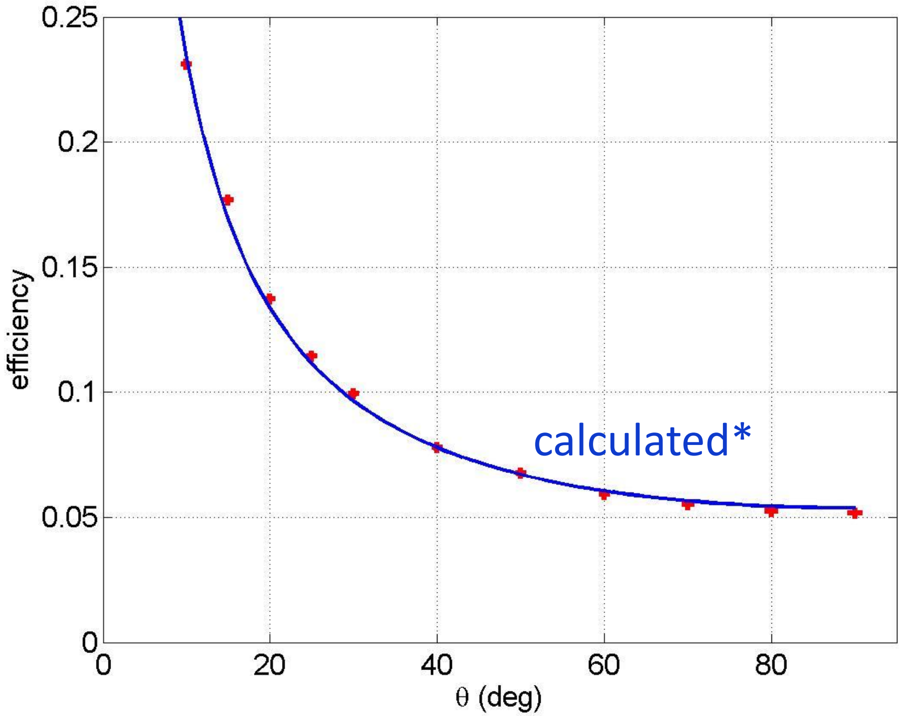

Pulse Height Spectrum

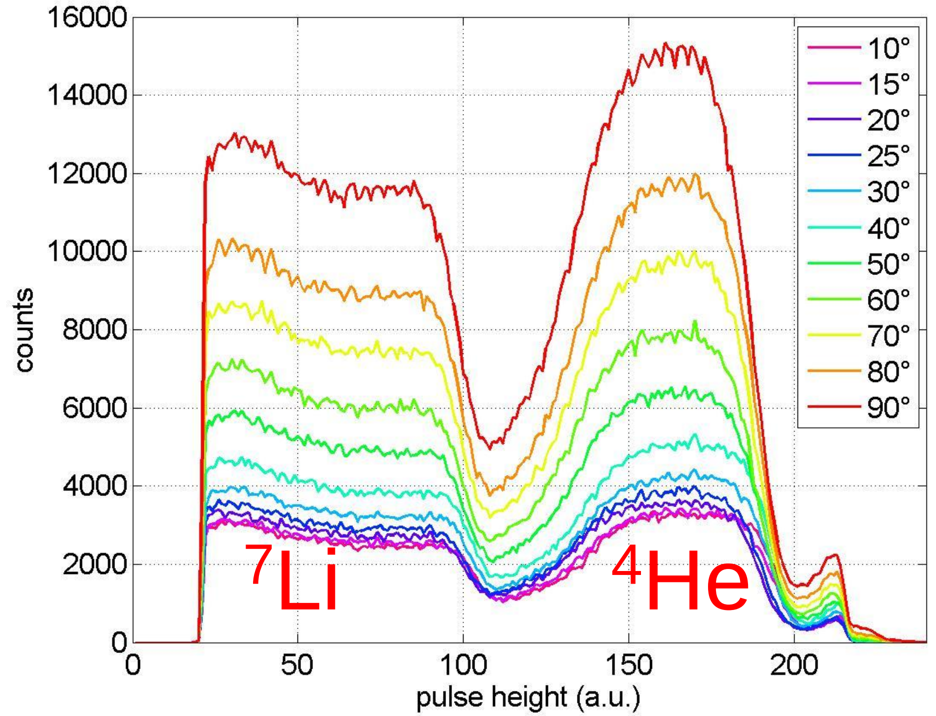

*F. Piscitelli and P. Van Esch, JINST, v. 8, p. 04020, 2013

(measured @ 2.5Å, 1um layer)

^{10}B-based Neutron Detectors: Multi-Blade

F. Piscitelli et al., accepted JINST 2014

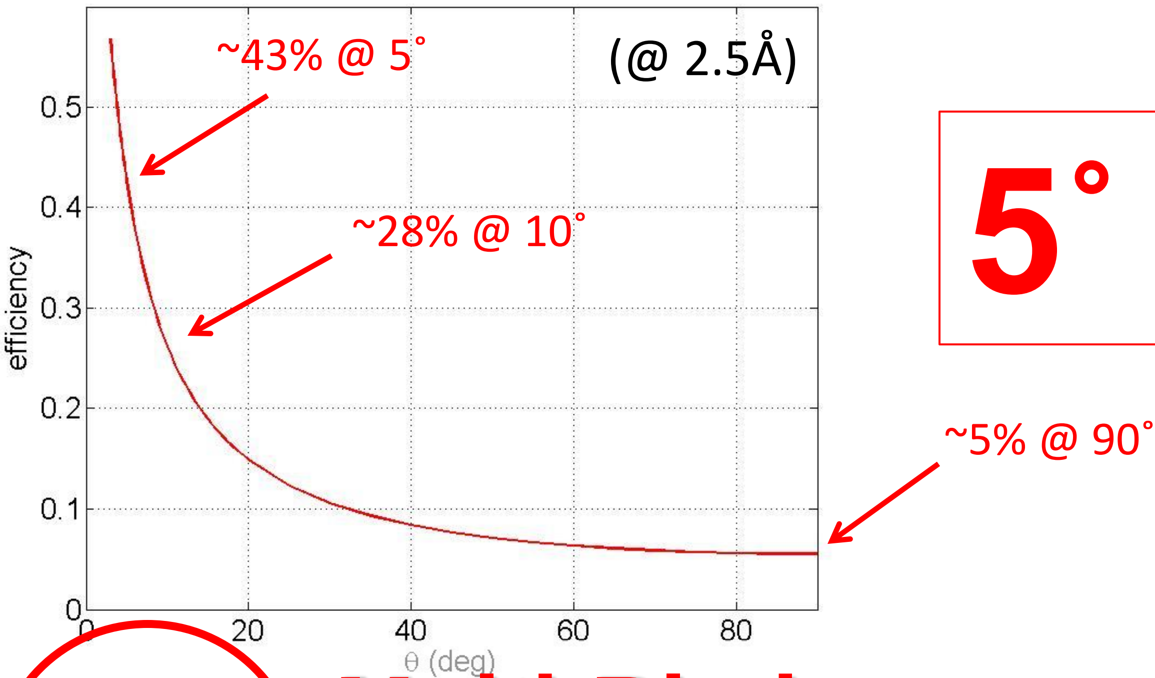

5˚ & 10˚

2

Multi-Blade

Grazing angle (<10˚)

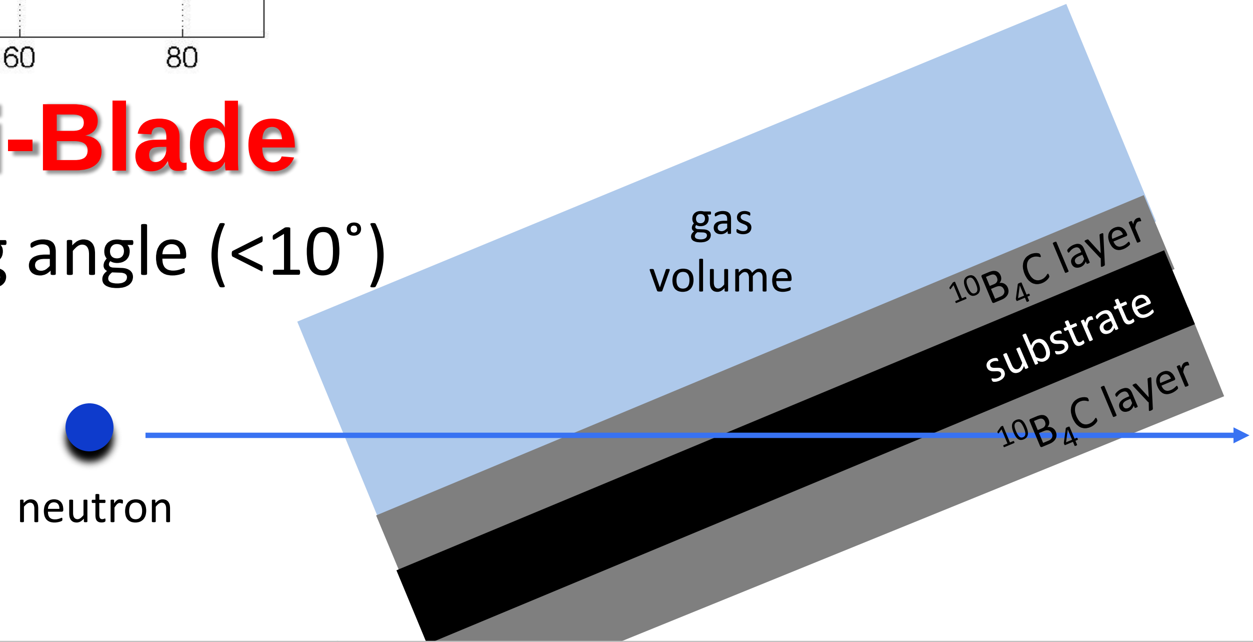

^{10}B-based Neutron Detectors: Multi-Blade

F. Piscitelli et al., accepted JINST 2014

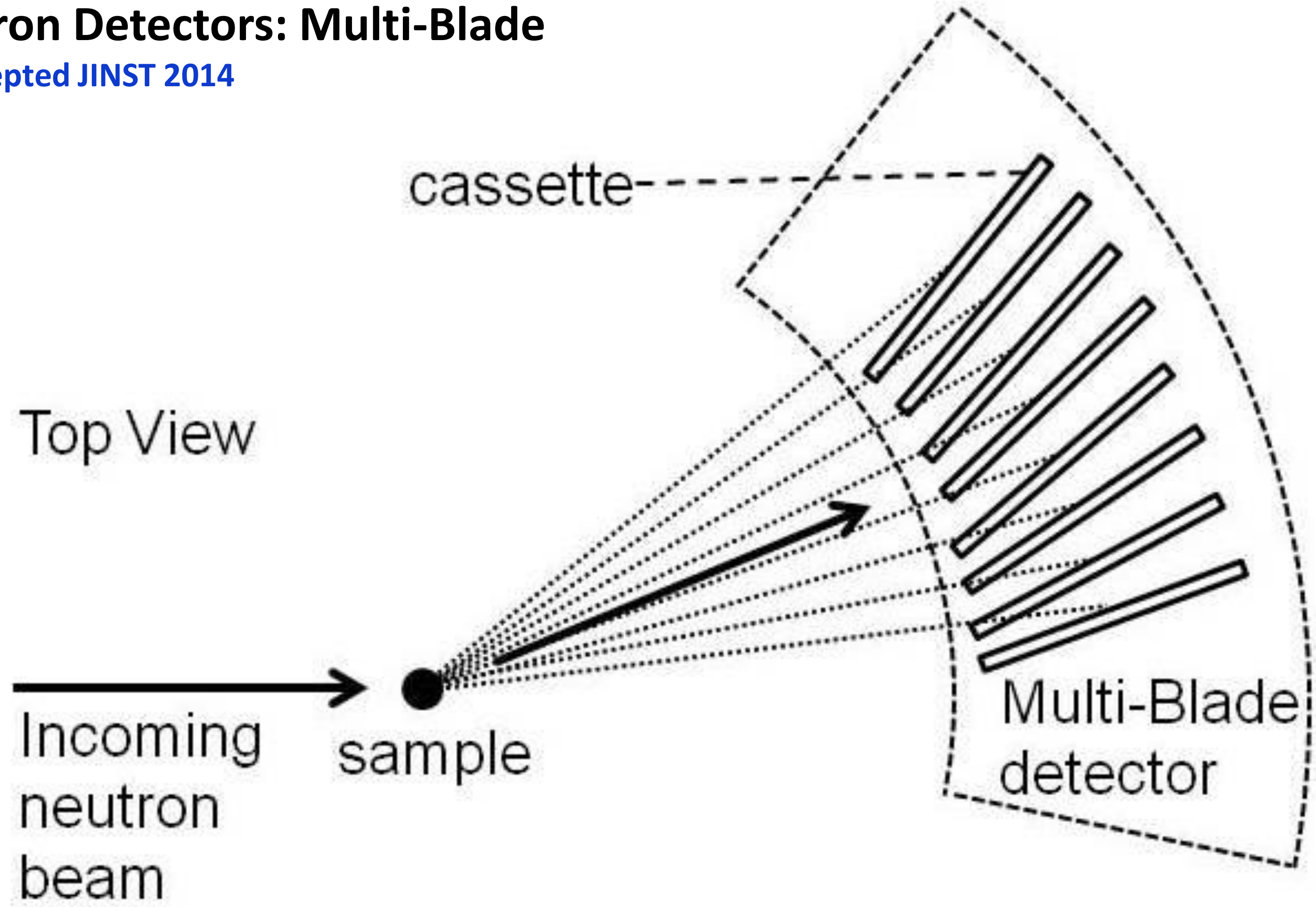

Suitable for Neutron Reflectometry
(for both monochromatic and ToF)

Introduced at ILL in 2005:

J.C. Buffet et al., NIM A 554, 1–3, 2005

^{10}B-based Neutron Detectors: Multi-Blade

F. Piscitelli et al., accepted JINST 2014

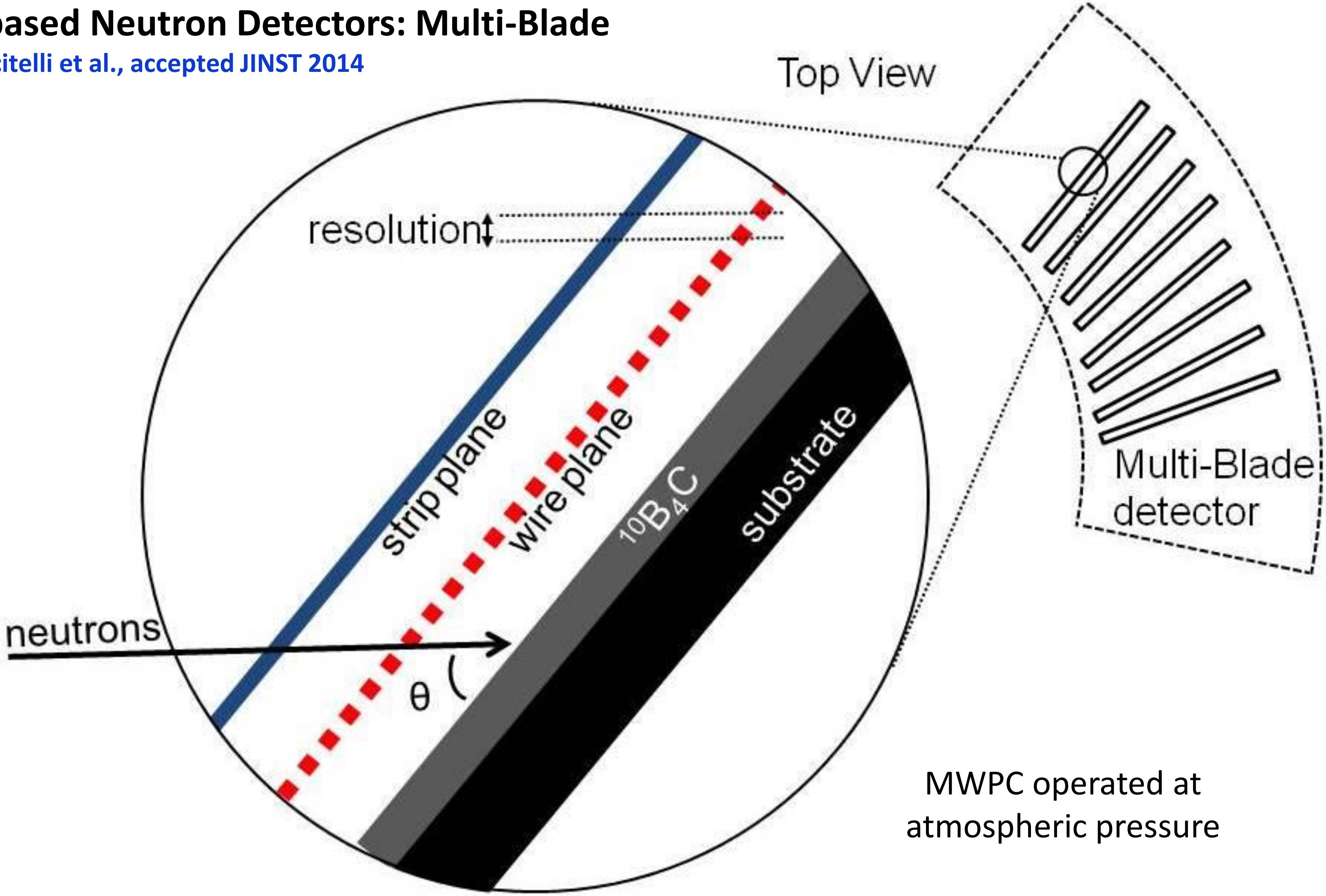

MWPC operated at atmospheric pressure

^{10}B-based Neutron Detectors: Multi-Blade

F. Piscitelli et al., accepted JINST 2014

A

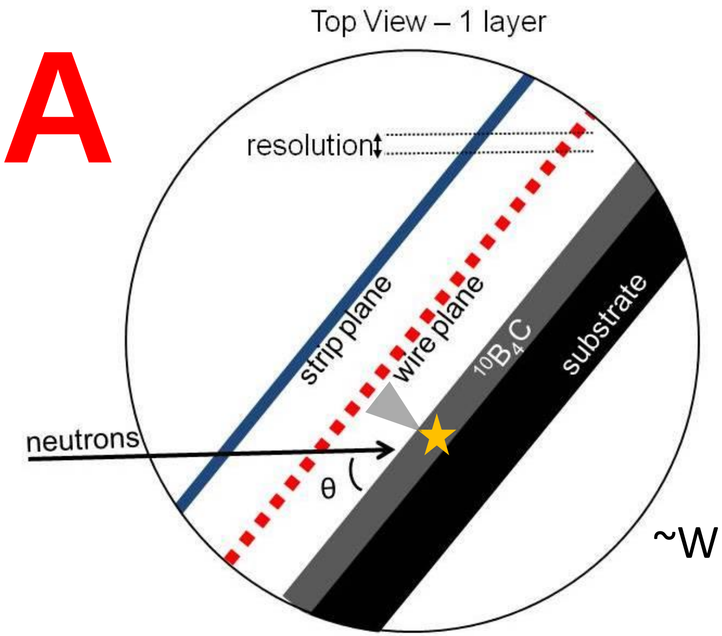

Resolution:
~Wire pitch x 5 at 10˚
(x10 at 5˚)

B

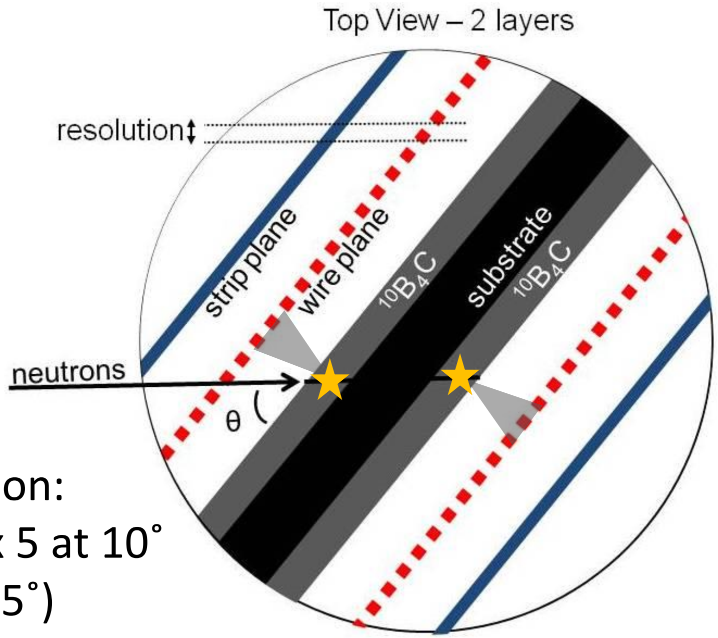

^{10}B-based Neutron Detectors: Multi-Blade

F. Piscitelli et al., accepted JINST 2014

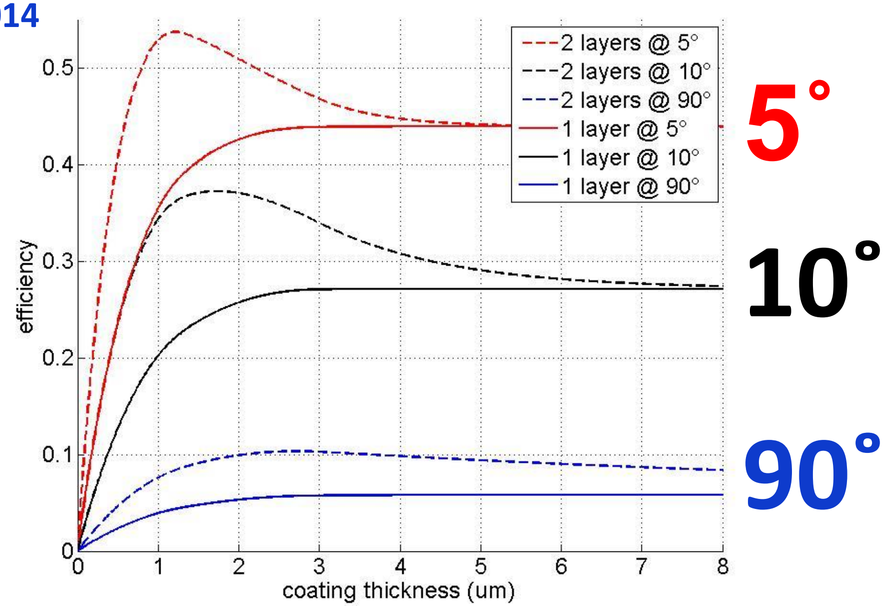

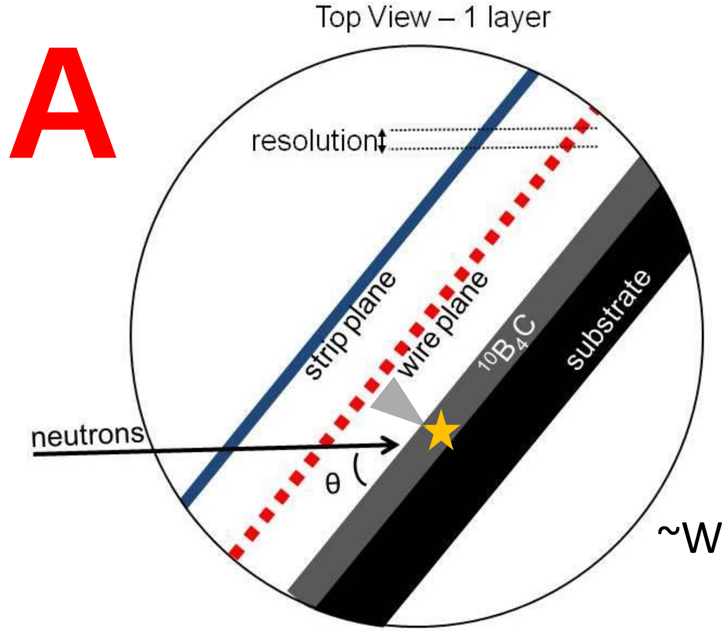

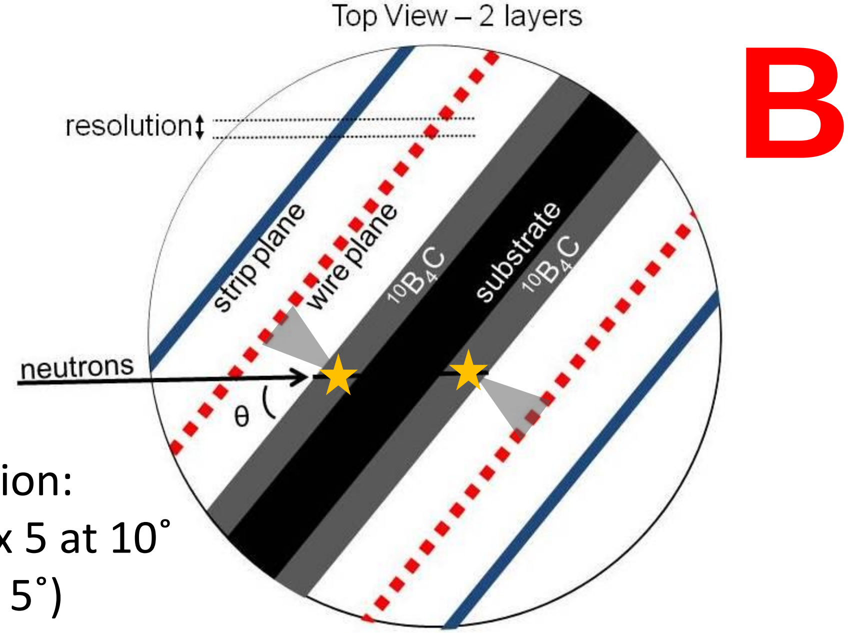

Resolution:
~Wire pitch x 5 at 10˚
(x10 at 5˚)

^{10}B-based Neutron Detectors: Multi-Blade

F. Piscitelli et al., accepted JINST 2014

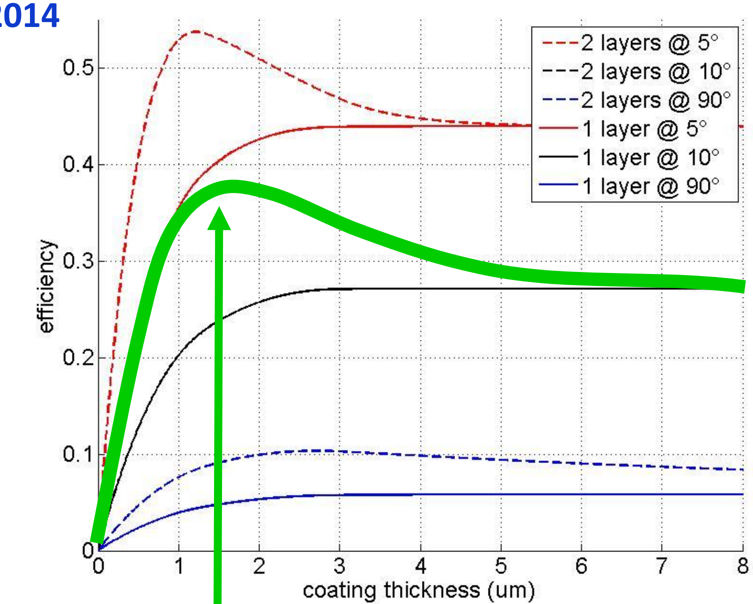

5°

10°

90°

higher efficiency

substrate choice

~1.5 µm

A

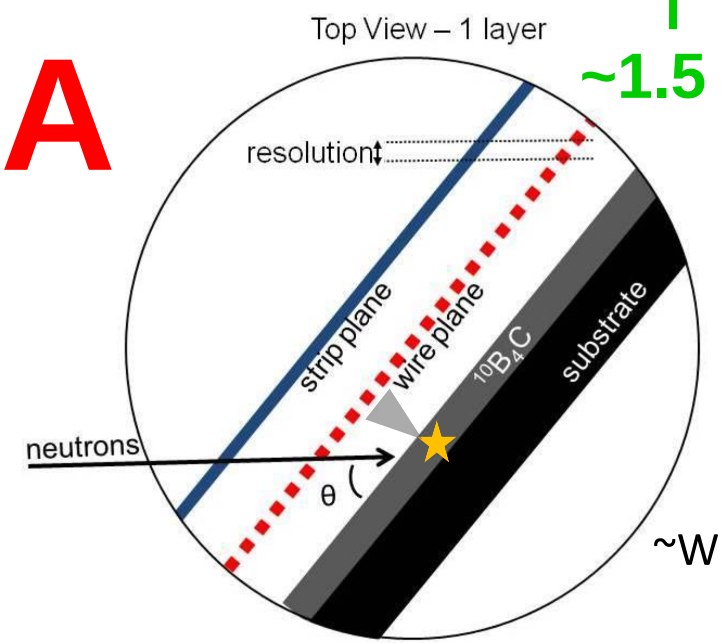

B

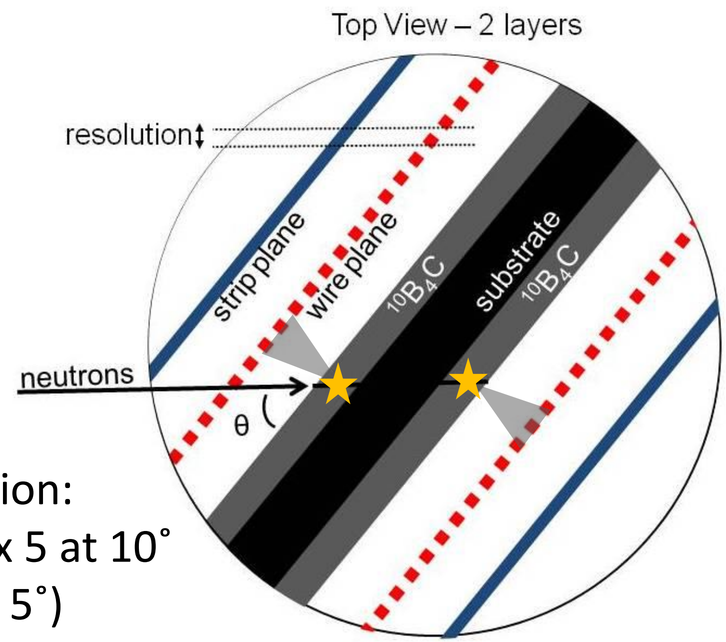

Resolution:
~Wire pitch x 5 at 10˚
(x10 at 5˚)

^{10}B-based Neutron Detectors: Multi-Blade

F. Piscitelli et al., accepted JINST 2014

lower efficiency

independent from layer thickness

no substrate problem

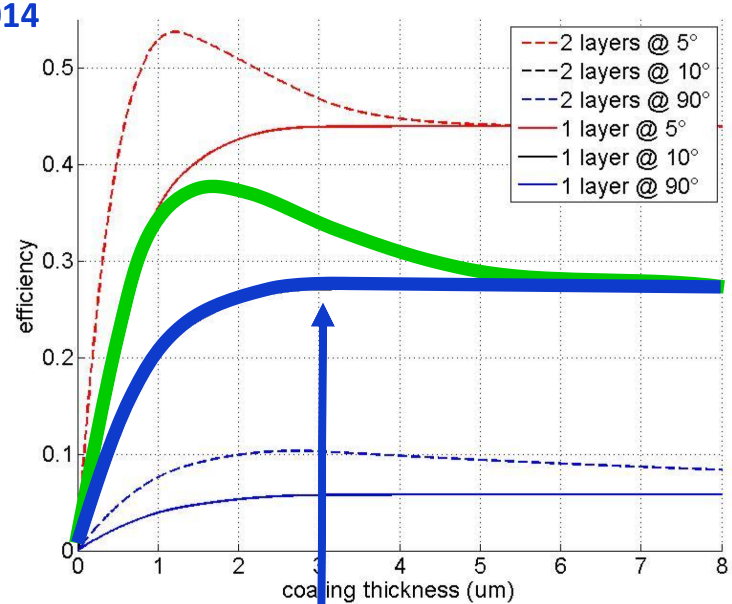

5°

10°

90°

~3 μm

higher efficiency

substrate choice

A

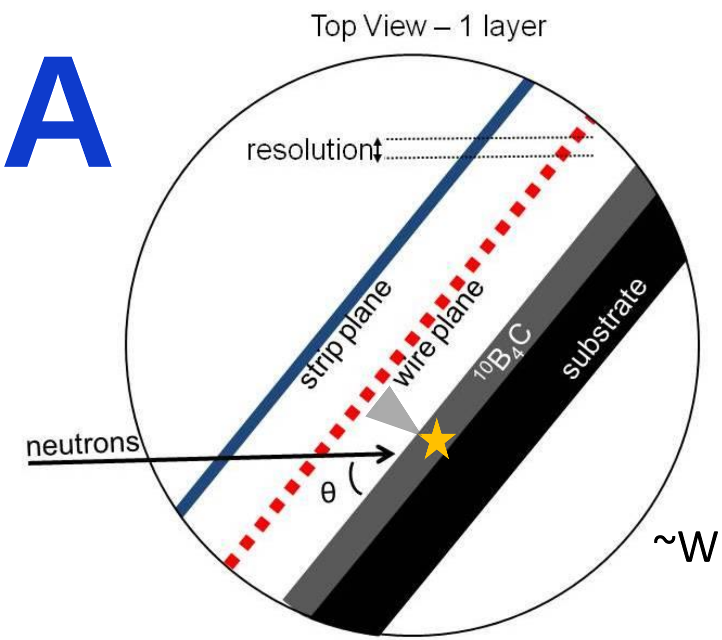

Resolution:
~Wire pitch x 5 at 10°
(x10 at 5°)

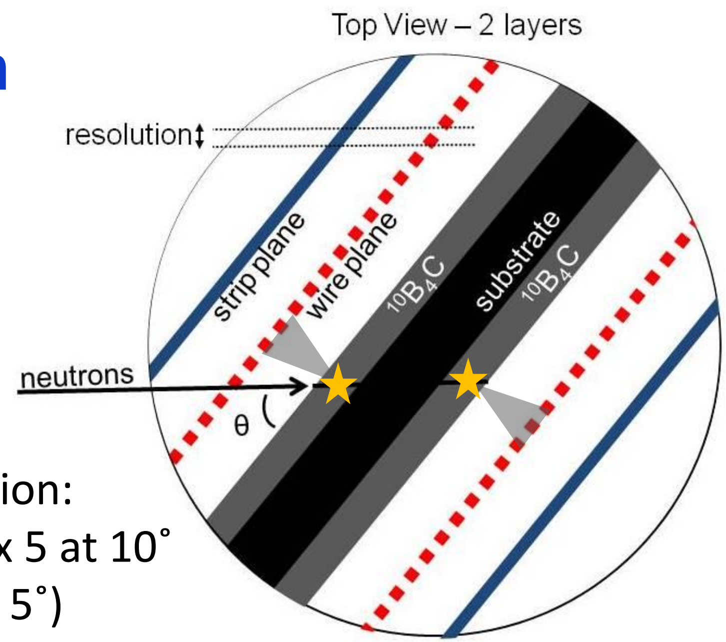

B

Triple GEM with Boron-10 converter (variant 1)

Drift cathode:
300 um Al coated with 1 um10B4C on both sides

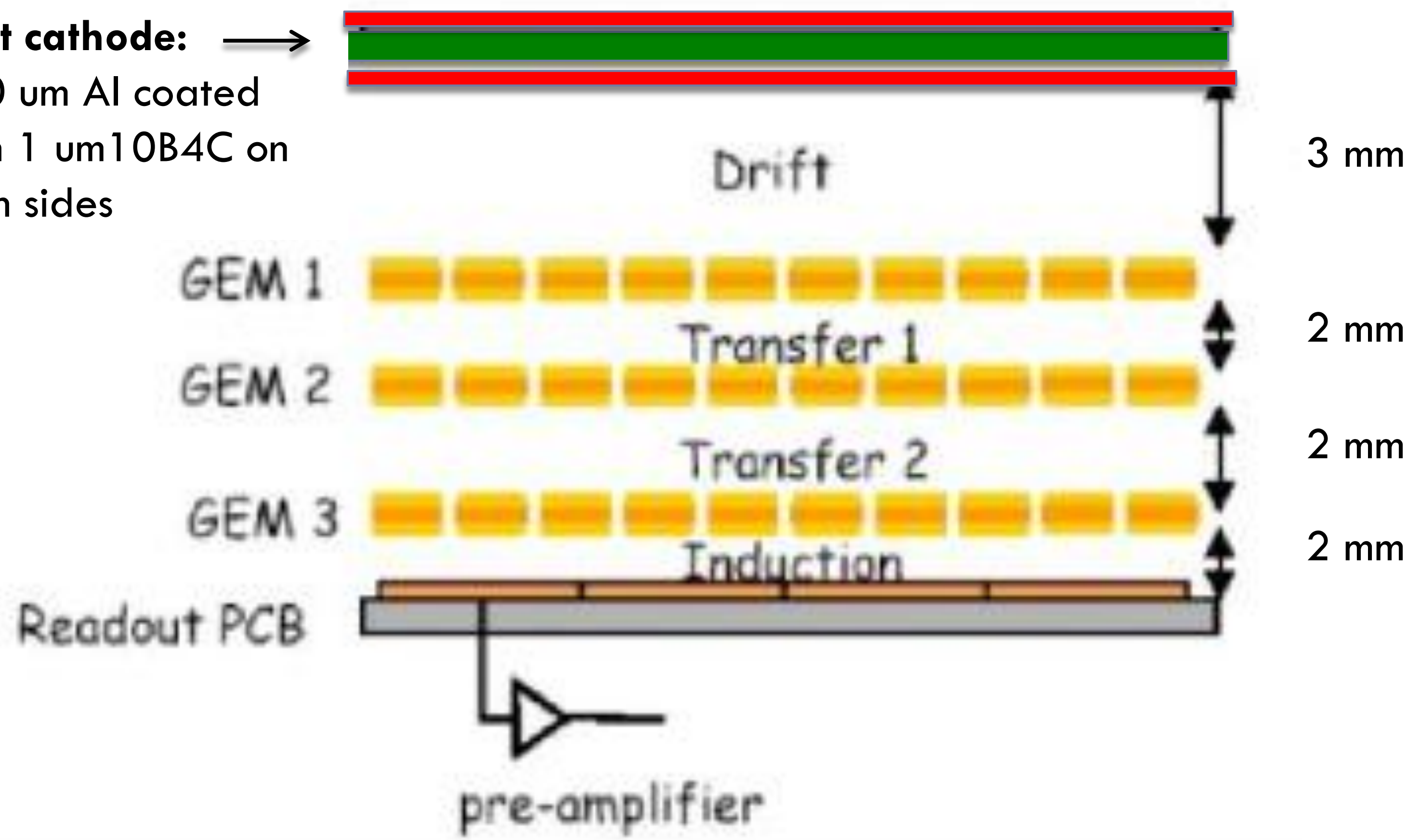

Boron GEM3: detector and support

Readout x direction

Readout y direction

Drift with10B4C

Support with O-ring

Gas flow (out)

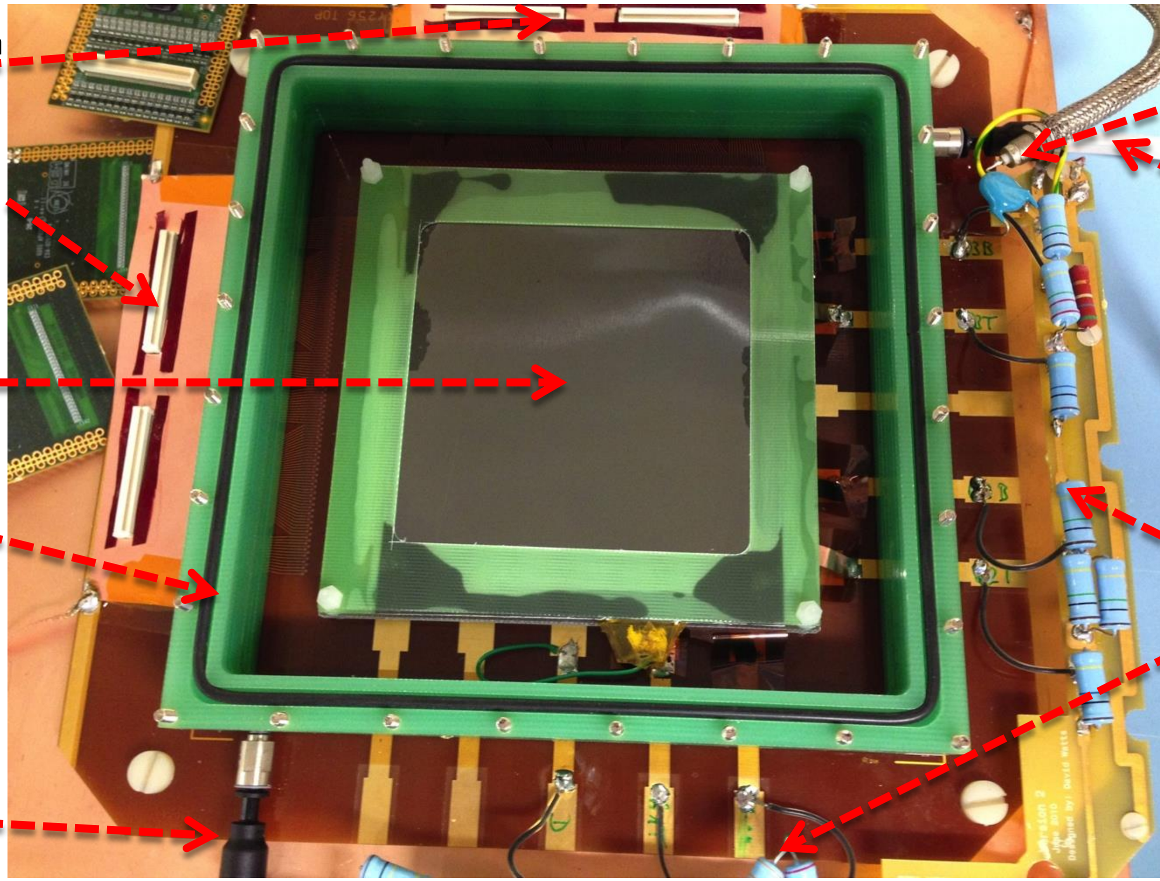

Readout for integrated signal induced at bottom of third GEM

Gas flow (in)

Voltage divider for HV for drift and 3 GEM foils

Spectrum 241Am Be source: 1 cm lead, gain ~200

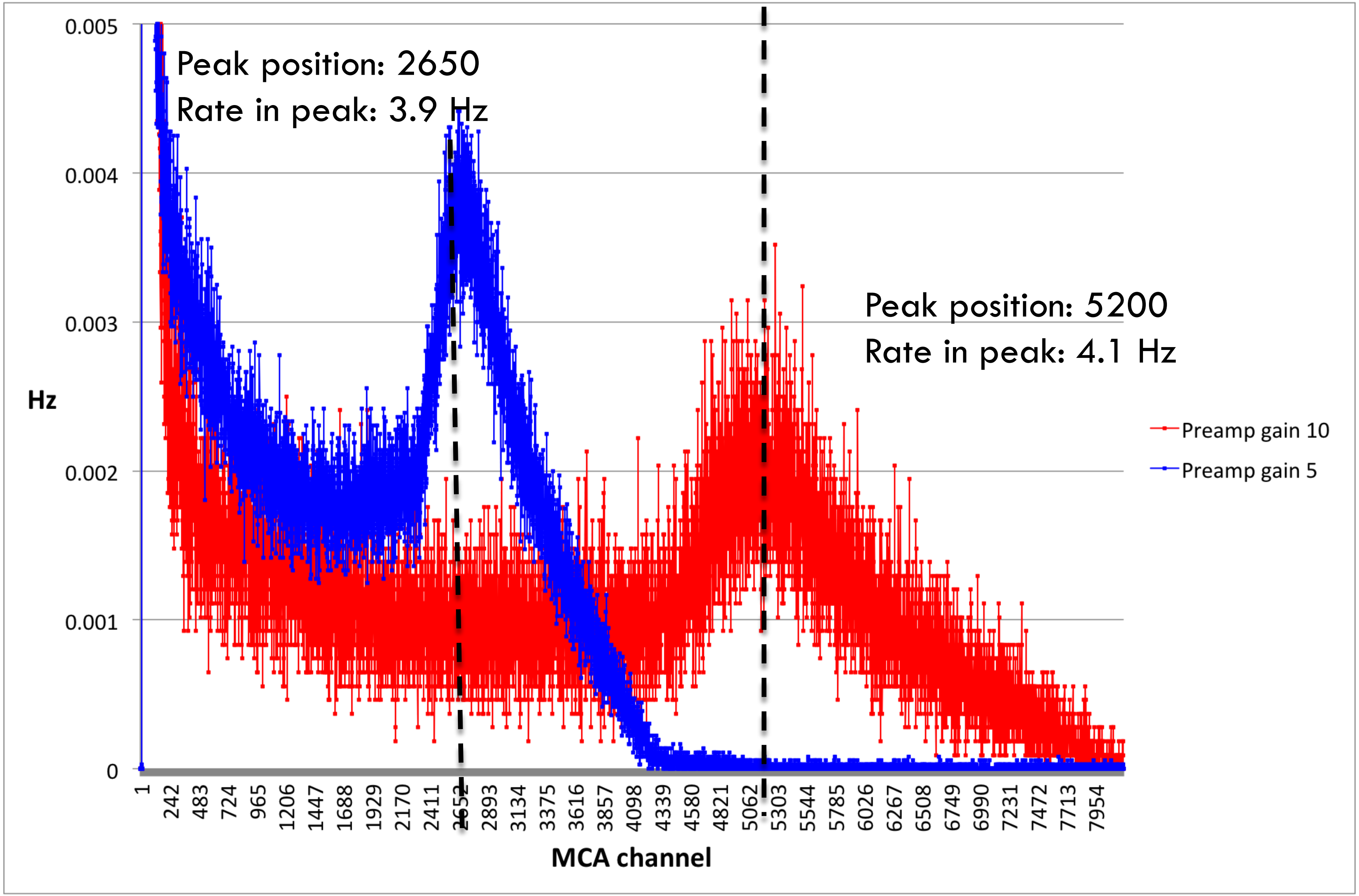

Triple GEM with Boron-10 converter (variant 2)

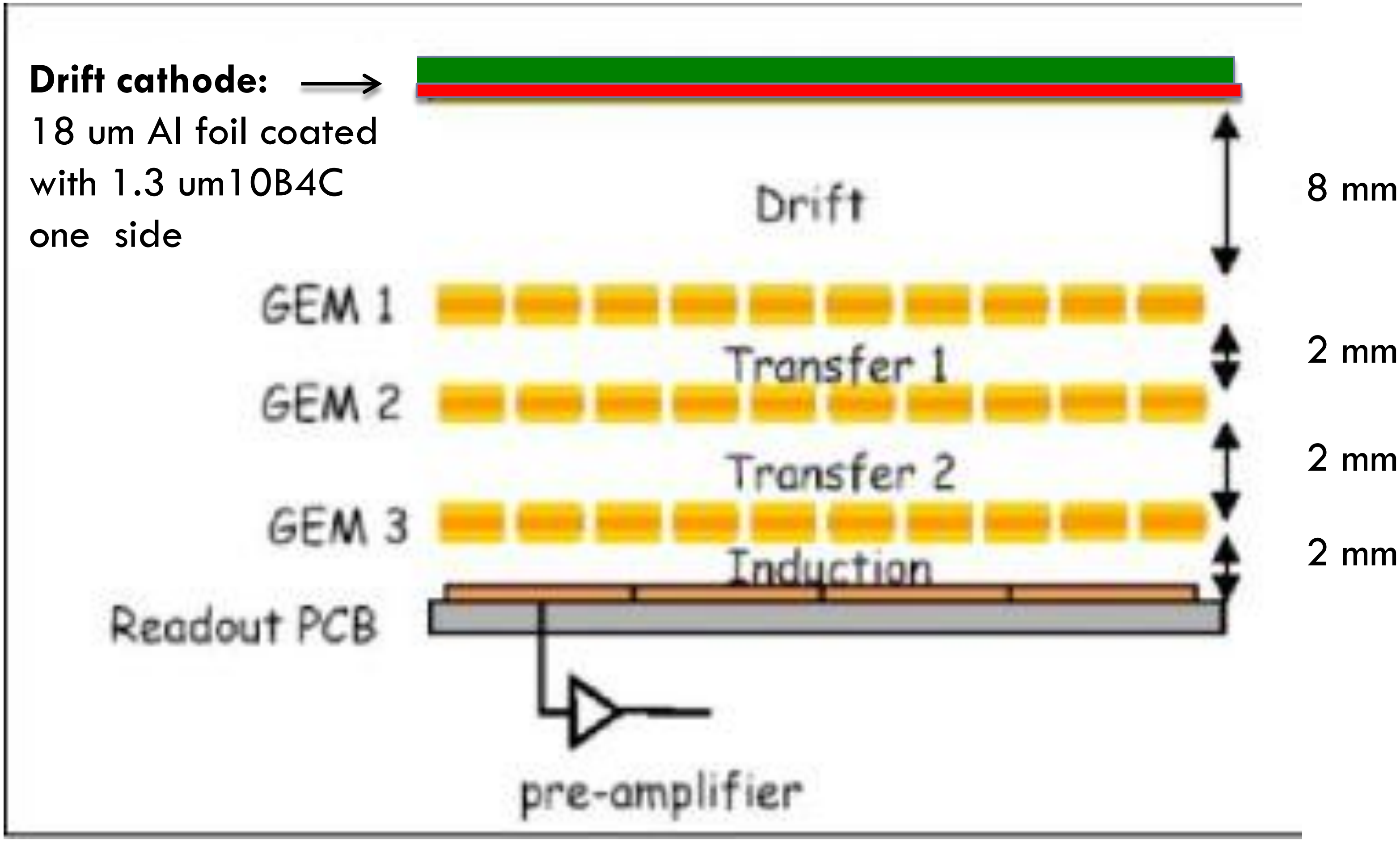

241 AmBe spectrum, drift gap 8 mm, gain ~ 200

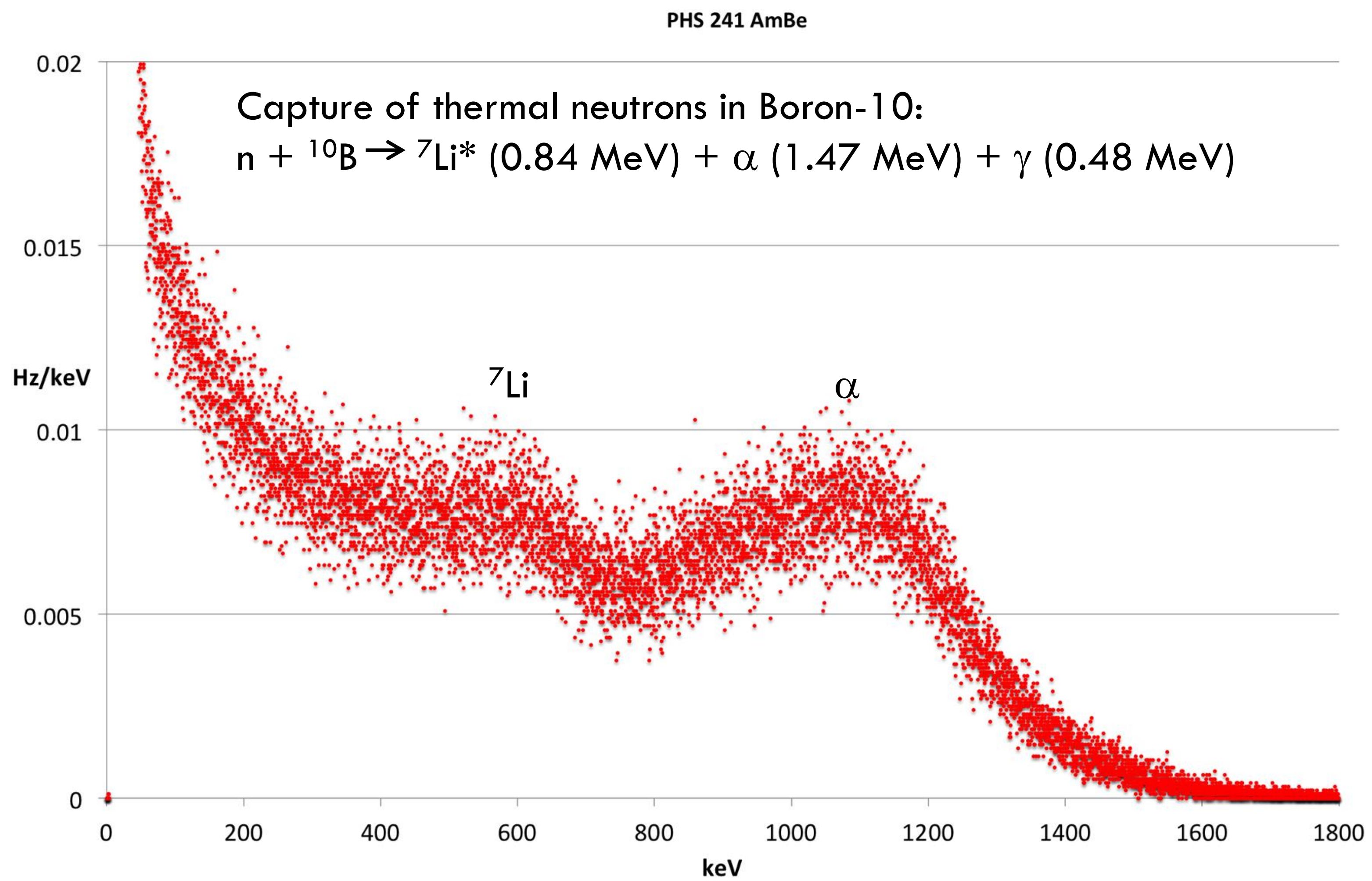

Boron GEMs

- It is quite straightforward to create a thermal neutron detector with a 10B4C coated cathode that has an efficiency of about 2%
- The bGEM of the Milano group has already been used at a neutron scattering experiment at ISIS and was able to reconstruct the TOF spectrum in similar quality as the He3 tubes (G. Croci et al.: GEM-based thermal neutron beam monitors for spallation sources, NIM A, Volume 732, 21 December 2013, Pages 217–22, http://dx.doi.org/10.1016/j.nima.2013.05.111)
- For higher efficiencies, different geometries or materials required
- A promising approach is the "lamella detector" of the Milano group. Detector uses inclined 10B4C coated lamellas and will have 50% efficiency and a spatial resolution in the mm range

uTPC

- Raw SRS data stored on disk contains timing information. Granularity depends on the read-out chip: APV25 (25 ns), VMM (1 ns)
- ATLAS team among George Iakovidis developed uTPC type analysis using this timing information and fitting algorithms to determine start, center and end of track
- So far this analysis if offline, but an online implementation in the FPGA of the SRS FEC card should be possible
- A quick analysis of the data of the Boron-GEM (done by Filippo Resnati) shows the potential of this method. First time such type of analysis has been done for neutrons

uTPC – alpha particle

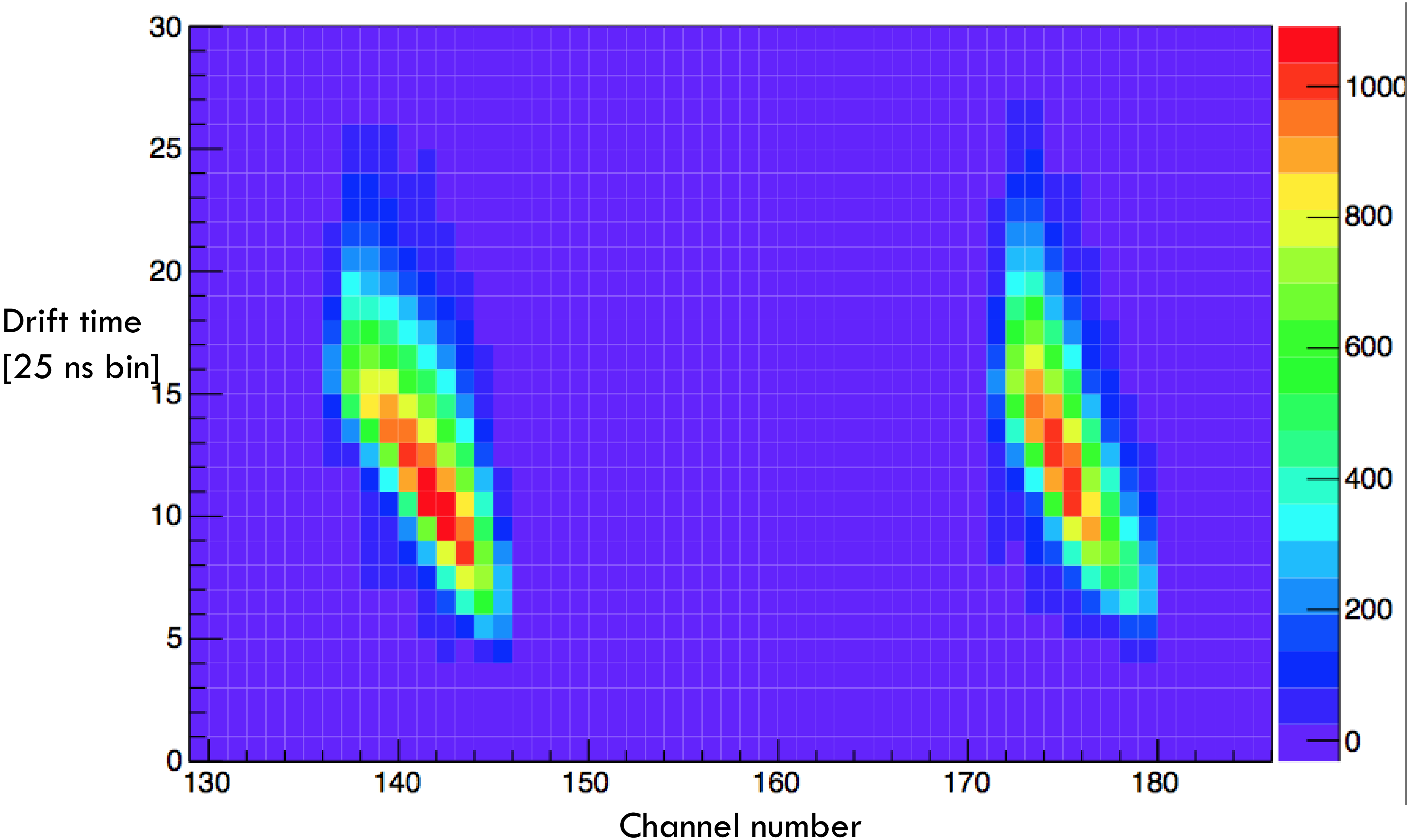

uTPC – alpha and gamma

Drift time
[25 ns bin]

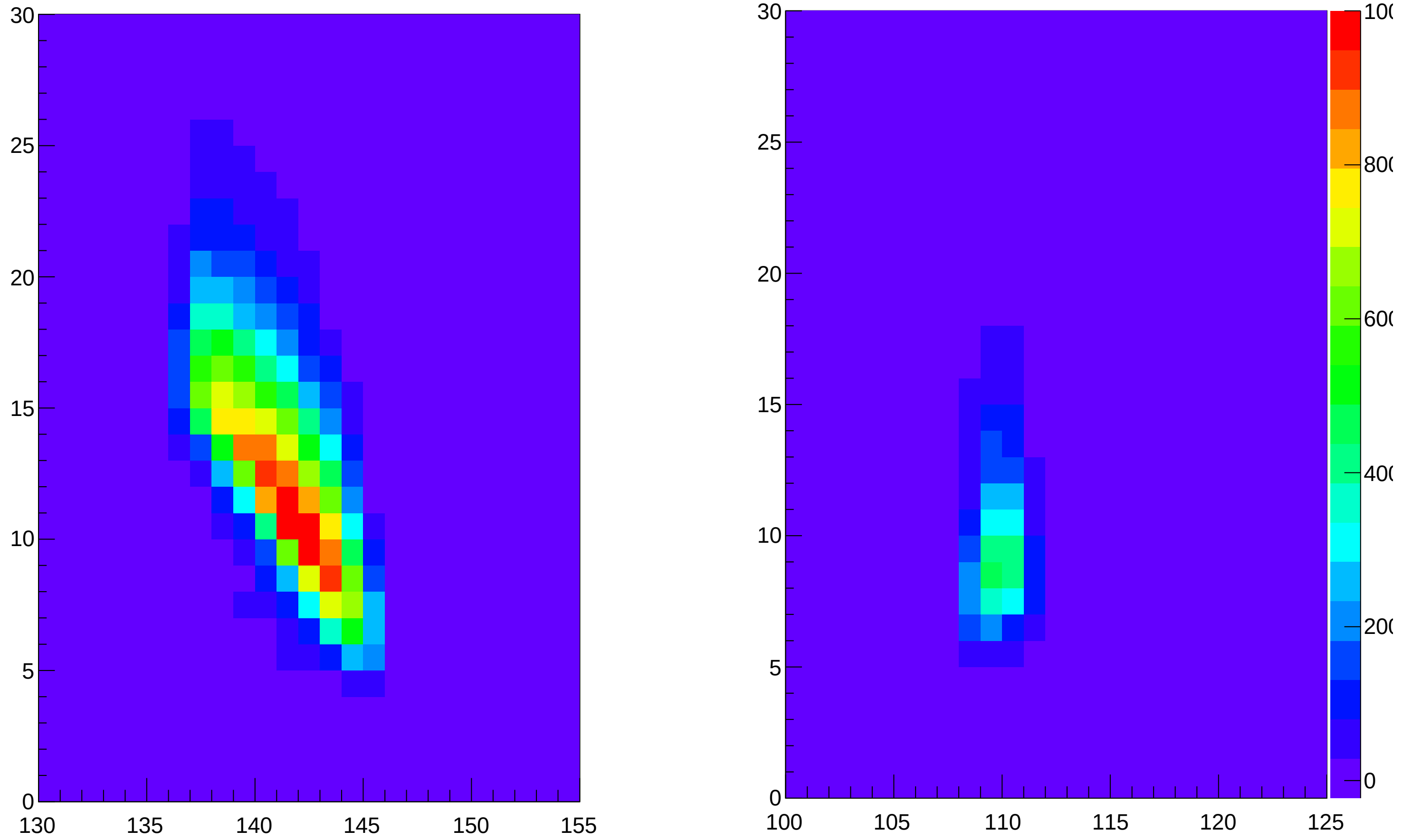

Channel number

uTPC – 3D reconstruction

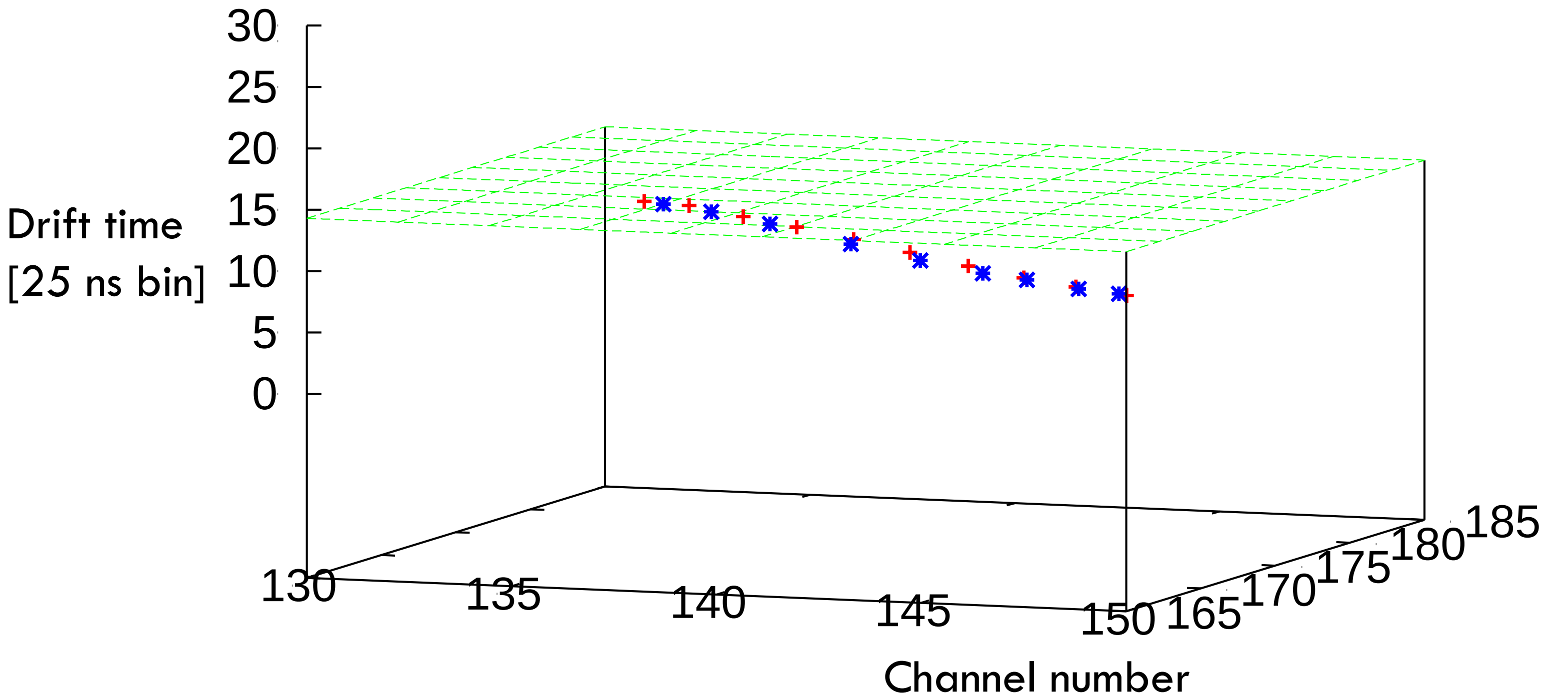

uTPC – large potential

- As we have seen, this method has a large potential to increase the spatial resolution compared to a centroid approach
- Method offers potentially both pattern discrimination and enhancement of position resolution
- With the Boron data it was also easy to distinguish between tracks created by gammas and alphas (amplitude AND shape)
- Real test case will be the Gd data and the discrimination between gammas and electrons

Converters for thermal neutrons

Isotope	Crosssection [barns]	Reaction	Range
^{3}He	5333	$n + {}^{3}He \to {}^{3}H$ (191 keV) + ^{1}H (573 keV) Q= 0.76MeV	R_p = 5.7 bar cm
^{6}Li	940	$n + {}^{6}Li \to \alpha$ (2.06 MeV) + ^{3}H (2.73 MeV) Q = 4.79 MeV	R_t=130 μm
^{10}B	3835	$n + {}^{10}B$ $\to {}^{7}Li^{*}$(0.84 MeV) + α (1.47 MeV) + γ (0.48 MeV) (93%) Q=2.3 MeV $\to {}^{7}Li$ (1.16 MeV) + α (1.78 MeV) (7%) Q=2.79 MeV	R_α = 3.14 μm
^{155}Gd	64000	$n + {}^{155}Gd \to {}^{156}Gd + \gamma$ (89, 199 keV) + conversion electron spectrum (39-198 keV) Q=8.5 MeV	
^{157}Gd	255000	$n + {}^{157}Gd \to {}^{158}Gd + \gamma$ (79, 181, 944 keV) + conversion electron spectrum (29-182 keV) Q=7.94 MeV	λ_{ce} = 11.6 μm

Gd-GEM

- For ESS macromolecular crystallography instrument (NMX) at least three movable detectors of 60 cm x 60 cm with100 um spatial resolution and ~30 % detection efficiency required
- Parameters difficult to achieve with 10B4C assuming normal neutron incidence
- Started investigating Gd GEM option

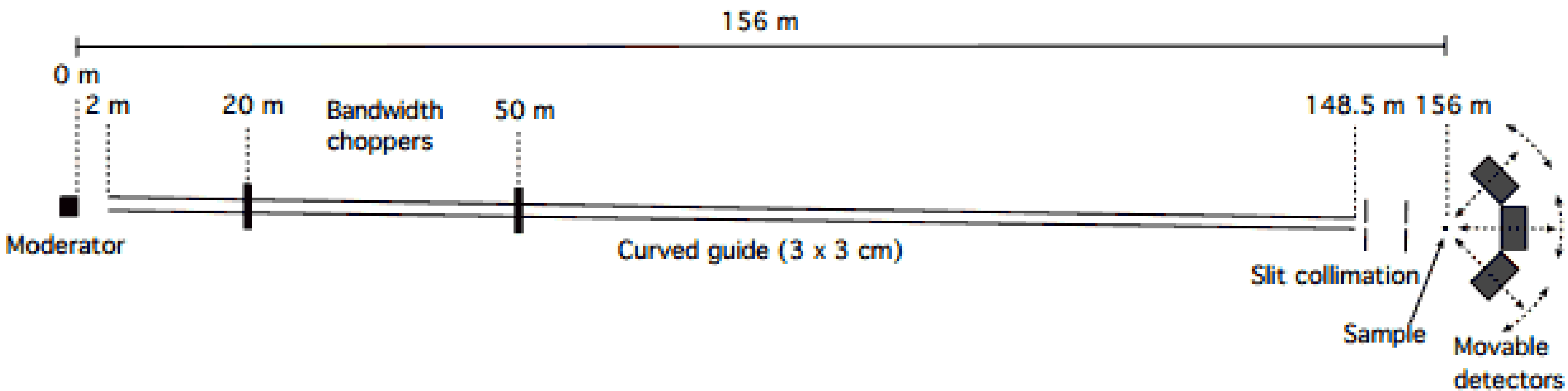

Gadolinium Simulation Setup

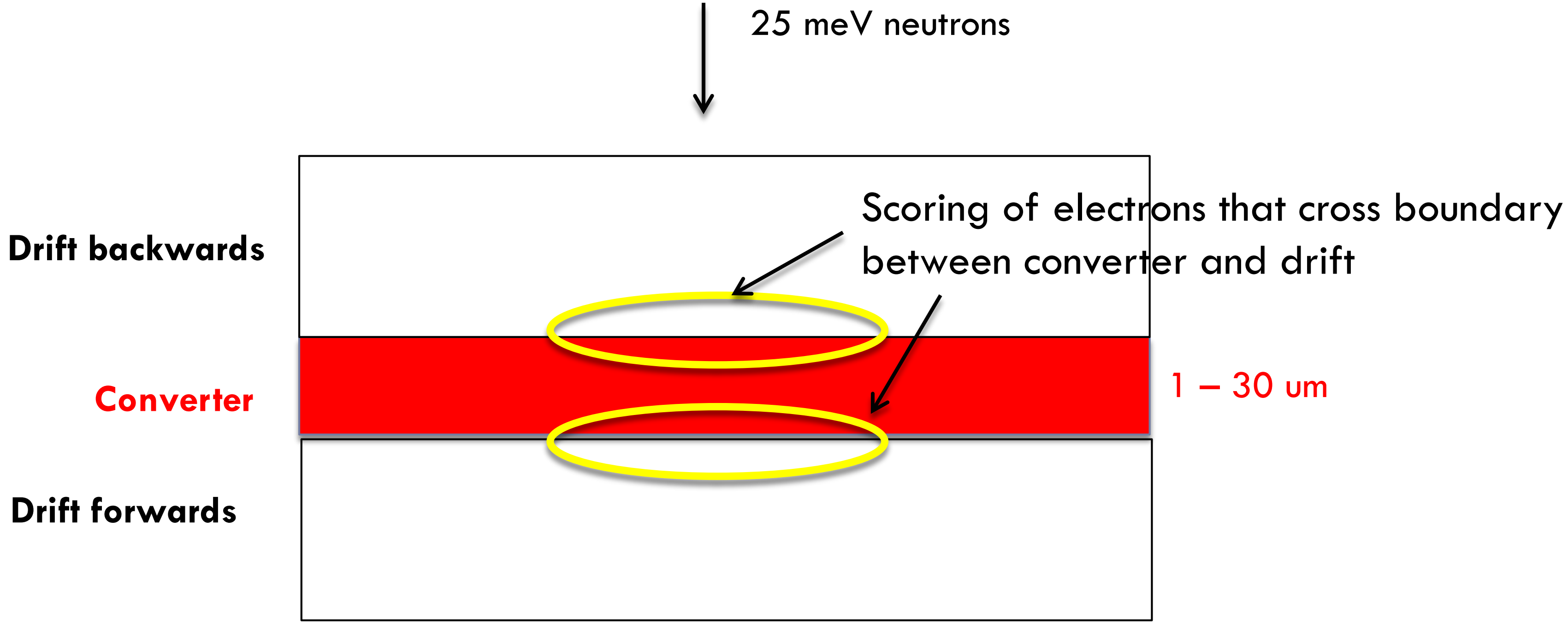

Converter efficiencies (25 meV neutron)

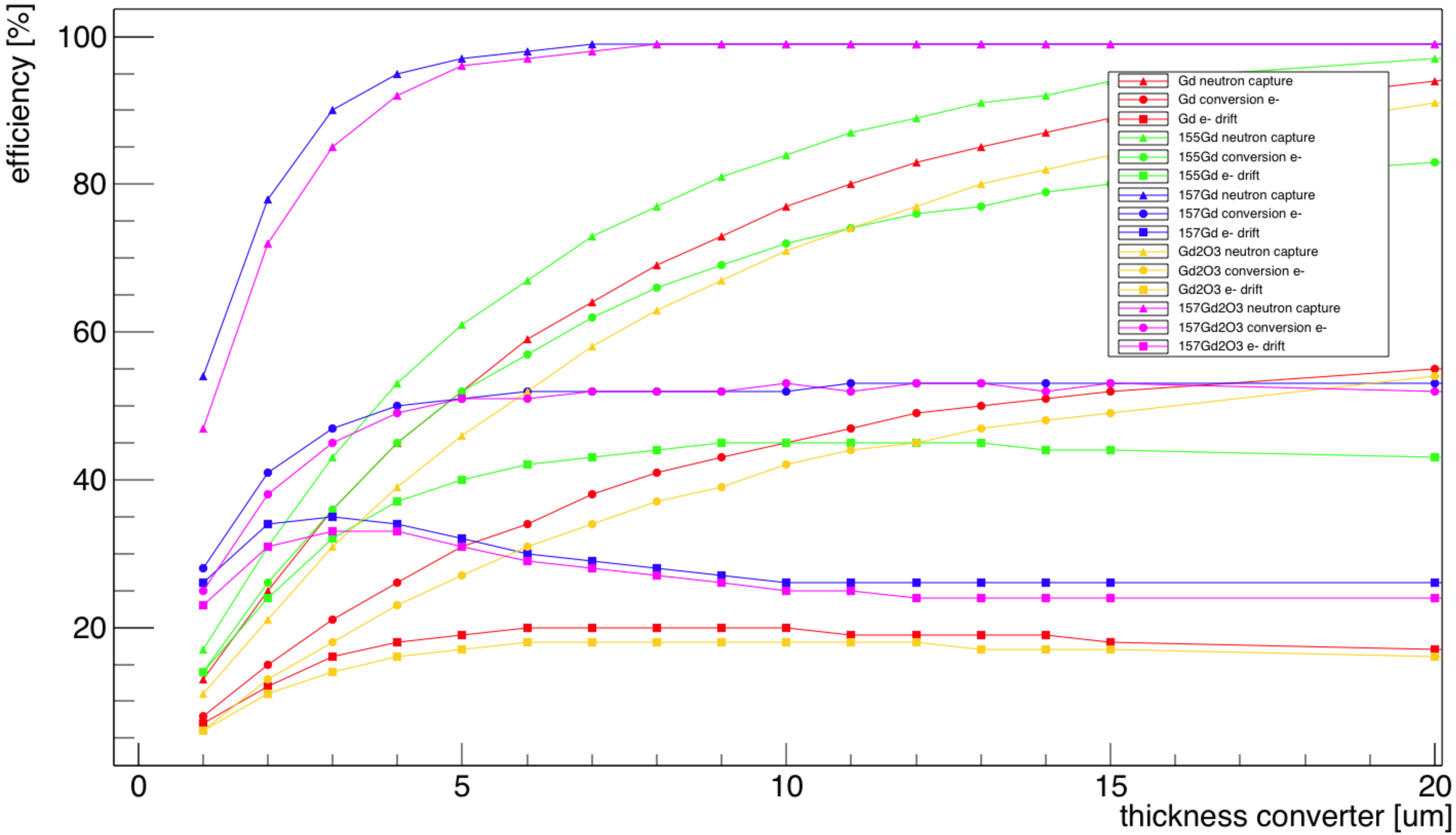

Electrons in drift

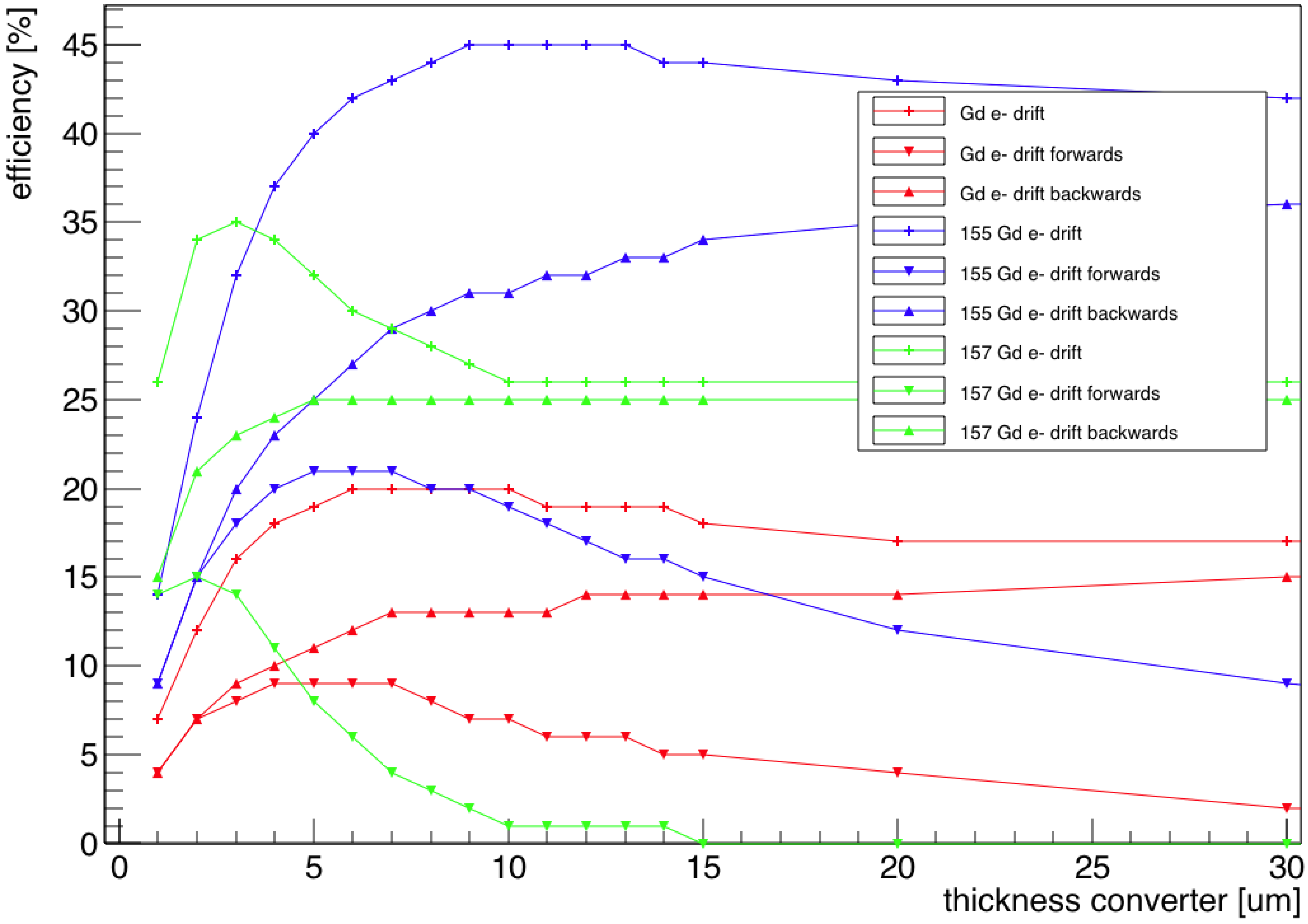

Conversion electrons 155 Gd

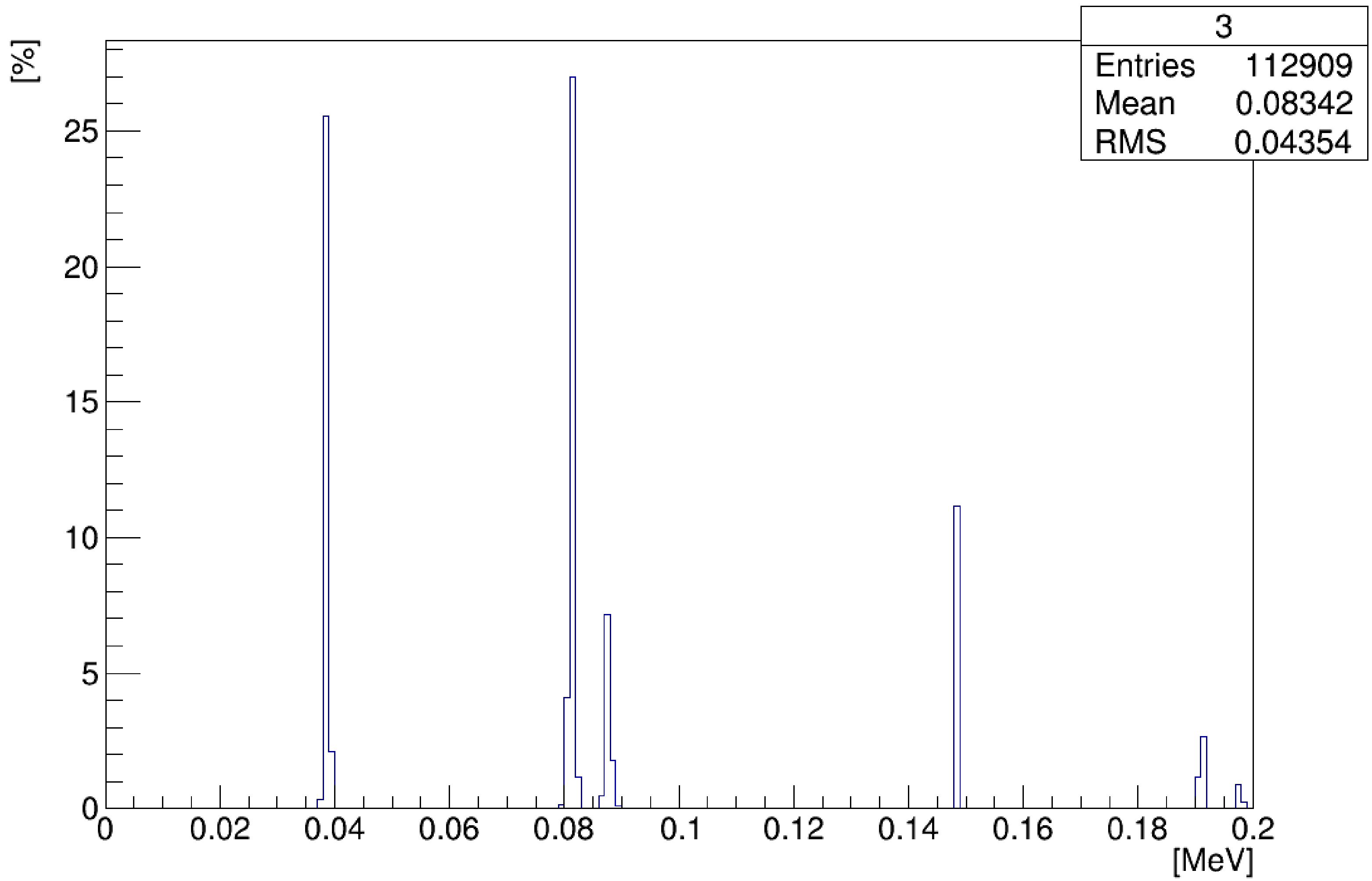

Conversion electrons 157 Gd

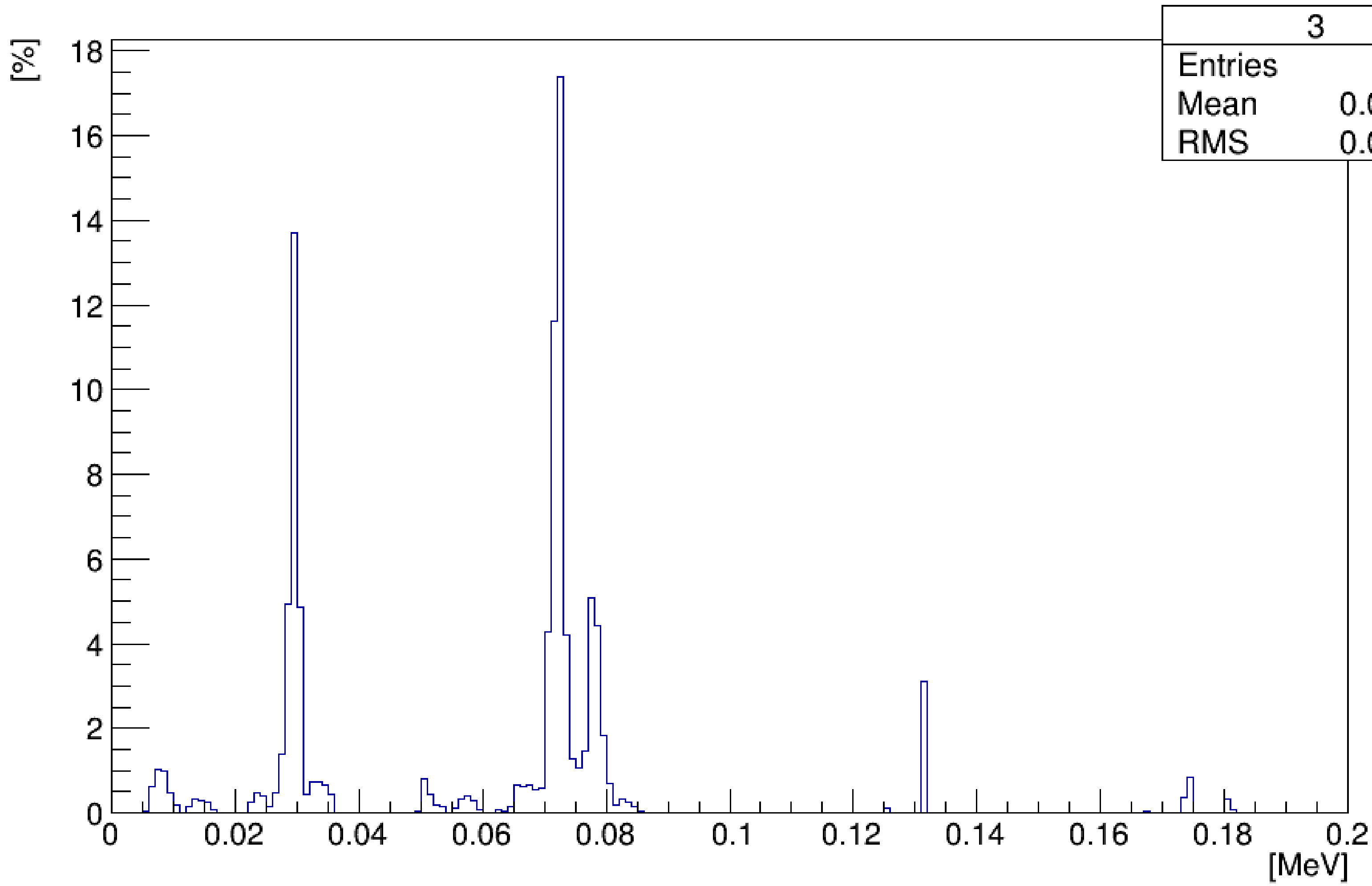

Conversion electrons natural Gd

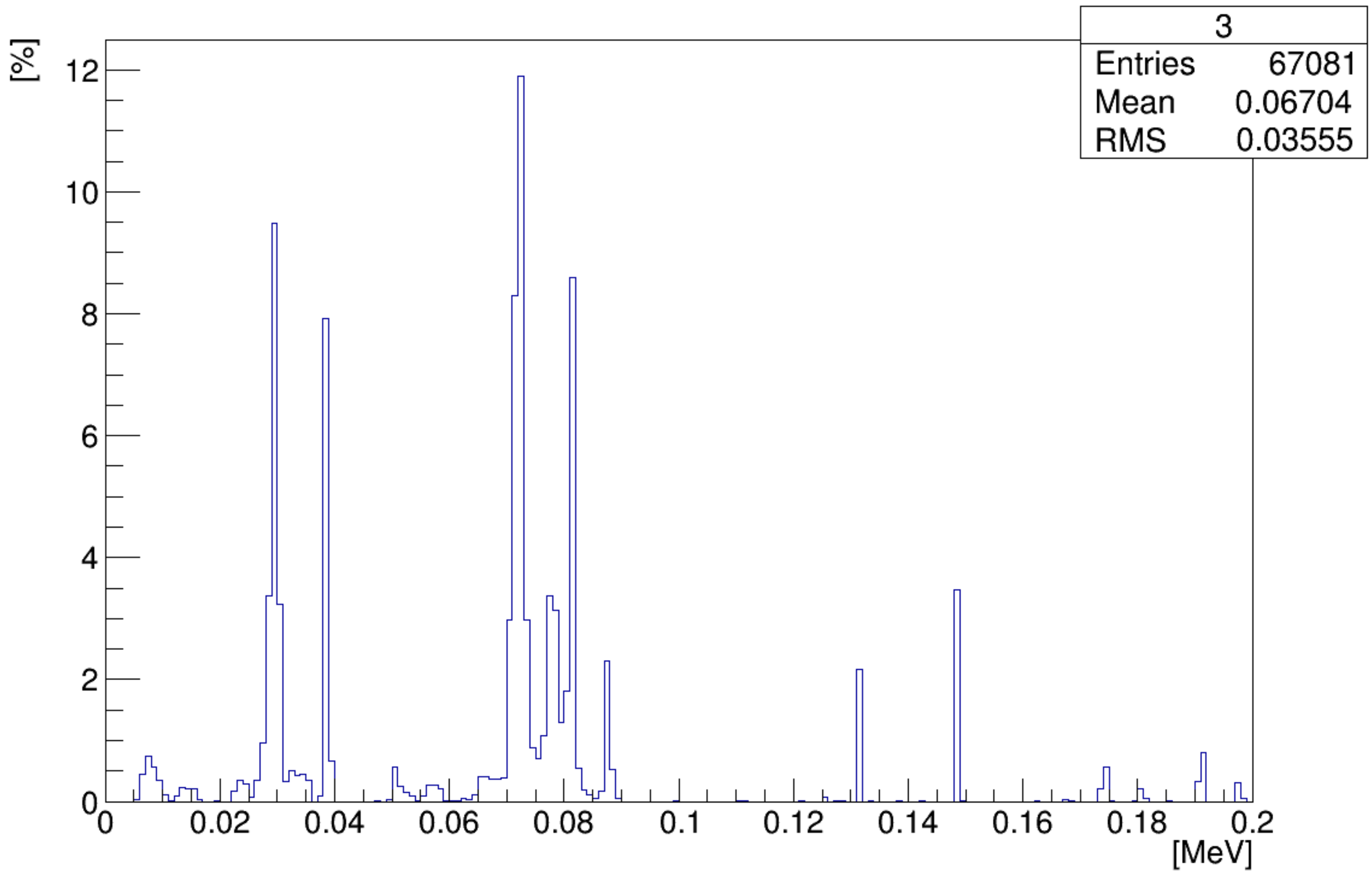

Gd GEM – first simulation results

- Simulations carried out with Geant4.10, G4NDL4.4 and flag G4NEUTRONHP_USE_ONLY_PHOTONEVAPORATION (final state data for gammas is not used)
- Oxides lead to comparable results for number of captured neutrons and conversion electrons created, but might be problematic due to charging up since they are not conductive
- Contrary to what is found in the literature, 155 Gd has a higher percentage of conversion electrons per captured neutron than 157 Gd
- The capture crosssection of 155 Gd is smaller than that of 157 Gd, therefore a thicker converter is needed. But since the spectrum of 155Gd (mean 83 keV) is considerably harder than that of 157 Gd (mean 61 keV), the conversion electrons can exit the converter

Geant4 simulation framework

Thomas Kittelmann et al., http://arxiv.org/abs/1311.1009

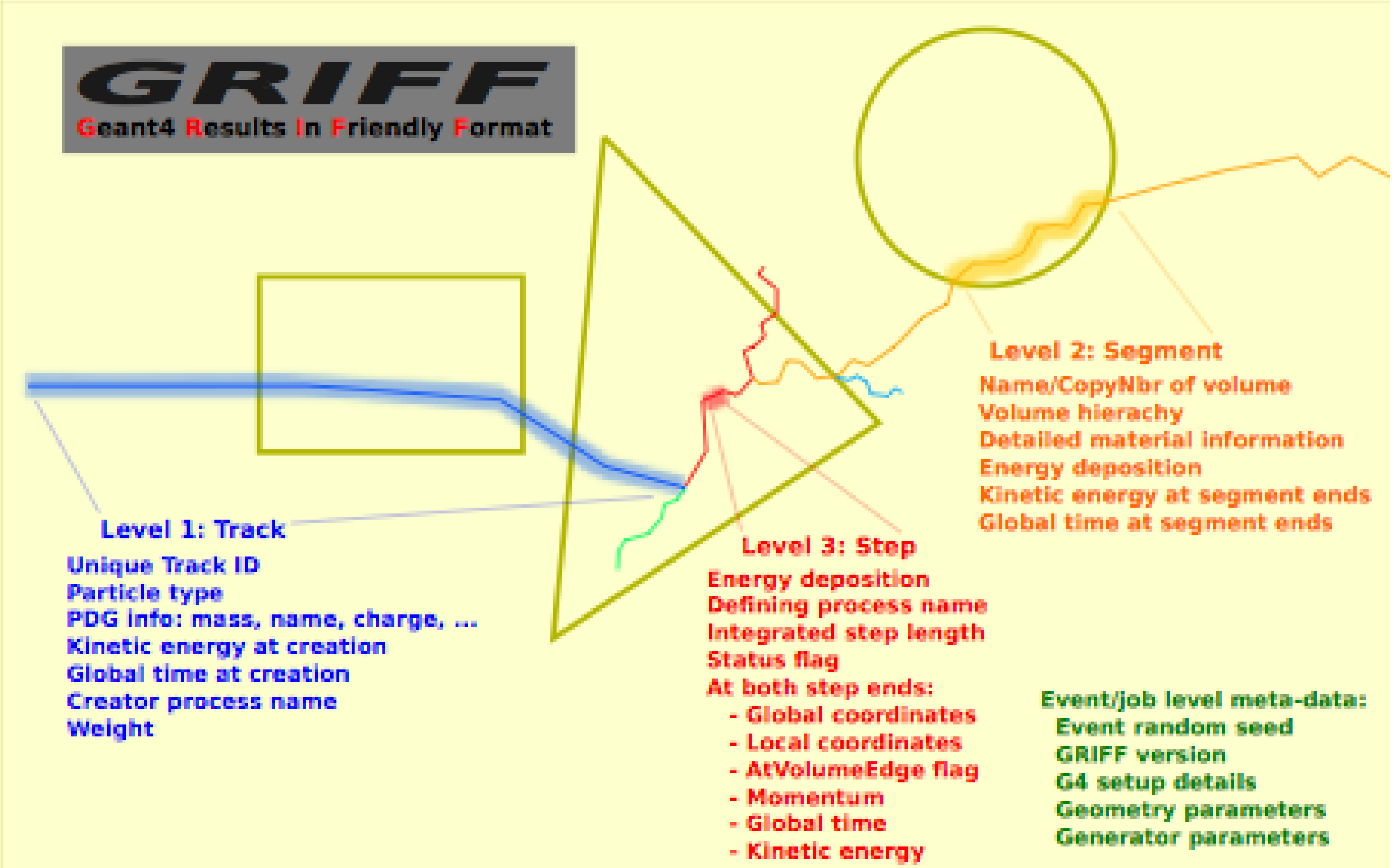

Geant4 simulation framework

- Includes description of neutron diffraction in polycrystals
- Plugin freely available for noncommercial purposes at http://cern.ch/nxsg4
- For simulations of neutron gas detectors it is desirable to use Geant4 and Garfield in the same simulation
- Discussions with Heinrich Schindler and Rob Veenhof resulted in a strategy to achieve a Geant4/Garfield++ interface

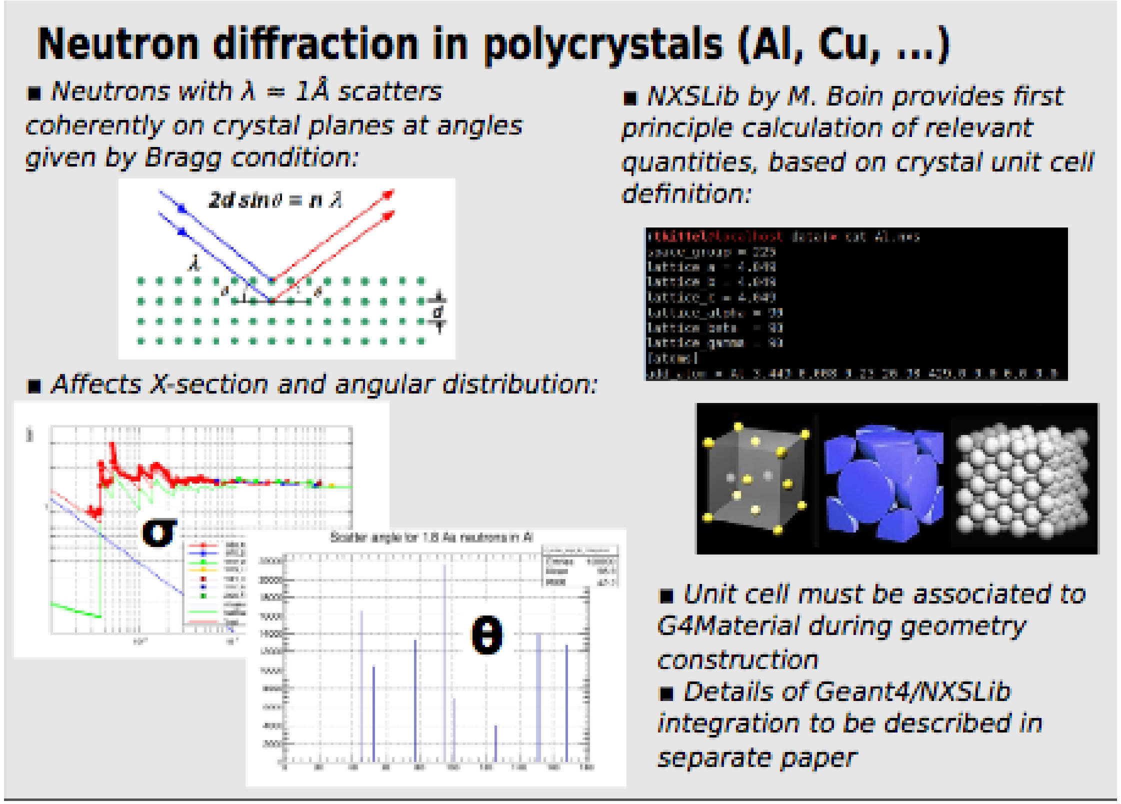

Geant4/Garfield++ interface

- The idea is to use Geant4 for the neutron capture and the creation of the prompt gammas and conversion electrons in Gadolinium and for the secondary electron creation in CsI
- The secondary electrons that arrive in the gas are then treated with Garfield/Heed. First Heed is used to create ionization clusters, then subsequently Garfield for the avalanches and the signal in the read-out
- With Gd and conversion electrons > 50 keV this approach should work well, but for Boron10 and the resulting alpha particles it is not so easy
- The alpha particles from the neutron capture have an energy < 1.47 MeV and are thus not relativistic. Heed works only for relativistic charged particles, the PAI is not applicable for slower particles. Geant4 is also not able to simulate the ionization of the gas by alpha particles
- Solution: Get the deposited energy in each step in Geant4, then create delta electrons in Heed

Geant4/Garfield++ interface

- Technical implementation:
  - Create region or parallel world with region in Geant4. In our case the region is the GEM detector below the cathode with the neutron converter
  - Create Garfield model class derived from G4VFastSimulationModel. The Garfield model is applicable for e.g. conversion electrons, kills the Geant4 primary track and uses the position, momentum and momentum direction to create a heed track (ionisation clusters). Subsequent steps are like in normal Garfield++ simulation
  - Attach the Garfield Model to the region
  - Add parametrisation to physics list. Create G4FastSimulationManagerProcess for the G4VFastSimulationModel
  - Update CMakeLists.txt to include Garfield++ sources and includes and link against library


THANK YOU
FOR YOUR ATTENTION!
MEMECREATOR.NET